Spatial modelling of soil and water conservation activities for a catchment in the Ethiopian Highlands

M.Sc. Thesis

M.Sc. Sustainable International Agriculture, specialization in Tropical Agriculture

Faculty of Agricultural Sciences

Georg-August-Universität Göttingen

James Ellison

Matriculation-number: 21363572

Supervisors

Dr. habil Katja Brinkmann (1st)

Prof. Dr. Andreas Bürkert (2nd)

Dr. Lulseged Tamene Desta

Dr. Gabriele-Johanna Lamparter

Accomplished at the

Dept. of Organic Plant Production & Agroecosystems Research in the Tropics & Subtropics

Witzenhausen

Universität Kassel

31 March 2016

Dr. Katja Brinkmann
Habilitated researcher
Dept. of Organic Plant Production & Agroecosystems Research in the Tropics & Subtropics
University of Kassel (Witzenhausen)
Email: brinkmann@uni-kassel.de

Prof. Dr. Andreas Bürkert
Full professor (chair)
Dept. of Organic Plant Production and Agroecosystems Research in the Tropics and Subtropics
University of Kassel (Witzenhausen)
Email: buerkert@uni-kassel.de

Dr. Lulseged Tamene Desta
Soil Scientist
Soils Research Area (Ethiopia, Malawi)
International Centre for Tropical Agriculture (CIAT)
Email: LT.Desta@cgiar.org

Dr. Gabriele-Johanna Lamparter
Scientific assistant
Dept. of Physical Geography
University of Göttingen
Email: glampar@gwdg.de

Author's email: jpellison5@gmail.com

Acknowledgements

I am grateful to Dr. Lulseged Tamene Desta ("Lule") for receiving me at CIAT in Ethiopia for six months during 2015 and who provided supervision during that time. My research stay in Ethiopia was made possible by the "Advisory Service on Agricultural Research for Development" (BEAF) of the Deutsche Gesellschaft für Internationale Zusammenarbeit (GIZ) GmbH. Their support, as well as the patience and cooperation of Mrs. Stefanie Zeiss from the BEAF, is gratefully acknowledged.

I thank also the CIAT team, Biyensa Gurmessa and Tesfaye Yaekob, who were always eager to help. This research was partly supported by Africa RISING, a program financed by the United States Agency for International Development (USAID) as part of the United States Government's Feed the Future Initiative. I thank both CIAT and Africa RISING for accommodating me into their programs and supporting my field visits.

I received help and encouragement from a number of people, including Dr. Zenebe Adimassu, Dr. Kindu Mekonnen, Dr. Tilahun Amede, Dr. Amare Haileselassie, Dr. Kifle Woldearegay, Dr. Sridhar Gummadi, as well as other colleagues from the ILRI campus in Addis Ababa. I'm also grateful to new friends I made in Ethiopia and to the people of Gudo Beret for being welcoming and patient.

In Germany, I'd like to thank both my official academic supervisors from Universität Kassel who accommodated me and particularly Dr. Katja Brinkmann who made time to consult me and looked through several drafts of this thesis. I thank also Dr. Gabriele Lamparter (Universität Göttingen) for her hydrological advice.

Abstract

This thesis focused on the use of soil and water conservation (SWC) planning tools to address two ecosystem services (ES's), erosion control (EC) and dry season baseflow enhancement (BF). The study site was a headwater catchment encompassing Gudo Beret town located in the central sub-humid highlands of Ethiopia. The aims of the thesis were to 1) model the current soil loss risk for the catchment, 2) to simulate a spatial allocation of recommended SWC activities throughout the catchment while giving different weights to the ES objectives, and 3) to estimate potential changes in soil loss and in the water balance as a result of those simulated activity scenarios. In the study, a number of tools and procedures were used: field observations to map erosion hotspots, participatory dialogues with focus groups, remote sensing to generate a land use/land cover (LULC) map, a water balance calculation, and GIS-based spatial modelling tools.

The current soil loss risk was predicted for the Gudo Beret catchment using the Revised Universal Soil Loss Equation (RUSLE). Erosion at Gudo Beret was found to far exceed safe limits, with soil loss from rainfed cropland estimated at 47 t ha^{-1} yr^{-1} (σ=82). Estimates of soil loss compared favorably with measurements and estimates from other sub-humid highland catchments in Ethiopia, but are believed to have significantly under-predicted total losses due to the prevalence of gullies in the study area.

The Resource Investment Optimization System (RIOS) tool was used to locate the most "responsive" sites to SWC. Three scenarios were tested in which EC and BF were weighted according to the ratios 1:1, 2:1, and 1:0. RIOS performed a spatial allocation of the activities and produced a hypothetical post-SWC LULC map to represent changes in biophysical parameters where activities were allocated. Soil loss was then estimated for the entire catchment for the hypothetical scenarios and a simplified water balance was performed for the rainfed cropland LULC class to assess the potential impact on baseflow, using the soil water storage/drainage term of the water balance as a proxy. The analysis that followed found that soil loss and soil water storage/drainage were not significantly different between the scenarios. The lack of significance between outcomes of the scenarios was attributed to low data quality for some inputs and the relatively small catchment size – both of which suppressed spatial variability which is needed to produce contrasting relative rankings for the ES objectives in RIOS. Recommendations for improving RIOS were given. Despite the results, the model's unique approach draws attention to both the need to target multiple ES objectives in future conservation goals as well as to account for the offsite benefits of SWC.

Table of Contents

List of Tables

List of Figures

Abbreviations and Acronyms

AET	Actual evapotranspiration
AfSIS	Africa Soil Information Service
ASTER	Advanced Spaceborne Thermal Emission and Reflection Radiometer (a DEM source)
BF	Baseflow
CN	Curve number
DEM	Digital elevation model
EC	Erosion control
ES's	Ecosystem services
ET	Evapotranspiration
ETB	Ethiopian birr
FAO	Food and Agricultural Organization of the United Nations
GIS	Geographical information systems
GPS	Global positioning system
GRASS	Geographic Resources Analysis Support System (a remote sensing tool)
InVEST	Integrated Valuation of Ecosystem Services and Tradeoffs (a modelling tool)
LULC	Land use/land cover
MAP	Mean annual precipitation
NRCS	Natural Resources Conservation Service (a division of the US Dept. of Agriculture)
PD	Person-day
QGIS	Quantum Geographical Information System (a GIS tool)
RIOS	Resource Investment Optimization System (a modelling tool)
RS	Remote sensing
(R)USLE	(Revised) Universal Soil Loss Equation (a modelling tool)
SCRP	Soil Conservation Research Program (a program of the Ethiopian government)
SDR	Sediment delivery ratio
SLM	Sustainable land management
SOM	Soil organic matter
SRTM	Shuttle Radar Topography Mission (a DEM source)
SWAT	Soil and Water Assessment Tool (a modelling tool)
SWC	Soil and water conservation
USD	United States dollars
$\Delta S + D$	The sum of the change in soil water storage (ΔS) and drainage (D)

1 Introduction

1.1 Land degradation in Ethiopia

Land degradation is major threat to livelihood security in the Ethiopian highlands where 85% of the country's population lives (Bewket & Sterk 2002). The Blue Nile, which is fed by a significant portion of the country's highlands, is famous for its dark brown color during the summer monsoon when the river carries high sediment loads and effectually "exports our soil to Egypt" - as one farmer from the study site put it. Some level of soil erosion by water is, of course, natural; since ancient times farmers of the Nile Delta have depended on rich sediments suspended in the Nile's waters to bring renewed fertility during the annual floods. But today's extent of erosion in Ethiopia – and especially in the highlands – comes at an ever-increasing cost to the nation.

The expansiveness of Ethiopia's land degradation problem is in part due to the pressure on land resources, which has resulted in extensive conversion of native vegetation to cultivated land (Dagnew et al. 2015). Evidence of this phenomenon was observed at the study site in the central highlands where no closed forest remains. Although some have estimated that 40% of Ethiopia was covered in forest in the 16th century (EFAP 1994; Tumcha 2004), some critics find the number too high given that the country has experienced widespread deforestation for over two millennia (EPA 1997). Nevertheless, there is consensus that a major decline in forest cover occurred in the second half of the 20th century and that today, less than 3.6% of the country is under forest (WBISPP 2004; Reusing 1998).

This land degradation is seen mainly in the form of soil erosion and nutrient depletion (Tekle 1999). The main land use contributing to the export of sediment is cultivated land (Adimassu 2013). Approximations of average annual soil losses from cultivated highland fields vary greatly, but 179 t ha^{-1} (Shiferaw & Holden 1999) seems to be a maximum. Tamene & Vlek (2008) translated the national land degradation crisis into a 2.2% annual decline in land productivity since the 1980s.

In recognition of this national threat, the Ethiopian government and donor organizations have promoted the adoption of soil and water conservation (SWC) measures by farmers. After land degradation was named a chief culprit of the catastrophic famine in northern Ethiopia in the early 1970s, a partnership between the government and the Food and Agricultural Organization of the United Nations (FAO) initiated the largest SWC campaign to date, called Food-for-Work (Tamene & Vlek 2008). Since then, despite millions of dollars and billions of hours invested, SWC adoption remains low (Adimassu et al. 2012; Tesfahunegn et al. 2011) and sediment concentrations in the Ethiopian Blue Nile continue to rise (Steenhuis & Tilahun 2014). Many factors have been blamed: the non-suitability of "imported" SWC technologies (Mitiku et al. 2006); the transfer of technologies between drastically different climates and landscapes (Tebebu et al. 2015); and the fact that local communities were not consulted in the choice of technologies (Badege 2001).

1.2 Ecosystem services

The decline in land productivity seen in Ethiopia can be said to be the result of the degeneration of ecosystem services. Ecosystem services (ES's) are the benefits obtained by people from ecosystems and have been categorized in four types of benefits: supporting, provisioning, regulating, and cultural (Millennium Ecosystem Assessment 2005). Because of the interconnectedness of ES's, this study will focus on two regulating services: erosion and water regulation.

Soil is a key asset for both erosion and water regulation. When soil is transported off a piece of land, plant nutrients like nitrogen and phosphorus bound to soil particles as well as soil organic matter are lost, representing a drop in fertility. Eroded materials often originate from the topsoil, which is more porous than deeper layers. It then follows that the loss of topsoil constitutes a drop in the water-holding capacity of soil column. Furthermore, the reduced capacity of the upper soil layer to absorb rainfall and slowly release it to deeper, less porous subsurface layers is reduced; this means that the parcel has a reduced capacity to infiltrate and store rainfall.

These shifts in regulatory services have onsite and offsite implications. Onsite, the decline in fertility, water-holding capacity, infiltration, and soil rooting depth render a piece of land less able to produce biomass. Offsite, the reduced infiltration capacity of the soil and the sediments that are transported lead to higher runoff flows capable of damaging downslope soils and crops; the clogging of natural vertical flow paths with fine sediments on downslope land; the perpetuation of soil erosion via sheet, rill, and gully erosion; the sedimentation and pollution of streams and water bodies; and a reduction in stream baseflow which is fed by subsurface water flows.

As shown, the loss of soil through erosion is linked to a decline in many ES's across a spatial range of the landscape. Aside from the reduced ability of the eroded land to support crop growth (a provisioning service), downslope lands along the flow routes to waterways are put at risk of degradation. As the water balance of the catchment shifts towards increased runoff flows, subsurface storage and drainage are diminished (Price 2011). Stream flows become increasingly energetic during rain events but with less subsurface drainage (responsible for baseflow), flows wane between events (Healy 2010). In tropical areas with long dry seasons, the water balance shift leads to streams and rivers running dry (Bewket & Sterk 2005). The downstream implication cannot be forgotten: a diminution of dry season flows means that less water is available for humans, animals, and - especially in the Ethiopian highlands - irrigated cultivation in the valleys.

1.3 Objectives of the thesis

This study took advantage of the established structure of the Ethiopian highlands component of a research-for-development program known as Africa RISING (Africa Research in Sustainable Intensification for the Next Generation). The study site, known as Gudo Beret, was a small catchment in the central, sub-humid highlands. The objectives of this thesis were three-fold:

1. Model the current soil loss risk for the Gudo Beret catchment.
2. Simulate a spatial allocation of recommended SWC activities throughout the catchment for three scenarios that give different weights to the targeted ES's.
3. Estimate potential changes in soil loss and the water balance as a result of the simulated activities.

Generally, this thesis focused on testing a new modelling tool which claims to facilitate SWC planning in a way that targets ES objectives. The objectives of interest in this study were erosion control and dry season baseflow enhancement since the study area faces high erosion risk and faces seasonal water scarcity. To facilitate the comparison of "status quo" and "post-SWC hypothetical" predictions, it was necessary to establish a baseline. Unfortunately, a shortage of time prevented the collection of enough data to accurately characterize the "status quo" of stream baseflow. However, regarding soil loss, a number of techniques were used to inform the modelling procedure: participatory focus groups, field surveys, literature reviews, remote sensing, and GIS modelling. After the modelling procedure, the

simulated post-SWC scenarios were assessed for their ability to lower soil loss risk in the catchment. Regarding baseflow, a simple water balance was performed in order to infer a potential impact as a result of the simulated SWC measures. Figure 1 provides a workflow for this thesis.

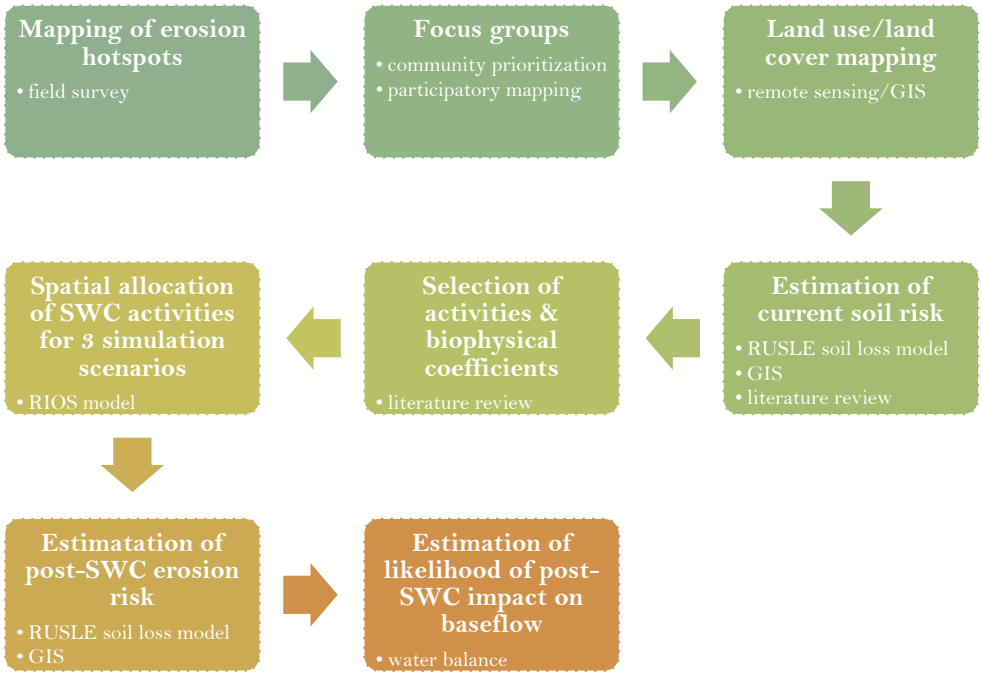

Figure 1: Workflow of thesis (tools used are bulleted)

1.4 RIOS as a tool for targeting ecosystem services

RIOS (Resource Investment Optimization System; Vogl et al. 2013) is a GIS-based tool used to locate "best-bet" sites for SWC interventions across a watershed. The first premise of RIOS is that conservation activities targeting certain objectives are most effective in the long-term when they are implemented in locations that would be most responsive. In other words, the most potentially responsive locations are those places (or, pixels in GIS) where SWC activities would be most likely to enhance ecosystem service (ES) objectives. The ES's of interest in this study were erosion control (EC) and baseflow (BF) enhancement. The second premise of RIOS is that the responsiveness of a particular location is presumed to be driven by a small set of biophysical factors. The RIOS documentation (Vogl et al. 2013) claims that, through an extensive review of published studies and hydrological model documentations on key drivers of ES enhancement, key factors have been identified which influence the magnitude of sediment or runoff sources.

RIOS requires spatially-explicit information for the study area. The main data inputs are biophysical factors that represent the variability of the climate, soil, land use/land cover, topography, and hydrology across the landscape. Indeed, a higher spatial variability – which often concurs with higher data resolution – is necessary for producing meaningful results. The tool is unique in its approach, but perhaps because of its relative novelty, is not yet widely used. The most relevant application of RIOS to this study was in developing scenarios for a water fund in Kenya (TNC 2015; Hunink & Droogers 2015; Vogl & Wolny 2015) which will be discussed in more detail in the discussion.

The spatial allocation of SWC activities by RIOS follows the following basic steps:

1. Spatial data corresponding to the two sets of biophysical factors - one set for EC and one for BF – is compiled.
2. For each objective, pixels are ranked across the landscape according to their biophysical factor weights. This is a relative ranking.
3. The two rankings are combined according to user-chosen weights for EC and BF. These weights could represent the value stakeholders associate with enhancing EC or BF.
4. Activities are allocated across the landscape, starting with pixels that ranked highest. The choice of activity is determined by settings given by the user. Activity selection can be influenced by activity costs (not used in this study) and other constraints if they are assigned. An activity allocation map is obtained.
5. In a second module, the user predicts the various land cover transitions expected to be caused by a particular activity on a particular land use/land cover type. A post-SWC land use/land cover map and biophysical coefficient table is produced.
6. The user can use this map and table to analyze the hypothetical impact on erosion and hydrological processes.

2 Materials and Methods

2.1 Description of the study area

2.1.1 Geography and climate

Gudo Beret, the study site is located in the central Ethiopian Highlands, about 25.7 km further north by road from Debre Birhan, a town located 132 km north of Addis Ababa along the Dessie Road. As the crow flies, the nearest town is Debre Sina, found 10.5 km to the northeast, however 25 km of road separate the two places due to the need for many switchbacks.

The study site is a sub-catchment of an upper reach of a tributary of the Blue Nile Basin, and consisted of a large portion of the Gudo Beret kebele as well as a small part of the Adisge kebele. For this reason, the study area will be called "Gudo Beret" henceforth. (Ethiopian administrative units are formed by kebeles, woredas, zones, and regions.) The woreda is Basona Worena, which is found in the North Shoa zone of the Amhara region. Within the study area, a small village called Gudo Beret occurs along the asphalt road and is located at 39.679 E, 9.801 N. The 25.76 km^2 (2576 ha) study area features a dramatic elevation gradient, from 2825 to 3562 meters above sea level. This gradient is seen foremost in the gradual incline from the wide valleys in the west to the high hills in the east. A second, less dramatic gradient is seen when one of the two main stream valleys are transected perpendicular to the westward flow of water; especially in the east of the sub-catchment, narrow stream valleys dissect steep hillslopes on either side. The area represents the very highest reaches of the Blue Nile tributaries, since the bordering catchment to the east would rather channel water eastward into the Great Rift Valley, feeding the Awash Basin.

The area contains two streams that run westward and merge en route to the Blue Nile. The streams flow continuously during the wet season. During the dry season, low flows persist at places where springs are present, but the flows diminish to nothing within meters. The northernmost stream has sufficient spring flows during the dry season in the downstream part to enable dry season irrigation of a vast valley plain. The southernmost stream is similarly perennial in its downstream portion, although because its riverbed is deeply incised, it does not contribute to irrigation within the study area.

The climate is temperate, with a tropical monsoon season from late June to early September. The period is caused by two moist air streams: a southeasterly stream originating from the Atlantic and the DR Congo's humid forests; and a southwesterly stream from the Indian Ocean (Osman 2001). During the wet season, the Inter Tropical Convergence Zone (ITCZ), a low-pressure system, lies north of Ethiopia's northern border; it is a combination of the effect of the ITCZ and the region's topography that have the most influence on the country's rainfall distribution (Osman 2001). The central highlands and parts of western Ethiopia receive the highest rainfall amounts in the country.

Following the wet season, the ITCZ traverses the country southward and then back northward. Historically, rainfall patterns in some parts of the central highlands exhibited an additional off season ("Belg") that allowed for short season cultivation, but unreliable rains in recent decades have rendered the practice of Belg cultivation obsolete in the study area (Kelemu et al. 2014). Farmers told Kelemu et

al. (2014) that the precipitation regime shifted from bimodal to unimodal after 1984, a year which marks a period of severe drought in Ethiopia.

A rainfall diagram (Figure 2) compares 30-arc-second interpolated precipitation data averaged for the 1950-2000 period (WorldClim.org; Hijmans et al. 2005) and 2015 data from a meteorological station established at Gudo Beret. Both datasets show the extreme seasonality of the region's unimodal precipitation regime. Temperatures hardly fluctuate throughout the year, hovering at around an average of 15.1 deg C. The total annual rainfall was measured as 1191 mm at the Gudo Beret weather station in 2015. At the same location, the 50-year average is predicted at 1087 mm.

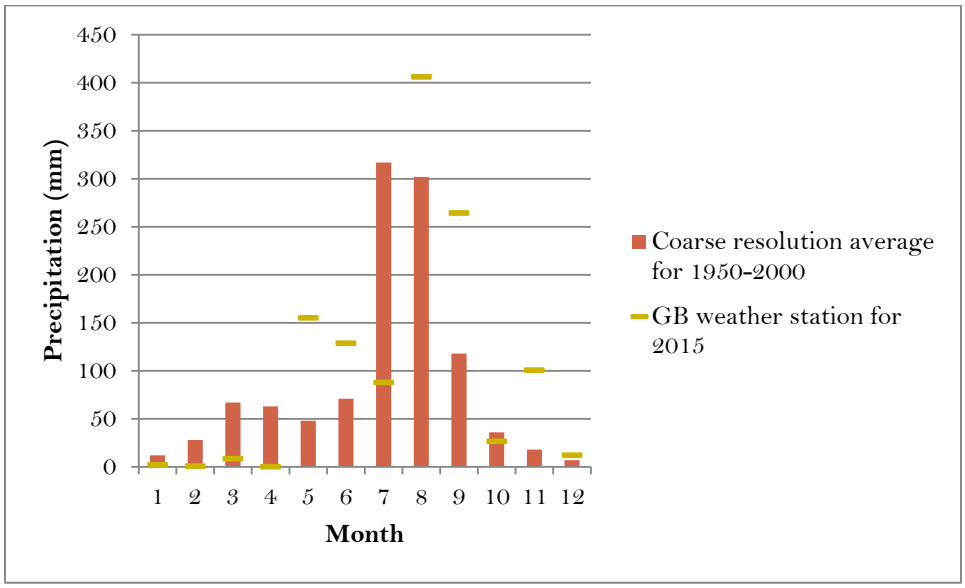

Figure 2: Long-term (1950-2000) precipitation data (Hijmans et al. 2005) and 2015 data from the Gudo Beret weather station

2.1.2 Vegetation and soils

According to Hurni's (1998) classification of traditional ecological zones in Ethiopia, since Gudo Beret experiences a MAP between 900 and 1400, a "moist dega" occurs at altitudes under 3200 m and a "moist wurch" occurs at altitudes over 3200 m.

Vegetative regimes in the highlands vary along the elevation gradient. The Gudo Beret landscape is completely artificial, meaning that the original, naturally-occurring species that would otherwise exhibit an altitudinal gradient have largely been displaced. Today, the lower, flatter western part of the sub-catchment is almost entirely under agriculture and pasture. The higher, more hilly eastern part of the sub-catchment is similar, except plantation forestry is additionally found here. It is only in the far eastern side, on the steep slopes hilltops, that a more typical afro-alpine landscape can be seen. This difficult terrain is dominated by shrubland that is relatively undisturbed.

While native tree species are extremely rare and highly localized - existing where farmers are deliberately protecting them - native shrubs and tussock can be seen on less-useful land, for example, on the banks of streams, steep areas, in gullies, around rock outcrops and at field borders.

Plantation forestry thus represents the main occurrence of trees in the landscape. Three species occur only, *Eucalyptus globulus*, *Eucalyptus camaldulensis*, and *Cupressus lusitanica*. Plantation forestry does not occur at riparian areas or along borders, but is also highly localized and its arrangement is based on ownership. Private woodlots occur close to homesteads, and normally consist only of eucalyptus. State-owned plantations managed by the Amhara Region Forest Enterprise are mono-cropped but may consist of either species. These plantations were established on highly degraded lands (steep land with only a shallow soil remaining) during the Derg era (1974-1991). Satellite imagery of this corridor of the Blue Nile Basin reveals that the state-owned plantations found in Gudo Beret are one of the few remaining swathes of woodland (Fig. 3).

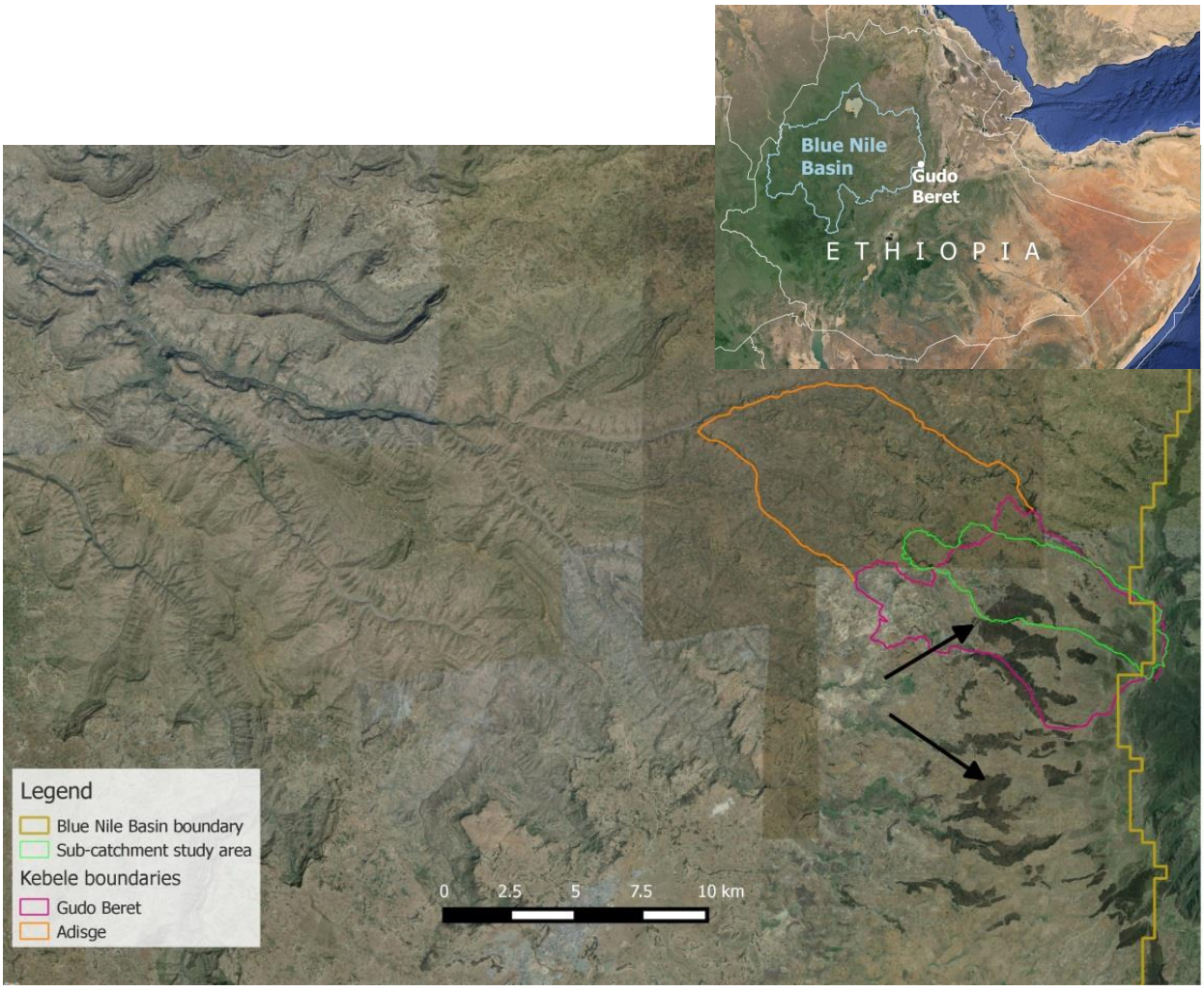

Fig. 3: Satellite imagery from the eastern edge of the Blue Nile Basin. Wooded areas, seen in dark green (like those indicated by the black arrows) are nearly void of the landscape in this part of the basin. The study area contains one of the few remaining wooded areas (albeit, plantation woodland) in the greater area. (Note: mismatching of the eastern sub-catchment and basin boundaries is due to the fact that the basin boundary is derived from coarser, 15 arc-second data.)(Source: Google)

An early participatory baseline survey by Kuria et al (2014) found that local farmers differentiated between seven soil types in Gudo Beret: two clayey soils, 3 loamy soils, a sandy loam, and a sandy soil.

These were each described in detail by farmers. Their relative differences in terms of fertility, gravel content, and waterlogging susceptibility were given.

Generally, valley soils (mainly in the west part of the sub-catchment) are deep, clayey soils that crack deeply in the dry season. However, a majority of the sub-catchment is sloped, and the soils are shallow and loamy. Rock fragments at the soil surface were common on upland farms, and in some cases, the rock cover was extreme.

Although it should not be interpreted as conclusive, ISRIC's soil maps offer perspective on the types of soils one may expect to find in the study area, as shown in Table 1.

Table 1: Expected soil types in the study area, acc. to 1-km ISRIC soil grids (Hengl et al. 2014)[1]

WRB[2] Soil type	Elevation distribution within study area	Description
Leptosol	Low, Mid	Shallow soils or soils over a gravelly or stony layer, common in mountains.
Cambisol	Mid	Relatively young soils, with little profile development.
Phaeozems	Mid	Prairie soils with accumulations of organic matter.
Andosols	High	Young, immature soils from volcanic materials.
Kastanozems	High	Soils with accumulations of organic matter.

[1] information should be interpreted loosely since data is based on rough interpolations between sampling points. For example, vertisols are known to be present in valley bottoms, though they may not be the dominant soil type at a 1-km resolution.

[2] World Reference Base

2.1.3 Land use activities

The Gudo Beret kebele is home to approximately 1500 households (Ellis-Jones et al. 2013). Agriculture, livestock, and forestry are the dominant livelihood sectors of the local society. The average farm size for a household is 2-3 ha. Cereals were mainly produced for household consumption, while other commodities were meant for the market. Livestock husbandry is dominated by sheep fattening, an activity pursued by nearly all households. Eucalyptus has become the most important income source across the woreda, with poles being the main commodity (Kelemu et al. 2014). Additional livelihood sources, although of lesser significance, include weaving, casual labor, beer-making, and carpentry (Ellis-Jones et al. 2013).

In Gudo Beret, the main crops were wheat, fava bean, chickpea, teff, barley, Irish potato, field pea, lentils, linseed, and some vegetables (garlic, cabbage, beet root, onions). Participatory information from a baseline study by Ellis-Jones et al. (2013) showed that (in order), barley, wheat, and fava bean were seen as most important for food security; on the other hand, potato, lentil, and field pea (in order) were seen as most important for generating cash.

The study by Ellis-Jones et al. (2013) also produced a cropping calendar for the area. Ploughing occurs in February and March, sowing in June, weeding in August and September, harvesting of wheat in October, harvesting of barley and beans in November and December, and threshing in January and February.

Livestock are an important part of the agriculture, and high stocking densities mean that digestible biomass is scarce in the dry season. Cows, oxen, sheep, donkey, and chicken are found in the area. The

baseline assessment of Kuria et al. (2014) found that crop residues were the main source of fodder for most farmers, and were utilized for about six months annually. Other feed sources included hay, by-products from the making of local beer (barley and leaves of *Rhamnus prinoides*), grasses, tree fodder, and weeds (Kuria et al. 2014).

2.2 Mapping of erosion hotspots

In late January 2015, we performed a total of seven transect walks throughout the landscape of the Gudo Beret kebele, two of which were within the study area. Erosion hotspots in the landscape consisted mainly of gullies, although some severe cases of rill erosion and landslides were also noted. Gully locations were needed because gullies and streams are not easily distinguishable from satellite imagery and are often confused by hydrological routing algorithms.

A total of 56 gully features were geo-referenced using a GPS unit with approximately 2-m accuracy. At all times, were accompanied by one or two local guides who could offer input as to the historical development of the gully and the surrounding land uses. Quotes from these key informants as well as personal observations (e.g., the relative "stability" of the gully) were additionally recorded in the gully database that would be created. Later, the GPS points were overlaid over the high-resolution SPOT satellite imagery, and the entire gully lengths were digitized manually. The full length of individual gullies is certainly not seen on the resulting map because gullies were digitized only along lengths that could be ascertained with a high level of certainty based on field records. Furthermore, an additional 21 gullies were digitized throughout the study area based on characteristic features seen in the imagery that were in common with the ground-truthed gullies; the transects also served to eliminate the possibility that these were natural streams.

In addition, the cross-sectional dimensions of 18 of these gullies were measured at the georeferenced points. Unfortunately, the high frequency of gullies in the landscape made it impossible to measure all gullies. Gully dimensions were measured at locations where the cross-section was at its widest in the vicinity. The gully edge was defined as the point along the cross-section where the land became unstable and un-vegetated (bare soil), or in the case when vegetation was present, the point where the slope dramatically increased. Depth was measured from the more vertical side; measurements were compensated when a slant in the measuring tape was inevitable. These measurements were used to establish an average gully size which was needed to calculate the cost of gully rehabilitation.

2.3 Focus group discussions and participatory mapping

Catchment-wide land management interventions are often implemented within hydrologically-sensible boundaries, which are often trans-boundary. This study targeted a sub-catchment that included parts of two kebeles, as mentioned previously. As such, it was necessary to collect participatory input from members of both the Gudo Beret and Adisge kebeles; nine and four community leaders, resp., represented their kebeles during focus group discussions.

The first meetings with both groups attempted to address community concerns and needs related to the sustainability of local livelihoods. Local leaders were assembled for focus group discussions that concluded with a prioritization of community concerns and needs.

Over the course of three meetings, community representatives – sub-kebele leaders, development assistants (DAs), and kebele chairs from both Adisge and Gudo Beret – assembled to discuss sustainable

land management (SLM). These meetings took the form of focus group discussions as described by Morgan (1996) in which local leaders were asked to focus on their SLM-related concerns that had previously been voiced during the prioritization activities (section 2.3.1) and to discuss land degradation pressures, outcomes, and acceptable mitigation approaches. The topics discussed helped to clarify local perceptions regarding the following questions:

1. What are the pressures and perceived causes that contribute to land degradation (defined as land that has a declining ability to support life)?
2. How has land degradation affected local people?
3. What are interventions and approaches that are found to be locally acceptable?

The three meetings previously mentioned were additionally used to engage local representatives in an interactive participatory mapping exercise. The purpose of the activity was to gain two pieces of information relevant to the modelling that would later be undertaken. These two questions were the foci of the exercise:

1. Where in the landscape have conservation activities already been undertaken through mass mobilization watershed management campaigns (a yearly event in the area)?

2. Where in the landscape are conservation initiatives seen as most critical?

Community resource or degradation mapping is traditionally performed on paper. However, due to the need for geo-referenced data and the availability of 0.5-meter SPOT imagery, an alternative approach was attempted. During the first session, the hi-resolution imagery was projected on a white screen and participants were given an hour-long training to help familiarize them with a bird's eye perspective of their landscape. Key landmarks and features – churches, schools, rivers, and roads – helped to familiarize participants with the technology.

Once participants were accustomed to the use of the imagery, the above questions became the focus. Participants agreed as to where former conservation interventions had been done. The facilitator would subsequently zoom in to the area and a participant would then demarcate the area of interest by tracing it on the screen (Figure 4). The facilitator would simultaneously digitize the traced area on the computer using QGIS.

The second question was tackled similarly. This time, representatives of the various sub-kebeles identified and traced the degradation hotspots within their jurisdiction that are seen as most threatening or requiring the most urgent intervention.

In the second and third sessions, participants who had used the satellite imagery in the first session were asked beforehand whether they preferred to carry out the mapping exercise using the traditional method (on paper) or using the projected imagery. Interestingly, participants preferred to use the imagery which was found to be novel and appealing.

Figure 4: Interactive mapping using high-resolution imagery projected on a screen

2.4 Land cover and land use classification

The modeling that would occur later in the project required that the study area be classified into distinct land use/land cover (LULC) classes. This is necessary because various biophysical parameters (e.g., C-factor and soil retention capacity) that must be mapped throughout the landscape can best be allocated to land units (such as pixels in GIS) if those units are grouped into a concise set of LULC typologies.

The following LULC classes were chosen after transect walks were undertaken that allowed for the identification of 15 preliminary classes: hi-biomass pasture, low-biomass pasture, sparse shrubland, dense shrubland, sparse woodland, dense woodland, clear-cut areas, newly-established woodland, native "guassa" grassland, barren land (including severely eroded land), buildings, paved roads, stony rainfed cropland, non-stony rainfed cropland, and irrigated cropland.

The land use classification procedure used was a remote sensing (RS) approach that relies on a user-supplied "training" of the classification algorithm and is known a supervised classification (as opposed to an unsupervised classification which might be used when the user cannot provide LU information with confidence to the algorithm). In both cases, classification is a two-step procedure. First, the spectral signatures of the data are analyzed for similarities; in a supervised classification, these are the spectral signatures of a user-defined "training set." A more homogenous spectral signature generally allows for a more accurate result. Secondly, pixels are allocated to the various classes (Neteler & Mitasova 2008).

GRASS GIS, an open-source RS tool, was used to perform the LULC classification. Two types of supervised classification methods exist in GRASS: maximum likelihood and *sequential maximum a posteriori* (SMAP) estimation. In the former, the spectral signatures calculated for each of the classes in the user-defined "training set" are used to classify each individual pixel. The latter method incorporates a geometric aspect into the algorithm by recognizing that nearby pixels are likely to be of the same class (Neteler & Mitasova 2008). The algorithm segments an image at different resolutions, and assigns the same LULC class to regions (or pixels) that have similar Gaussian distributions. To prevent overly-large regions of the same class from resulting, the algorithm reduces its smoothing behavior when

abrupt changes in spectral signatures are detected in neighboring pixels or regions (GRASS Development Team 2015).

A common challenge to algorithm-based classifications is the occurrence of multiple objects (or LULC classes) within the same pixel; this results in LULC class assignments of low confidence (Neteler & Mitasova 2008). Since the classification was based on very high resolution (0.5 meter) SPOT imagery, the likelihood of mixed pixels was minimized.

A supervised SMAP estimation was accomplished by the following steps. First, training areas were digitized in QGIS for each LULC class. These were small (<300 pixels, or 75m^2) polygons demarcating regions of nearly homogenous pixels. The imagery was then imported into GRASS and the four bands were grouped. The region to classify and a cell size of 1-m were defined. Next, the training set was converted to raster format and imported into GRASS. Training signatures were then produced via the *i.gensigset* command. Finally, the *i.smap* command produced an initial LULC map.

The above procedure had to be performed five times because of the size of the imagery that needed to be classified (of which the study area is a small part) as well as to prevent certain LULC classes from appearing where it is known they don't exist. For example, the far eastern part of the watershed was classified as a single unit with a training set that did not include any type of woodland since this area was void of woodlands. In a similar way, irrigated areas were digitized and classified as a single unit using a training set that included only the LULC classes that occur within.

Finally, the various partitions that had been classified separately (using the same training set minus those representing the classes that did not occur therein) were mosaicked (using SAGA GIS). A "sieve" was performed to remove small clusters of polygons under 4 pixels (4 m^2) in size. A final step in the post-processing was to adjust the original 15 classes such that they represent more practically-relevant classes (rather than simply homogenous-looking areas). In this regard, the sparse woodland, clear-cut areas, and newly-established woodland were reclassified into a single class since the latter two represent eucalyptus that had either been coppiced or planted in early 2013 (since the imagery is dated May 2013) and were likely to be equivalent to a young, sparse plantation woodland by present day. It should be noted that eucalyptus (and *C. lusitanica* though it is far less common in the area) is fast-growing and provides a little soil cover due to its canopy type. Paved roads and buildings were combined under a new category "Built-up" since they can be described by the same biophysical parameters. Stony rainfed cropland and non-stony cropland were reclassified simply as "rainfed cropland" because they were observed to have not performed well as separate classes. Similarly, sparse and dense shrublands were combined due to poor performance. The final LULC map thus contained just ten classes.

The accuracy of the resulting LULC map was assessed using a database of 110 ground-truthed GPS points that had been collected in March 2015 during a soil survey exercise. GRASS's "kappa accuracy assessment" (*r.kappa*) was used to compare the LULC map to these data points, which had been assigned to one of the 10 final LULC classes. In this circumstance, a kappa score is more revealing of the accuracy because, unlike a an accuracy score (percent correct), the kappa score takes into account the fact that some "correct" classifications could have been due to random chance (Landis & Koch 1977). The kappa score compares the observed accuracy to an "expected accuracy" which represents the accuracy when classification is by random chance. The GRASS function compares two overlaid maps and produces an error matrix, a kappa score, percent commission error, percent omission error, and the overall percentage of correctly classified pixels.

2.5 Digital elevation model

Three choices of DEM sources were available for the study area:

1. Advanced Spaceborne Thermal Emission and Reflection Radiometer (ASTER) Global DEM of 1 arc-second resolution; Version 2 released October 2011
2. Shuttle Radar Topography Mission (SRTM) Global DEM of 1 arc-second resolution; released September 2015 for Africa; Version 3 released September 2014
3. Topographic map-derived DEM of 1/3 arc-second resolution

The ASTER and SRTM are available as open source products while the latter was created from a manual digitization of a 1:50,000 scale topography map published in 1986 by the Ethiopia Mapping Agency. After the map was scanned, contour lines (at 20 m intervals) and 24 spot heights were digitized manually. Streams were rather digitized from the satellite imagery (and using ground knowledge to distinguish between streams and gullies) since there were significant discrepancies with the topography map. Next, the *Topo to Raster* tool in ArcGIS was used to create the DEM. Incorporation of the streams in the algorithm produced poor results (nearly 100 m difference as compared to ASTER and SRTM DEMs), so the final 10-m resolution topograph-derived DEM (henceforth referred to as TOPO) was derived from spot heights and contour lines only.

The series of transect walks performed in January 2015 had yielded 152 GPS points that fell within an area that encompassed the study area. The GPS device used, a Garmin eTrex 20, had approximately a 2-meter horizontal accuracy. The manufacturer does not publish a vertical accuracy for the device, but some experts claim that the vertical accuracy of a handheld GPS device is generally about 50% worse than the horizontal accuracy. This is the case because the satellites in space needed for trilateration are in a horizontal plane and not a vertical plane, the latter of which is not possible since GPS signals cannot be sent from below the horizon. By making the assumption that the vertical accuracy was about 50% worse than the horizontal accuracy – so about 3 meters - this dataset of elevation points was seen as far more accurate than any DEM source and suitable for comparing the accuracy of the different DEM sources.

To prepare the three DEM sources for comparison, the sinks in each raster were filled and the TOPO was resampled via the *regularized spline and tension* function in GRASS to 1 arc-second resolution so as to provide for a standard comparison across the three sources, which was the procedure of Datta & Schack-Kirchner (2010). Finally, elevations were extracted from each DEM source and a comparison was made based on the root mean square error of each DEM source relative to the GPS data.

Comparison of the three DEM sources revealed an underreporting of the elevation in all cases, seen by the negative means of the differences between measured elevations and DEM data (Table 2). The SRTM was found to be the superior elevation model because it had the lowest spread, root mean square error (RMSE), and standard deviation. Thus, the SRTM DEM was chosen for the catchment delineation and for the extraction of topographic conditions in the subsequent RUSLE and RIOS modelling.

Table 2: RMSE and univariate statistics showing DEM errors by subtracting field measured elevations from the DEM elevation values.

DEM source	RMSE	Error			
		Min	Max	Mean	St. dev.
TOPO	14.3	-33.6	44.8	-6.3	12.8
ASTER	11.8	-77.1	34.4	-1.2	11.8
SRTM	7.1	-25.4	26.9	-1.3	7.0

2.6 Catchment delineation

The study area was the sub-catchment containing the Gudo Beret village. In order to be able to link future water yield predictions with changes in irrigation capacity, a point in the stream near the large valley irrigation area was chosen as an outlet point. The sub-catchment was delineated based on this outlet point. TauDEM (version 5) hydrological analysis algorithms were used for the delineation procedure, and followed the method described by Tarboton (2011).

First, the *pit remove* function was used to fill any sinks in the DEM; the function simply raises the elevation of depressions such that they equal the elevation of the pixels along their rim. This is necessary to improve the accuracy of hydrological calculations which would otherwise channel water to these sinks which are often just a result of coarse data. Next, the *D8 flow directions* produced both a slope raster and a raster indicating the steepest downward slope from a pixel to one of its neighbors. Next, *D8 contributing area* function is used to count the number of pixels draining through each pixel. The output raster was used as the preliminary input for the *stream definition by threshold* function. An arbitrary initial stream definition threshold value – the minimum contributing area a pixel must have to be considered part of a stream channel - was given since the output is only used to correct the location of the outlet. The *move outlets to stream* function makes the correction, shifting the outlet a few pixels to coincide with a stream channel. Next, the *D8 contributing area* function was rerun, but this time with the new outlet shapefile so that only the areas upstream of the outlet will be calculated. The *stream definition by threshold* function was then used to correctly identify stream channels. A threshold value of 550 was identified as appropriate because it most accurately predicted stream channel locations while excluding gullies that had been ground-truthed. The "stream network" and the new "contributing area" rasters, as well as the new outlet shapefile, were the inputs for the final function, *stream reach and watershed*. The output is a raster which was polygonised in order to function as a delineation of the study area.

2.7 Modelling of soil losses using the RUSLE

The Revised Universal Soil Loss Equation (RUSLE), an empirical model, describes the spatial heterogeneity of potential soil loss (Wischmeier & Smith 1958, 1978; Renard et al. 1991). The RUSLE and its predecessor, the USLE, are the most commonly used erosion risk models in Ethiopia (Nigussie et al. 2014). As such, it was selected in order to predict the impact of applying the SWC activities as RIOS had allocated them. The RUSLE (Renard et al. 1997) is calculated for pixel i by:

$$A_i = R_i K_i LS_i C_i P_i \qquad \text{Equation 1}$$

Where, A is the average soil loss in t $ha^{-1}yr^{-1}$, R is the rainfall erosivity factor in MJ mm $ha^{-1}h^{-1}yr^{-1}$, K is the soil erodibility factor in t ha h $ha^{-1}MJ^{-1}mm^{-1}$, LS is the dimensionless slope-length gradient factor, C is the dimensionless cover factor, and P is the dimensionless support practice factor.

The RUSLE was performed within a program called InVEST (Integrated Valuation of Ecosystem Services and Tradeoffs; Sharp et al. 2015) since this program requires the same biophysical parameter data setup as RIOS. InVEST adjusts the RUSLE calculation for the sediment delivery ratio (SDR), the percentage of lost soil that actually reaches the stream. For each cell, the program calculates the soil lost and then the soil that is lost but is thereafter captured by vegetative or topographic features prior to reaching a stream channel. Both values are reported for each cell. In addition to the raster data required for the RUSLE, the SDR adjustment (Vigniak et al. 2012) requires three additional calibration values and is calculated at pixel i by:

$$SDR_i = SDR_{max} * \{1 + \exp((IC_{0,i} - IC_i)/(k_{b,i}))\}^{-1} \quad \text{Equation 2}$$

Where, IC is the hydrological flux connectivity, k_b and IC_0 are parameters that describe the sigmoid relationship between hydrologic connectivity and SDR, and SDR_{max} is used to cap the SDR at a maximum level. IC_0, which is suspected by Vigniak et al. (2012) to be landscape-independent, was kept at its default value of 0.5, as other authors have done (Jamshidi et al. 2013). k_b was left at its default of 2 since Vigniak et al. (2012) recommend it only be changed to calibrate using sediment yield information. SDR_{max} has been defined as the proportion of the soil particle distribution finer than coarse sand, for which insufficient information was known; however, SDR_{max} was changed from a default of 0.8 to 0.9 due to a recommendation by Vigiak et al. (2012) that applies when vertisols are present. Although the option was available to add a "drainages layer" to improve flow routing, for example, by incorporating gullies which are artificially connected to streams, these were not used since the model treats those drainage lines as final destinations for exported sediment and would therefore not allow us to see the soil loss contribution of those pixels. However, one should be aware that without this information, the model will under-predict exported sediment (sediment reaching channels, and thus becoming non-recoverable).

Since the Revised Universal Soil Loss Equation (RUSLE) was used to analyze the erosion component of the conservation planning exercise, it was important to acquire the best-possible input data. The LULC classification and the Digital Elevation Model (DEM) are the most important inputs; the former influences both the cover (C-) and practice (P-) factors while the latter influences the slope length gradient (LS-) factor.

2.7.1 Slope length gradient factor (LS factor)

InVEST calculates the LS factor automatically, requiring only the DEM as input data. While convenient, this means that adjustments to the LS factor cannot easily be made. For example, since terracing effectually increases the slope length (by increasing the surface area of the hillside), SWAT (Neitsch et al. 2005) - a popular model for erosion and runoff modelling - adjusts the LS factor on terraced locations. Without this adjustment, a margin of error is added to the soil loss prediction for terraced sites.

Desmet & Govers (1996) LS factor equation is used in InVEST's calculation of the RUSLE. It differs from the original USLE by viewing the landscape two-dimensionally which became increasingly feasible with the advent of computer-based GIS. Slope length (i.e. distance to the divide) is thus replaced with

unit contributing area (i.e. upslope drainage area per unit contour length) – a far better predictor for soil loss since it allows for the convergence or divergence of flows which are commonplace on topographically complex terrains such as Gudo Beret (Desmet & Govers 1996). The LS factor at pixel i is calculated according to:

$$LS_i = \{S_i (A_{i\text{-}in} + D^2)^{m+1} - A_{i\text{-}in}^{m+1}\} \cdot \{D^{m+2} \cdot x_i^m \cdot (22.13)^m\}^{-1} \quad \text{Equation 3}$$

Where, S_i is the slope factor for pixel i calculated as,

$S = 10.8 \cdot \sin(\theta) + 0.03$ for θ (in radians) < 9%, or
$S = 16.8 \cdot \sin(\theta) - 0.50$ for θ >= 9%,

$A_{i\text{-}in}$ is the contributing area in square meters for pixel i calculated using the d-infinity flow direction method, D is the raster pixel's dimension in meters, x_i is the sum of the absolute values of $\sin\alpha_i$ and $\cos\alpha_i$ when a_i is the aspect direction for pixel i, and m is the length exponent factor from the original USLE equation from Wischmeier & Smith (1978).

2.7.2 Rainfall erosivity (R-factor)

Rainfall erosivity (R-factor) is an index value that describes both the intensity and duration of a rain event (Wischmeier & Smith 1978). The parameter is not easily measured, so most erosion studies in Ethiopia have turned to Hurni's (1985) empirical results which give a regression equation that require only mean annual precipitation. However, in 2007 a student of Hurni re-calibrated the original equation using meteorological data from seven meteorological stations in Ethiopia (Kaltenrieder 2007). The new equation is taken as superior since it is adjusted to measurements across the country and is used in recent publications (i.e., Tamene & Le 2015). It is:

$$R = 0.36 \cdot MAP + 47.60 \quad \text{Equation 4}$$

Where, MAP is the mean annual precipitation and R is in units of MJ mm $ha^{-1}h^{-1}yr^{-1}$.

For the R-factor calculation, 30 arc-second (about 0.93 km) resolution data averaged the 1950-2000 timespan was acquired from WorldClim.org (Hijmans et al. 2005). Despite some distinct differences with the measured 2015 rainfall data (Figure 2), the 50-year average data was deemed more suitable for the RUSLE and RIOS modelling.

2.7.3 Soil erodibility (K-factor)

Soil erodibility, an indexed value indicating the potential for soil particles to detach from a unit area of soil surface, was need for the erosion components of the modelling exercises. The chosen method was a set of equations developed by Auerswald et al. (2014, 2015) that improves on the original K-factor nomograph developed by Wischmeier et al. (1971) and the nomograph restrictions later published in Wischmeier & Smith (1978). Auerswald et al.'s set of equations accounts for these restrictions which occur for soils with a high silt content, soils with low erodibility, soils with a high organic matter (SOM) content, and soils covered in rock fragments. Soils high in SOM and with large stone cover particularly applied to parts of the study area.

Raw data for the K-factor was acquired from AfSIS source. A collaboration between AfSIS (African Soil Information Service) and several partners (ISRIC, CIAT, ICRAF, and the Earth Institute) has produced

open source predictions for a number of soil characteristics for the African continent at 250-m resolution (Hengl et al. 2015). Specifically, 250-m resolution rasters for bulk density, soil organic carbon (SOC), FAO drainage classes, clay percent, silt percent, and sand percent. Data for each of these was acquired for three standard depths, aside from drainage classes which accounted for an entire soil profile. K-factor is commonly calculated for the upper 20-cm soil layer (e.g., Tamene & Le 2015), but since the AfSIS standard depths did not include a cut-off at 20-cm, it was decided to take weighted averages (identical to Equation 5) for each of the aforementioned parameters for the 0-30 cm range. The Auerswald et al. (2014, 2015) K-factor method consists of four steps of calculations. However, a lack of data for the percent stone cover on the soil surface prevented the adjustment provided by the fourth equation from being used although it is recognized that stone mulches could cause up to a 10% reduction in erodibility (Wischmeier et al. 1971). For this reason, three steps (Equation 5) were used for the calculation:

1. $K_1 = 2.77 * 10^{-5} * (f_{Si + vfSa} * (100 - f_{Cl}))^{1.14}$ for $f_{Si + vfSa} < 70\%$
   $K_1 = 1.75 * 10^{-5} * (f_{Si + vfSa} * (100 - f_{Cl}))^{1.14} + 0.0024 * f_{Si + vfSa} + 0.16$ for $f_{Si + vfSa} > 70\%$
2. $K_2 = (12 - f_{OM})/10$ for $f_{OM} < 4\%$
   $K_2 = 0.8$ for $f_{OM} > 4\%$
3. $K_3 = K_1 * K_2 + 0.043 * (A-2) + 0.033 * (P-3)$ for $K_1 * K_2 > 0.2$
   $K_3 = 0.091 - 0.34 * K_1 * K_2 + 1.79 * (K_1 * K_2)^2 + 0.24 * K_1 * K_2 * A + 0.033 * (P-3)$ for $K_1 * K_2 < 0.2$

Equation 5

Where, f_{Si} is the percentage of silt, $f_{Si + vfSa}$ is the combined percentage of silt and very fine sand, f_{Cl} is the percentage of clay, f_{OM} is the percentage of soil organic matter, P is the permeability index, and A is the structure code.

Since data for "very fine sand" was not explicitly available, it was estimated as 20% of the total sand fraction - a work-around used by Panagos et al. (2014) that is applicable when the cutoff for sand follows the USDA (US Dept. of Agriculture) standard (50-2000 μm). The conversion of SOC to SOM followed the Wischmeier et al. (1971) recommendation that SOM be calculated as approximately 1.72 times that of SOC. Permeability index corresponds to the FAO drainage class data; seven levels of drainage are given, from "excessively drained" to "very poorly drained" (FAO 1990). Structure code was determined from the calculated packing density, a method suggested by King & Jones (1995), who warns that land use also impacts structure. Packing density (PD) is found by:

$$PD = \rho_b + f_{Cl}$$ Equation 6

where, ρ_b is bulk density in g/cm^3 and f_{Cl} is the percentage of clay in the top 30 cm. Structure classes were then assigned based on the pedotransfer rule shown in Table 3.

Table 3: Packing density – structure code associations (King & Jones 1995)

Packing density (g/cm^3)	Packing density class	Structure class	Structure code
< 1.4	Low	Good	1
1.4 – 1.75	Medium	Normal	2
> 1.75	High	Poor	3

The authors state that most soils must be assumed to have a "normal" structure class. A "poor" class would be assigned to a soil exhibiting a massive or large ped structure while a "good" class would be found on highly developed soils with small peds.

2.7.4 Cover management factor (C-factor)

The RUSLE utilizes the C-factor, or plant-cover factor to distinguish between differences in plant cover characteristics. The C-factor represents the localized degree of plant cover, production level, and vegetation management and can range from 1 on bare soil to 1/1000 under forest (Roose 1996). The models use C-factor as an index of the sediment that is exported from a particular pixel which has a defined LULC class. It has been estimated by a large number of studies involving various land uses in various locations. These studies have determined C-factor values by approximating the soil loss that occurs under a specific vegetation regime in relation to that which would occur should the soil be tilled and bare. No less than eight Ethiopia-specific references were consulted before selecting values thought to be appropriate to the vegetative conditions found in Gudo Beret (BCEOM 1998; Hurni 1985; Vogl et al. 2013; Kaltenrieder 2007; Morgan 2005; Eweg & van Lammeren 1996; Neitsch et al. 2005; Shiferaw & Holden 1999). C-values for forests in Gudo Beret were selected with regard to their characterization as monoculture (mostly eucalyptus) plantations. C-factor values for cultivated areas were related to literature values for the three dominant crops found in Gudo Beret, wheat, barley and faba bean.

2.7.5 Practice factor (P-factor)

The RUSLE equation uses the P-factor, or "practice" factor, to take erosion control measures into account (Renard et al. 1991). Values can range from 1/10 for tied ridging on a gentle slope to 1 for bare soil tilled up-and-down the slope (Roose 1996). Since erosion control is generally only found among cultivated lands, P-factors of 1 were assigned to non-cultivated LULC classes. An Ethiopian-specific journal article was the source for the other values (Haregeweyn et al. 2013).

2.7.6 Sediment retention

Since InVEST performs the RUSLE calculation alongside a Sediment Delivery Ratio (SDR) calculation, sediment retention information is needed. Sediment retention efficiency represents the ability of a LULC class to cause the deposition of suspended sediments contained in overland flow. In the literature, sediment retention efficiency has been extensively studied for vegetative filter strips and riparian buffers, kinds of conservation measures used to enhance the deposition of suspended sediments downslope of their origin. However, little information could be found to differentiate sediment retention efficiencies between different LULC classes, and no information could be found for the Ethiopia condition. Thus, default values for different LULC classes were used.

2.7.7 Pre-processing of raster input data

All raster data was re-projected in QGIS to a common datum and projection; the World Geodetic System of 1984 (WGS 84) and the Universal Transverse Mercator projected coordinate system (for the 37 North zone) were chosen, respectively.

Furthermore, in order to facilitate accurate raster calculations before and during modelling, the data needed to match in both resolution (cell size) and alignment. A common resolution of 10-m was chosen since the RUSLE model relied most heavily on the LULC classification (originally 2-m) and the DEM (originally 30-m). Although the weather and soil data were significantly coarser datasets (Table 4), this

resolution was justified by the argument that the LULC and DEM data account for two-thirds of the RUSLE inputs. Note that the rainfall, AET, and soil depth data were used only for the spatial optimization in RIOS but not in the RUSLE.

To resample coarse resolution rasters to finer resolutions, the bicubic (also known as cubic convolution) method in GRASS's *r.resamp.interp* function was used. This method creates a smoothed interpolation while not clipping local peaks and valleys (GRASS 2015). In contrast, *nearest neighbor* interpolation does not smooth and *bilinear* interpolation tends to clip the extremes.

The only data requiring fine-to-coarse resampling was the LULC classification. The GRASS function *r.resamp.stats* was used because it allowed for an aggregation of cells based on the "mode" value of those cells. It was important to use the mode in this case since the LULC map consists of integer values, of which the most frequently occurring value (in a 10 by 10 meter area) is most likely to be the value for the dominant land use.

Table 4: Resampling of raster data

Raster data	Models	Approx. original resolution (m)	Resampling method
DEM[1]	Both	30.5	Bicubic interpolation
Rainfall[3]	RIOS	918.7	
R-factor	Both		
AET[3]	RIOS	917.5	
K-factor	Both	250.1	
Soil depth	RIOS		
Soil texture	RIOS		
LULC classification[2]	Both	1.0	Mode aggregation

[1] For the RUSLE, the LS-factor is derived from the DEM.

[2] For the RUSLE, this map represents the resolution of the C- and P- factors as well as sediment retention information; for RIOS, this map represents these factors in addition to surface roughness and vegetation cover.

[3] Used in the RIOS pre-processor only

2.8 Inputs and settings for the RIOS simulation

RIOS required a variety of input data in addition to the inputs collected for calculating the RUSLE (Table 5).

Table 5: Input data for the RIOS simulation

Data category	Input data	Data form	Description	Unit	Origin
Topography	DEM[3]	raster	Spatial elevation data	m	SRTM
	Slope index[1]	raster	Spatial slope calculation	(index)	RIOS preprocessor
Climate	Mean annual precipitation (MAP)	raster	Spatial interpolation of rainfall data	mm/year	1950-2000 rainfall average, interpolated for Gudo Beret
	Rainfall erosivity (R-factor)[3]	raster	Potential for rainfall to cause soil particle detachment	(MJ mm)/(ha h yr)	Kaltenrieder's (2007) calibration of the Hurni (1985) equation for Ethiopia
	Actual annual evapotranspiration (AET)	raster	Atmospheric water losses, regulated by soil-vegetation regimes	mm	1950-2000 averaged, interpolated data
Soil	Soil depth	raster	Depth to a restricting layer	mm	AfSIS interpolated (Hengl et al. 2015)
	Soil erodibility (K-factor)[3]	raster	Vulnerability of a soil to soil particle detachment	(ton h)/(MJ mm)	AfSIS data and Auerswald's (2014) nomograph-derived equations
	Soil texture	raster	Classification according to textural classes	(index)	AfSIS texture data (Hengl et al. 2015)
Land cover/land use	LULC map[3]	raster	Spatial classification of local land use/cover types	(integer)	Ground data; SPOT imagery; SMAP procedure
	Cover factor (C-factor)[3]	table	Ratio of soil loss under present vegetation to soil loss from barren, tilled soil	(index)	Literature
	Sediment retention efficiency[3]	table	Potential of a LU to cause settling of suspended solids	(index)	Literature
	Manning's n	table	Surface roughness	(index)	Literature
	Cover rank	table	Fraction of a surface covered by vegetation	$s/(m^{1/3})$	Literature
	Practice factor (P-factor)[3]	table	Factor compensating for management practices	(index)	Literature
	Riparian continuity[1]	raster	Indication of the continuity of a vegetative riparian barrier along streams	(index)	RIOS pre-processor
	LULC transitions	table	Defining of new C, P factors and sediment retention values for activity-LU class combinations	-	Ground observations; expert consultation
Cross-cutting	Upslope source index[1,2]	raster	Potential for upslope areas to produce suspended sediments or runoff	(index)	RIOS pre-processor
	Downslope retention index[1,2]	raster	Potential for downslope areas to retain suspended sediments or runoff	(index)	RIOS pre-processor
Local perspectives and	SWC activities	table	Indication of which SWC activities are allowed on each LU class	-	Literature/local perspectives
	SWC activity costs and	table	Costs associated with implementing an	Person-	Literature; local information

conditions	study area budget		activity	days	
	Prohibited/preferred areas[4]	polygon shapefile	Input prevents activities where they are inappropriate, or causes activities to occur in a certain area before elsewhere.	-	Ground observations; local information

[1] These rasters are created using the RIOS pre-processor

[2] Separate rasters are produced for either the erosion or baseflow objectives

[3] Also used for the RUSLE/SDR calculation

[4] Sections 2.2 and 2.3 describe the local information included in the model

2.8.1 Raster data inputs

RIOS requires topographic, climatic, soil, and land use/land cover information, as well as two inputs that cross-cut these themes. The previous section on RUSLE inputs has already described the DEM, R-factor, and K-factor inputs, which are also used in RIOS. Mean annual precipitation (MAP), needed to derive R-factor, is an input for RIOS, but has already been described. Further inputs are described below.

2.8.1.1 Actual evapotranspiration

Although actual evapotranspiration (AET) was eliminated from the baseflow ranking procedure, it was required for the creation of the upslope source index raster created with the RIOS pre-processor (see next section). The crop coefficient (K_c) is the ratio of the actual evapotranspiration to the reference evapotranspiration (ET_0) (Allen et al. 1998). This relationship means that AET could be derived by multiplying rasters that contain K_c and ET_0 values throughout the study area. However, to match the rainfall data resolution and time span – and due to a lack of multiple-year meteorological data with which to calculate ET_0 - it was decided to use 30 arc-second data provided by Trabucco & Zomer (2010). The acquired raster data contains annual averages for the period from 1950 to 2000, and is derived from the WorldClim.org data.

2.8.1.2 Soil depth

Soil depth was necessary for the modelling procedure for two reasons. Firstly, greater depths mean there is more material available for transport downslope and thus a greater potential for erosion. Secondly, greater depths provide more storage capacity for water during rain events, increasing the potential for percolation to subsurface layers which is the source of baseflow. Raster data for "depth to bedrock" was acquired from AfSIS (Hengl et al. 2015). The maximum possible depth is 175 cm.

2.8.1.3 Soil texture

The baseflow model in RIOS required a raster containing indexed soil texture values since texture is an indicator of pore space and greater porosity enhances infiltration, which can enhance baseflow. Data containing the percentage of clay, silt, and sand for three standard depths was acquired from the aforementioned AfSIS source. The standard depths used were 0-5 cm, 5-15 cm, and 15-30 cm – referred to as sd_1, sd_2, and sd_3, respectively. Deeper layers were not used because it is the topsoil that first receives rainwater and which is the better indicator for infiltration. For each of the texture datasets (sand, silt, and clay), a weighted average was taken over the 0-30 depth according to:

$$sd_1\,(1/6) + sd_2\,(1/3) + sd_3\,(1/2) \qquad \text{Equation 7}$$

Where sd_n refers to the sand/silt/clay percentage at one of the aforementioned standard depths, n. Next, an indexed map had to be created according to index values provided by the RIOS documentation (Table 6).

Table 6: Assignment of RIOS texture coefficient to textural classes

Common name (general texture)	**RIOS texture coefficient**	**Sand %**	**Silt %**	**Clay %**	**Textural class**
Sandy (coarse)	0.2	86-100	0-14	0-10	Sand
		70-86	0-30	0-15	Loamy sand
Loamy (moderately coarse)	0.4	50-70	0-50	0-20	Sandy loam
Loamy (medium)	0.6	23-52	28-50	7-27	Loam
		20-50	74-88	0-27	Silty loam
		0-20	88-100	0-12	Silt
Loamy (moderately fine)	0.8	20-45	15-52	27-40	Clay loam
		45-80	0-28	20-35	Sandy clay loam
		0-20	40-73	27-40	Silty clay loam
Clayey (fine)		45-65	0-20	35-55	Sandy clay
		0-20	40-60	40-60	Silty clay
		0-45	0-40	40-100	Clay
Built-up	1.0				

Source: based on the RIOS documentation

A comparison of the weighted average texture maps for the study area revealed that only two textural classes were predicted by the data: clay loams and clays. Since clay loams represent the lower end of the fine-textured soils (Table 6), it was decided to index these soils (containing less than 40% clay) with a value of 0.75 while clays were indexed at 0.8.

2.8.1.4 Rasters created with the RIOS pre-processor

RIOS required an upslope source index, a downslope retention index, a riparian continuity index and a slope index for the ranking procedure during simulation. All four indexed rasters were generated with the RIOS pre-processing extension for ArcGIS. Input rasters used to create the following indexes were first normalized to a 0-1 range.

- The upslope source index represents the magnitude of the source from the upslope area that reaches a pixel. It is calculated by first producing average on-pixel values for source, retention and slope. In the case of soil erosion, the sediment source factors are the sediment export (C-factor), erosivity, erodibility and soil depth factors; retention refers to sediment retention. In the case of baseflow, the runoff source factors are rainfall, AET, vegetative cover, soil texture, and soil depth; retention refers to the cover roughness, which is a proxy (Vogl et al. 2013, p.31, 55). After each cell is weighted individually, a weighted flow accumulation is performed for each pixel by summing the on-pixel weights with upslope source weights from any neighboring in-flowing pixels.

- The downslope retention index represents the ability of the downslope area (of a given pixel) to retain sediment (in the case of soil erosion) or runoff (in the case of baseflow). It is calculated using a weighted distance - of sediment retention or surface roughness for erosion and baseflow, resp. - along the flow path from each cell to the nearest stream (Vogl et al. 2013, p.31, 55). Flow

length is calculated until the stream by defining a threshold accumulation value. This value determines how much flow must be received by a pixel before it is considered part of a stream, and then replaces stream pixels with null values. An appropriate value was determined by trial-and-error by inputting a wide range of values and comparing the outputted flow accumulation raster to the ground-truthed stream network shapefile. A relatively high value of 4500 was found to be optimal because it minimized the number of false streams (mostly known gully channels) in the flow accumulation raster.

- The riparian continuity index represents the continuity of vegetated riparian buffers, which is important only for the erosion control objective. Values are only needed for pixels within a user-provided buffer width of the streams. Since this raster will increase the likelihood that activities are allocated within the buffer zone, a buffer width of 9 m was chosen since this is the distance from channels where riparian management is allowed. The raster is created by assigning high index values to pixels that are vegetated (and currently act as a riparian buffer) or have high sediment retention values, or neighbor pixels that have these characteristics.
- Slope index represents the potential for rainfall to become runoff as opposed to infiltrating where it falls. It is important only for the baseflow component. Higher slopes infiltrate less water and thus have lower potentials to regulate baseflow. The raster is derived by indexing a rise-to-run calculation based on the DEM.

2.8.2 Land use/land cover coefficients

Biophysical values were defined for each LULC class. RIOS required input values for C-factor, sediment retention efficiency, P-factor, cover roughness, and surface cover. The first three of these have been covered in the RUSLE inputs section, and the remaining coefficients are described below.

2.8.2.1 Cover roughness (Manning's n)

The cover roughness parameter represents the ability for a LULC class to slow the flow of erosive overland flow. A greater cover roughness renders greater frictional forces that oppose the flow of surface water, thereby decreasing flow velocities. The vegetative regimes associated with each LULC class were ranked using estimated Manning's n coefficients. Manning's n is an index of cover roughness which was developed for the calculation of fluid velocity in open channels. Due to the absence of Ethiopia-specific values, Manning's n values were chosen after a review of six publications.

2.8.2.2 Surface cover ranking

The surface cover ranking is the fraction of the soil surface that is covered by vegetation. A higher degree of surface cover lowers the likelihood that a land cover type will produce runoff. While the cover roughness (described in the previous section) can be thought of as a lateral (horizontal) resistance to flow, the surface cover can be thought of as a vertical resistance which counters the production of runoff. In an experimental setting, surface cover can be approximated from leaf area index (LAI) measurements. Ethiopia-specific surface cover values were not available, so RIOS default values were adopted and adjusted slightly for the Gudo Beret condition in some cases. The values selected for non-cultivated LULC classes do not account for seasonal changes in vegetative cover. Surface cover values were not adjusted for seasonality because precipitation data seems to indicate that the onset of erosive rain events (possibly in July) is normally preceded by two months of lower rainfall (May-June) (see Figure 2). This indicates that perennial vegetation has time to resume its "normal" wet season surface cover levels prior to the onset of erosive rains.

2.8.2.3 Predicted coefficients for post-SWC LULC transitions

For the purpose of predicting future sediment and water yields after activities have been implemented, a second module in RIOS produces a table containing "transitioned" biophysical parameters which corresponds to a post-activity "transitioned" LULC map. This map and table depict the changes in LULC classes and biophysical parameters that would occur should the SWC activities be implemented in the places they have been allocated. Of course, locations that will undergo activities will not necessarily change their LULC class. The module allows the user to assign LULC transitions in one of two ways: a LULC can transition towards an existing LULC class and thereby adopt the parameters of that class (to an extent defined by the user); or, a LULC can shift to a new user-defined LULC class with newly defined parameters.

Due to the lack of Ethiopian highland-specific information regarding the changes in biophysical characteristics of LULC types following conservation measures, the LULC transitions had to be defined through alternative means. Photos from the transect walk of areas that had been conserved in recent years (especially previously degraded areas) in addition to anecdotal information from informants familiar with the area helped to establish the succession of a particular LULC class.

This analysis led to the creation of eight new post-conservation LULC classes. A five-year transition period is assumed for each of the predicted transitions. Biophysical factor values (for C-factor, sediment retention, cover roughness, surface cover ranking, and P-factor) were established for new LULC classes via several methods:

- Use of literature-derived values for conserved LULC classes
- Averaging of values for the original LULC and a LULC to which it is becoming more similar
- Weighted averaging of values from two LULC classes based on their proportions on a unit area (e.g. weighted averaging of cropland and grassland values for cropland on which grass strips had been established)

A summary of the predicted LULC transitions used in this module as well as the biophysical coefficients assigned to them are summarized in a table in the results section.

2.8.3 Selection of soil and water conservation (SWC) activities

Different soil and water conservation activities were simulated within RIOS to show the possible impact of implementing these measures in strategic locations in order to assess the costs and benefits. During this modelling exercise, RIOS did not choose between different SWC activities for a given pixel (although, as described earlier, this can be done using activity costs and relative differences between the expected transitions an activity is expected to cause), but was only used to choose activity locations based on one of the three objective weighting scenarios.

The user defines the activities by restricting activities to certain LULC classes, preventing an activity from being allocated to certain defined areas, or by preferring them to occur in certain defined areas before they can occur elsewhere. Although not used in this simulation exercise, users can also choose to distinguish between the LULC transitions an activity can cause (which only has an effect if transitions are weighted differently for an objective or between objectives) or they can price activities differently such that pixels are allocated to activities based on a kind of proxy for return on investment.

SWC activities to be included in the model were selected systematically. First, the national guidelines were consulted. The standard manual for SWC in Ethiopia is published by the Ministry of Agriculture and Rural Development (Desta et al. 2005). The document, titled "Community Participatory Watershed Management," presents activities in sections that refer to the intended purpose: physical soil and water conservation, flood control and improved drainage, water harvesting, soil fertility management & biological soil conservation, agroforestry, and gully control. Transect walks and participatory discussions in the study area made it possible to establish a short-list of activities that could be acceptable.

The short-list of activities was narrowed through personal communication with technical assistants who had knowledge of the area and the type of SWC activities that have not been effective in the area. Activities were narrowed due to a variety of reasons: their complexity, their non-suitability to the type of cultivation being practiced in Gudo Beret (ox tillage for cereal production), their inappropriateness for large-scale community mobilization campaigns (e.g., activities that can be easily done by individual farmers).

Each activity is prescribed only for certain LULC classes. Based on recommendations and personal knowledge of the study site, a matrix was created to indicate the applicability (0/1 binary) of an activity on a certain LULC class. This LULC – activity matrix was an input for RIOS to ensure that activities were targeted to the appropriate LULCs.

The aforementioned guidebook for SWC in Ethiopia (Desta et al. 2005) further prescribes each of the various SWC activities to a precise range of slope gradients. With this information, for each LULC class, a different SWC activity was selected for each slope class. To force RIOS to only allow certain activities on certain slope classes of certain LULC classes, exclusion polygons were created. In the case of agricultural and degraded lands, this was done by polygonising the slope raster and dissolving the polygons of the slope classes for which an activity should be prevented.

Aside from rules to limit activities to certain slope classes, several other exclusions were necessary: limiting riparian and gully interventions to riparian and gully areas, preventing other interventions in gully and riparian areas, and limiting the homestead-appropriate intervention to homestead areas.

Furthermore, the participatory input regarding the "priority" areas for conservation were incorporated here; "preference" polygons were used to force the model to apply interventions here before allocating activities to other parts of the catchment. Finally, initial runs of the model made it clear that activities should be preferred on land where the individuals or the community is in charge of land management, as opposed to state-owned plantations or wild (and seldom frequented) shrubland. A list of the "exclusion" and "preference" polygons that were created are given in Table 14.

2.8.4 Costs of SWC activities

Although some recent studies have used RIOS to compare scenarios for different budget levels (e.g., Hunink & Droogers 2015), this study had no reason to compare budget scenarios since there was little uncertainty as to current and future expected annual budgets available for watershed management activities in Gudo Beret. This is because SWC activities in rural Ethiopia are carried out by farmers during annual "labor campaigns." These mandatory 30-day public work campaigns have their roots in the late 1970s when the communist "Derg" regime took power; the approach to implementation of the campaigns has been altered a number of times, gradually becoming more participatory and including

more integrated measures (vegetative in addition to structural measures) (Rahmato 2001). The mass mobilization of peasant farmers to engage in SWC work is generally accomplished with little monetary funding but is rather most limited by labor availability as opposed to funds. Although differences exist between regions and between areas within a region, the program utilizes the voluntary labor of kebele residents and often requires that participants use their own tools (e.g., hoes and pick-axes). Activities mainly utilize locally-sourced materials although external inputs (e.g. tree saplings and wire for gabion construction in gullies) may be provided through local government funds earmarked for watershed management. Although the campaigns receive a number of criticisms (see, for example Wolancho 2015) and have been little-studied for their effectiveness, they seem to be a mainstay for most of the country and are nevertheless the current approach to SWC in Gudo Beret.

Although yearly budgeting and SWC costs can be used to limit the land area converted by RIOS, use of this setting did not allow for a proper testing of RIOS's ability to address multiple ES's. This is explained in the results and the results of using this setting can be seen in the Annex. Nevertheless, costs for the various activities were needed for the analysis in order to assess labor and time requirement differences between the different scenarios. Costing was assessed on the basis of labor. Thus, local data was needed to approximate the labor availability for the study area. For this, the kebele chairman was consulted, and information regarding the number of persons that have both previously participated as well as the number that are expected to participate in the 2016 campaigns was acquired. A summary of that information can be found in the results.

Labor requirement data in terms of person-days (i.e., the labor one man could perform in a single day) were found in the standard manual for Ethiopia by Desta et al. (2015). Labor costs accounted for the time needed for physical construction (earth-moving), re-vegetation, and compensation for land owners – so much as each was required for an intervention. Maintenance costs in years subsequent to establishment were not included since interventions that occur on private lands are considered the responsibility of the land owner and because private and public lands and not easily distinguished. A table giving the costs of each activity, and the basis for each calculation can be seen in Table 13 in the results.

2.8.5 Simulation of SWC activities

The premise of RIOS is that conservation activities targeting certain objectives are most effective in the long-term when they are implemented in locations that would be most responsive. Responsiveness refers to the impact on (enhancement of) ES's The ES's of interest in this study were erosion control (EC) and baseflow (BF) enhancement.

Through an extensive review of published studies on key drivers of ES enhancement as well as hydrological model documentations, key factors have been identified which influence the magnitude of sediment or runoff sources as well as the effectiveness of different types of conservation activities. The key factors linked to erosion control and baseflow enhancement are given in Table 7 and Table 8, respectively. Responsiveness of a particular location is driven by a small set of biophysical factors. Biophysical factor coefficients are normalized so relative differences are important. After normalization, the biophysical factors are assigned weights and each pixel in the landscape is ranked. Pixels are first ranked separately for each ES objective since each objective is related to a different set of biophysical factors. Factors are either minimized or maximized based on the justifications given in the tables.

By default, RIOS assigns equal weights to the on-pixel (sediment or runoff) source, the on-pixel (sediment or runoff) retention, downslope (sediment or runoff) retention, and upslope (sediment or runoff) source factors. This weighting was maintained, although weighting of some factors was changed due to data quality differences.

Weighting was performed systematically by ranking data quality as low, medium or high. This was based on the available resolution of the data and the relative confidence in the spatial distinctions of the data. To derive the new weights, high, medium, and low quality data was assigned a weight of 30, 20, and 10, resp.. Finally, the weights were normalized.

Furthermore, two factors were deleted (assigned a weight of "0") from the ranking procedure. Soil depth - which is maximized for the EC ranking in order to favor pixels where greater amounts of soil are present (i.e. there is potential for greater soil loss) - was eliminated due to local circumstances; in Gudo Beret, nearly all arable land is used for production (be it cultivation, grazing, or plantation) so it is highly important to conserve soil on lands with only shallow soils. Secondly, actual evapotranspiration - which is minimized for the BF ranking in order to favor pixels where less vegetation is present and thus less water is removed (transpired) from the available pool contributing to groundwater recharge – was eliminated since the coarse data did not make distinctions between land cover types.

Table 7: Factors and their weights for the ranking procedure for the erosion control objective

Factor	Action[1]	Justification	Data Quality	Weight[2]
On-pixel sediment source				
C-factor (sediment export)	+	Do conservation on pixels with higher susceptibility to erosion.	High	~~0.25~~ 0.50
Rainfall erosivity	+		Low	~~0.25~~ 0.17
Soil erodibility	+		Medium	~~0.25~~ 0.33
Soil depth[4]	+	Do conservation on pixels where greater amounts of sediment are available for transport downslope in the long-term.	-	~~0.25~~ 0
On-pixel sediment retention				
Sediment retention efficiency[3]	-	Do conservation on pixels with low abilities to remove sediment from runoff. If the pixel is riparian, do conservation where formerly discontinuous stream buffers can be made continuous.	High	1.0
Off-pixel sediment effects				
Downslope retention	-	Do conservation on pixels downslope of which there is little ability to retain sediment.	High	1.0
Upslope source	+	Do conservation on pixels that are receiving higher amounts of sediment from upslope.	High	1.0

[1] "+" indicates that a higher rank will be assigned to higher factor values; "-" indicates the opposite

[2] RIOS defaults are struck-through when overridden

[3] In riparian areas (within a 9 m buffer of stream channels), the sediment retention value is the average of the riparian continuity index and the sediment retention efficiency.

[4] Soil depth found to be unsuitable for Gudo Beret where there is great value in preserving soil where it is shallow due to land scarcity.

Table 8: Factors and their weights for the ranking procedure for the baseflow objective

Factor	Action[1]	Justification	Data quality	Weight[2]
On-pixel runoff source				
Rainfall	+	Do conservation on pixels having greater potential of producing more runoff.	Low	~~0.2~~ 0.125
Soil texture	-	Do conservation on coarser texture soils that are more likely to infiltrate water and enhance groundwater recharge.	Low	~~0.2~~ 0.125
Slope index	-	Do less conservation on steep areas which have a lower potential to infiltrate water.	High	~~0.2~~ 0.375
Vegetative cover	-	Do less conservation on pixels with greater rainfall interception which generally produce less runoff.	High	~~0.2~~ 0.375
Mean AET[3]	-	Do conservation on pixels with a lower AET where there is a greater proportion of water available for baseflow enhancement.	-	~~0.2~~ 0
On-pixel runoff retention				
Surface roughness (Manning's n)	-	Do conservation on pixels where runoff is not being slowed by the surface cover. Manning's n is a proxy for retention.	High	~~0.5~~ 0.6
Soil depth	+	Do conservation on deep soils where water can be stored and slowly released to streams.	Medium	~~0.5~~ 0.4
Off-pixel runoff effects				
Downslope retention	-	Do conservation on pixels downslope of which there is a low ability to retard flow velocity.	High	1.0
Upslope source	+	Do conservation on pixels receiving the greatest quantities of runoff from upslope areas.	High	1.0

[1] "+" indicates that a higher rank will be assigned to higher factor values; "-" indicates the contrary

[2] RIOS defaults are struck-through when overridden

[3] The available AET data did not distinguish between LULC types and was disregarded

The sediment-based erosion control (EC) ranking and the runoff-based baseflow (BF) enhancement rankings were performed according to $R_{EC} = 1/4 * \{U + (1 - D) + (0.50 * SE) + (0.17 * R) + (0.33 * K) + (0.0 * SD) + (1 - SR)\}$ Equation 8 and $R_{BF} = 1/4 * \{U + (1 - D) + (0.125 * MAP) + (0.2 * (1 - AET)) + (0.375 * (1 - C)) + (0.125 * (1 - T)) + (0.375 * (1 - SI)) + (0.4 * SD) + (0.6 * (1 - N))\}$

Equation 9.

$$R_{EC} = 1/4 * \{U + (1 - D) + (0.50 * SE) + (0.17 * R) + (0.33 * K) + (0.0 * SD) + (1 - SR)\} \quad \text{Equation 8}$$

$$R_{BF} = 1/4 * \{U + (1 - D) + (0.125 * MAP) + (0.2 * (1 - AET)) + (0.375 * (1 - C)) + (0.125 * (1 - T)) + (0.375 * (1 - SI)) + (0.4 * SD) + (0.6 * (1 - N))\}$$

Equation 9

Where, U = upslope source index, D = downslope retention index, SE = sediment export (C-factor) coefficient, R = erosivity coefficient, K = erodibility coefficient, SR = sediment retention index, MAP = mean annual precipitation, AET = average annual actual evapotranspiration, C = vegetation cover index, T = soil texture index, SI = slope index, SD = soil depth, N = vegetation roughness coefficient. Note that SR is averaged with the riparian continuity index when the pixel is in a riparian area. Each

factor is weighted such that each major process – on-pixel source, on-pixel retention, upslope source, and downslope retention – has a total weight of 1. With a total factor weight of 4, the normalization for each objective was thus performed by dividing by 4.

The result of this procedure is two rankings – one for EC and one for the BF objective – at every pixel. Next, RIOS combines these two rasters using weights given by the user. These objective weights could represent the degree to which stakeholders value an objective relative to another objective. To evaluate RIOS's utility in targeting different ES objectives, it was decided to test three different scenarios. Thus, the model was used to perform the spatial optimization of SWC activities across the landscape for the following scenarios:

1. Activities are allocated to the highest-ranking EC pixels.
2. Activities are allocated to the highest-ranking EC and BF pixels, each having an equal weight.
3. Activities are allocated to highest-ranking EC and BF pixels, with EC weighted twice that of BF.

Using one of the three objective weights described above, a final objective score map is created that ranks the pixels.

Aside from allocating *where* activities should occur, RIOS can also decide *which* activities should be chosen if the user gives different activity costs. In this mode, the model creates cost-effectiveness maps for each activity by dividing the objective scores by an activity's cost to produce activity score maps for each activity. These maps represented the return-on-investment of a particular activity whereby the investments are in terms of activity costs and the return is in terms of relative rankings. This is justified by the fact that the pixel ranking procedure shows where (i.e. on which pixels) interventions have the most potential to impact the current erosion and baseflow status.

Users have the option to distinguish between activities in terms of their potential to cause one or several preset transitions (assisted revegetation, unassisted revegetation, agricultural vegetation management, ditching, pasture management, preservation of native vegetation, and fertility management). However, unless transitions are weighted differently among themselves or between objectives – not done in this modelling exercise – they do not influence the activity selection. Since transitions were disregarded, RIOS decides between two activities allowed on a given pixel simply by choosing the cheaper activity if activity costs are differentiated. RIOS is too simplistic to account for relative differences in benefits of two activities (unless costs are adjusted based on benefits).

A preliminary run of RIOS using activity costs in terms of labor costs (in person-days) found that activity selection was dominantly driven by activity costs. (See the Annex.) Activities were thus chosen based more on cost (with cheaper activities more often chosen) than "responsiveness" because often the sites that would benefit most from activities required the more expensive activities. This circumstance was highly inappropriate for Gudo Beret where SWC is performed by residents during the annual voluntary labor campaigns. Far more relevant than labor availability or costs is the need to target sites that will be most "responsive" in terms of ES provisioning.

To adapt RIOS to this circumstance, all activity costs were set as equal. Furthermore, activities were pre-determined for unique land characteristic combinations so that RIOS would not be choosing

between different activities for a given pixel. This was done firstly by limiting each activity to only the appropriate LULC classes. Secondly, where multiple activities were appropriate for a particular land use (e.g. rainfed cropland), activities were assigned to unique slope classes.

In this way, after landscape constraints were met (prevention of certain activities on certain LULC classes and in certain user-defined areas as well as incorporation of community preferences - described in the next section), RIOS was limited to selecting pixels only based on objective scores, starting with the highest ranked pixel. Activities were allocated to pixels in stages; first 200, then 400, then 600 hectares were allocated for each scenario. These stages allowed us to analyze three sets of selected pixels: those of highest priority (the first 200 pixels), those of lesser priority (the second set of 200 pixels), and those of even lesser priority (the third set of 200 pixels). Figure 5 is a schematic summarizing the way in which RIOS was adapted for this simulation exercise.

Figure 5: Schematic highlighting activity allocation procedure by RIOS

2.9 Water balance calculation

Due to the non-availability of long-term stream discharge data for the study site, the likelihood of a change in dry season baseflow as a result of SWC was investigated by performing a simplified water balance. This calculation was performed with regard to only the rainfed cropland in the catchment so as to test the effects of SWC on this LULC class (the class for which the most land area was converted by RIOS, as the results will show). The control volume for the water balance was a rectangular prism soil column unit bounded at the soil or plant (if present) surface (including any water on top of the soil) and extending down to the water table. By disregarding lateral subsurface flows, the flows into and out from the soil column can be described according to the following equation (Healy 2010).

$$P = ET_c + Q_r + \Delta S + D \qquad \text{Equation 10}$$

Where, P is the precipitation entering the control volume, ET_c is the crop evapotranspiration, Q_r is the surface runoff that exits the control volume, D is the drainage out of the bottom of the column (reaching the water table), and ΔS is the change in water storage inside the column; all units are in terms of water depth per unit time. Baseflow, the slow release of water to stream channels, can either originate from the unsaturated zone or from groundwater; the movement of water from these sources to the stream channel is called throughflow and hyporheic flow, respectively (Price 2011). For the simplified equation ($P = ET_c + Q_r + \Delta S + D$

Equation 10), baseflow is captured in both the ΔS and the D term, although it is not known the contribution of each. Such a distinction goes beyond the scope of this study and hence, $\Delta S + D$ was calculated as a proxy for "change in baseflow."

The P and ET_c terms were derived from hourly meteorological data from a weather station installed in Gudo Beret in 2014. For the water balance a daily time step was chosen and a period of exactly one year was used, starting on 1st January 2015. Crop evapotranspiration is given by (Allen et al. 1998):

$$ET_c = ET_0 \cdot k_c \quad \text{Equation 11}$$

Where, ET_0 is the reference evapotranspiration in mm/day and k_c is a dimensionless coefficient representing the transpiration of the crop. The dual crop coefficient method, which distinguishes between soil evaporation and crop transpiration, was followed according to the FAO-56 procedure (Allen et al. 1998) for optimal moisture conditions. This method accounts for daily soil moisture fluctuations at the top 10 cm of the soil. ET_0, in turn, was calculated according to the modified Hargreaves equation (Hargreaves & Samani 1985):

$$ET_0 = 0.0023\ (T_{mean} + 17.8)(T_{max} - T_{min})^{0.5}\ R_a \quad \text{Equation 12}$$

Where, T_{mean} is the mean daily temperature in ºC, T_{max} is the maximum daily temperature in ºC, T_{min} is the minimum daily temperature in ºC, and R_a is the extraterrestrial radiation in MJ m^2 day^{-1}. The following assumptions were made for the daily ET_c calculations:

- Barley was used as the sole crop due to its dominance in Gudo Beret (Kuria et al. 2014) and the appropriate kc values for each of the growth stages and the growth stage lengths were taken from Allen et al. 1998. This was a reasonable simplification because these values for the second and third important crops in Gudo Beret, faba bean and wheat, were similar.
- 9th May 2015 was chosen as the sowing date since soil moisture first passes 40% on this day after four continuous days of rainfall.
- During non-growing periods, the transpiration component for barley was assumed to be zero.
- Converted land was assumed to gain a perennial 9% shrub cover 1.5 m in height, representing perennial agroforestry. Descheemaeker's (2009) $K_{c,mid}$ value for shrub in a young exclosure in Ethiopia is used.
- Since the crop is growing during the wet season, the FAO-56 procedure for optimal (non-stressed) moisture conditions was used; the shrub was assumed to be deep-rooting and therefore non-stressed year-round.

Surface runoff (Q_r) can be estimate by the NRCS curve number method (NRCS 2004) according to:

$$Q_r = (P - \lambda S)^2\ (P - \lambda S + S)^{-1} \quad \text{Equation 13}$$

When $P > \lambda S$, where P is the daily precipitation in mm, λ is the dimensionless initial abstraction ratio, and S is maximum potential retention in mm. When $P < \lambda S$, then surface runoff is zero because λS is the initial abstraction, that amount that wets the soil and cannot runoff. S is related to the curve number (CN) by:

$$S = 25400/CN - 254 \quad \text{Equation 14}$$

Several adaptations should be noted. An initial abstraction ratio (λ) of 0.05 was used in line with recommendations by Hawkins et al. (2003) and its adoption by Descheemaeker et al. (2008) in Ethiopia. A correction for antecedent moisture conditions was not performed in accordance with the decision by the NRCS to abandon the adjustment (Hawkins et al. 2009) due to the lack of correlation between the

CN and antecedent rainfall (van Mullem et al. 2002). Because the curve number method uses CN values developed for slopes of 5%, and because slope classes have been distinguished in this study, adjusted curve numbers (CN_{adj}) were calculated for these classes according to Williams' (1995) technique:

$$CN_{adj} = \{(100 - CN)/3\} \cdot (1 - 2 \cdot \exp(-13.86 \cdot \theta) + CN \quad \text{Equation 15}$$

Where, CN is the original CN value for a 5% slope and θ is the percent slope, in this case the average slope of the slope class (classes were >58%, 35-58%, 15-35%, 8-15%, 3-8%, and 0-3%).

Choice of the curve number depends on dominant hydrological conditions and the hydrological soil group. Regarding the former, the conditions were assumed to be "poor" both before and after given the local conditions which made it uncertain that residues would remain on the field and livestock browsing would be reduced after the SWC activity. A "D" hydrological soil group was chosen since AfSIS data (Hengl et al. 2015) predicts "imperfect drainage" for the entire study area and because all cropland is clay (as opposed to clay loam). The following assumptions were made for the runoff calculations:

- Current "status quo" land was assumed to be in "straight rows," resulting in CN = 88
- Post-SWC "converted" land (land under bench terraces, stone bunds, fanya juu or soil bunds, grass strips, or vegetative fencing) was assumed to be "contoured and terraced, resulting in CN = 82
- For each day, runoff was weighted according to the relative proportions of converted and non-converted cropland after adjusting for slope.

The water balance calculation was performed for the two scenarios that weighted baseflow most differently, EC1BF1 and EC1BF0, and only for the 600 ha benchmark. The method described above, while simple, is meant to capture both the structural (contouring and terracing) and vegetative (agroforestry) components of the Q_r and ET_c terms of the water balance.

3 Results and discussions

3.1 Mapping of erosion hotspots

Of the 56 gullies identified during the transect walks, 11 fell within the study area. 21 additional gullies were added to the final map based on heuristic knowledge (Figure 6). The gully vector map was used to differentiate between gullies and streams in RIOS through the creation of prohibition shapefiles. Gullies were found both at high gradient areas as well as in low-gradient valleys.

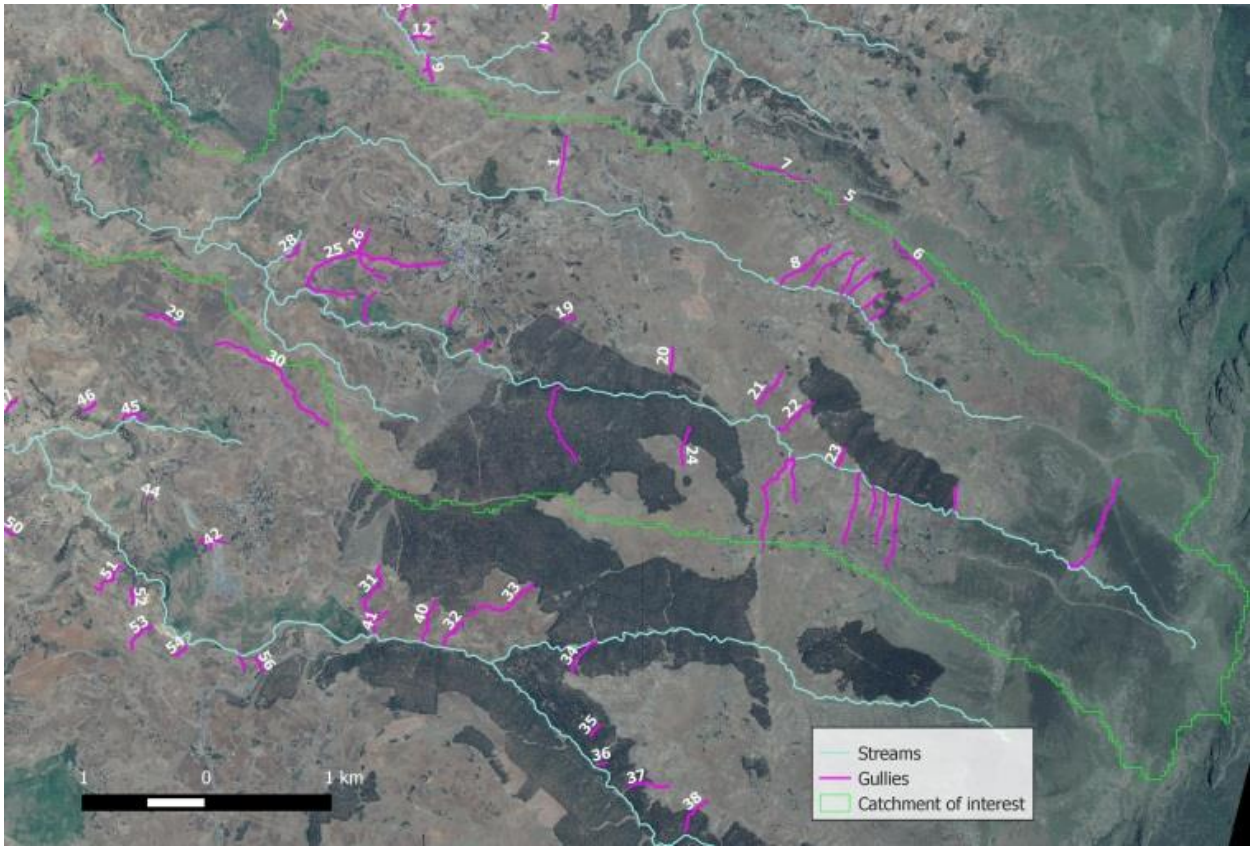

Figure 6: Compilation of ground-truthed gullies (numbered gullies) and heuristically-derived gullies in Gudo Beret

The main sources of runoff contributing to gully formation were identified. Farm drainage channels (Figures 5 and 6) constructed to cope with excess water on cultivated land was the most common source. These were normally small hoe-constructed furrow-like channels (Figure 11) that routed water downhill either off-the-contour or directly along the slope gradient. Often drainage channels from neighboring fields emptied into larger purpose-built waterways that emptied to natural waterways. Normally these manmade waterways were unreinforced and constructed directly along the slope gradient – facilitating highly energized concentrated flows – and thus, their "gullification." In other cases, farm drainage channels diverted water from fields to overgrazed pasture areas, without purpose-built waterways. The use of graded soil or soil/stone bunds on cultivated areas might be concentrating flows on soils that saturate, a phenomenon also observed by Nyssen et al. (2007). Because of the shallow soil and low potential for infiltration in the uplands, authorities often advise farmers to construct graded

(off-the-contour) bunds in these areas. Graded bunds also diverted water to unreinforced waterways which concentrated flows and turned into gullies.

Figure 7: Farm drain channel leading to gully which is fed by a number of channels from different farms above (left); Within the cultivated areas, small drain channels direct excess water downhill, either directly along the slope or off-the-contour (right).

Perhaps the second-most frequent cause of gully formation was runoff from cattle paths (Figure 8) which were sometimes eroded down to a layer of decomposed rock. These nearly always showed signs of either rill or gully erosion, and were often the origin of more typical-looking gullies downhill. A number of gullies were found to originate from state-owned eucalyptus plantations established during the Derg regime on steep lands. Although these gullies might have predated the plantation establishment, many woodland gullies still show signs that they are active and unstable. Conditions are likely exacerbated during harvest periods during which clear-cutting occurs on steep slopes. Eucalyptus woodland soils were highly degraded, with minimal understory vegetation or soil surface cover and the absence of an O-horizon. As a property of the regional government, these plantations give little benefit to residents.

Figure 8: Litter collection in state forests is a vital income source for the community (left); Cattle paths exhibited signs of gully or rill erosion, and were often stripped to the subsoil (right).

Other sources of gullies were homesteads from which flows were sometimes directed downslope with dug drains, and upland pastures with shallow, compacted soils. The latter has probably developed as a gully source over time as the soils compacted from overly intensive grazing which lowered infiltration capacity. Finally, a word must be said of currently used gully rehabilitation methods in Gudo Beret since the remains of failed check dams were frequently seen. Check dams were either made from poles and plant residues or from labor-intensive wire mesh filled with large stones. While the former had nearly always failed due to its weakness, even gabion-type check dams had often failed - probably due to their establishment at lower parts of the gully (as opposed to check dams that start from the top). Furthermore, active gullies showed evidence of rapid sideways expansion seen by the collapsing of the steep gully banks. The cutting and grading of the gully head as well as grading and vegetative stabilization of the banks, commonly recommended rehabilitation techniques (see Desta et al. 2005), were not observed.

The aforementioned observations from the transects led to several useful insights with regard to model inputs: the need for a reduction in the volume of concentrated flows through measures that promote point-source infiltration; the need to avoid allocation of SWC activities to inappropriate slope classes; the ability to predict the occurrence of severely degraded areas from the whitish-gray color of the subsoil as was commonly found along cattle paths (a technique incorporated into the LULC classification); the apparent futility of advising SWC on state-managed plantation lands in which gullies persisted due to management choices (monocropping, species choice, harvesting method) and from which residents would derive little benefit if SWC activities were done; the importance of not overlooking runoff originating from homesteads; and the need to incorporate SWC activities on pasture lands; and the need to include gully head and side grading, vegetative stabilization, and sturdy check dam construction in future gully rehabilitation attempts.

Figure 10. This natural stream has taken on gully characteristics; massive flows continue to destabilize its sides, causing landslides

3.2 Local perceptions on soil and water resource vulnerabilities and SWC activities

Community need prioritization exercises confirmed that issues related to catchment hydrology and conservation ranked high for residents of both Gudo Beret and Adisge kebeles (Table 9), the two kebeles in the study area. Gudo Beret leaders cited seasonal water scarcity, landslides, and gullies as the 2nd, 3rd, and 5th most important issues, respectively. Adisge leaders cited SWC/SLM activities as their foremost concern.

Table 9: Prioritization results from Adisge (n=4) and Gudo Beret (n=9) kebele meetings with local leaders

Ranking	Adisge kebele	Gudo Beret kebele
1	SWC/SLM-related concerns	Faba bean and field pea diseases
2	Unexploited irrigation potential	Seasonal water scarcity
3	Improved crops and crop varieties	Landslides
4	Fruit production	Wheat rust
5	Livestock-related concerns	Gullies
6	Capacity building and experience sharing	Irrigation infrastructure concerns
7		Seed quality
8		Introduction of technologies without adaptation studies
9		Climate change

Focus group discussions revealed local perceptions as to the various pressures contributing to land degradation. The following highlights are paraphrased or directly quoted from the translation from Amharic:

- *Livestock was perceived to be a major driver of degradation, with leaders admitting that their **populations exceed the number that can be sustainably supported** by the given land. It was said that trampling by animals during the dry season was "**pulverizing the soil** which could thereafter be blown away by the wind."*
- *Gullies were said to be the result of excessive amounts of runoff that could "not be safely disposed of." The immense pressure on land was said to have rendered farmers **unable to fallow parts** of their land as had previously been done. As nearly all arable land had been converted to farmland, more land than ever before was contributing to concentrated flows. **Cattle paths** and an increase in the number of homesteads utilizing **iron sheet roofs**, especially within Gudo Beret town, was thought to be responsible for the numerous gullies. Gullies can also form when **ill-maintained terraces** break. Another reason cited for the high amounts of runoff was the **large eucalyptus plantations** "which are concentrating flows." This was in contrast to the Cupressus lusitanica (or, "Tid") woodlands, which were not seen as contributing high amounts of runoff.*
- *The reduction in yields from natural springs was attributed to the planting of **water-hogging** eucalyptus trees in their vicinity as well as the **deepening of gullies** and landslides which have lowered the water table. Finally, the gargantuan river flows during the wet season was attributed to a long-term loss of soil depth and **infiltration capacity**: "When we were children, the soil was deep and rich and held a lot of water, but nowadays the river widens every year."*

The following were seen as the outcomes of land degradation:

- *Landslides have "changed the landscape," rendering land "wasted" and "**forcing people to move away**."*

- *"A lot of land has been lost to gullies." Thoroughfares have been interrupted by gullies, "forcing us and our animals to walk longer distances because many of these gullies have become* ***"too big to cross****." As gullies deepen, the water table descends,* ***impacting irrigation****. Similarly, rivers that were "very thin and easy to cross when we were children are today very wide and flows are tremendous."*
- *State-owned eucalyptus plantations established in the Derg era were formerly cultivated, so their presence adds to the pressure on land, because it means there is* ***less land to cultivate****, and because "we have* ***no control*** *over these plantations." "Government plantations have made it* ***impossible to have fallow land****."*
- *Water scarcity in the dry season means that cattle become physically weak and vulnerable. Many* ***springs have disappeared*** *from the Gudo Beret landscape, necessitating longer walks to rivers for fetching water. Because descending water tables lower flows from natural springs that supply irrigation areas, irrigation schemes experience* ***constrained production****.*

The following were identified as acceptable mitigation approaches to address land degradation:

- *Exclosures were said to be "****useful for restoring degraded pasture areas****." although it was said that this would need to occur simultaneously with some changes in livestock management. Livestock populations need to be reduced, and that this could be possible by producing higher quality animals.*
- *Participants emphasized the need for biological conservation techniques employing* ***fruit trees and "fertilizer" trees*** *around the homesteads and as parts of agroforestry systems on and around cultivated land. Trees and shrubs (Cytisus proliferus and Sesbania sesban were mentioned) could be used to stabilize terraces and bunds where they could be kept at a low height to prevent shading and used as feed for livestock. Eucalyptus was unwanted near the homestead or near cultivated land where they have been observed to cause problems. C. lusitanica was preferred to eucalyptus because it creates less runoff problems.*
- *Participants trusted expert opinions regarding appropriate conservation structures, although they preferred these technologies to be first demonstrated on experimental plots before being mandated as part of the annual labor campaigns. Technologies need to be "sold to farmers" which will facilitate uptake even outside of campaigns and incentivize follow-up necessary maintenance by farmers.*
- *Involving women in new income-generating activities, especially* ***near the homestead*** *(fruit tree and poultry production were mentioned), could help to diversify household assets and reduce pressure on forested and cultivated land.*

The above-quoted discussions helped to inform model inputs. Above all, the high prioritization of SWC-related concerns as well as seasonal water scarcity by participants meant that the RIOS model could be justified for an optimization of both erosion control and dry season baseflow. It was emphasized that the latter has implications for the irrigation potential, which is currently constrained. Additionally, the following aspects from the discussions helped to inform the model: exclosures were seen as an acceptable SWC method; biological measures should be used in parallel to physical structures since they add benefits; and activities near the homestead are desired.

A final model input derived from the focus group sessions was the result of the interactive participatory mapping exercise (Figure 9 and Table 10). Participants located and guided the demarcation of 8 areas in the kebele where SWC measures had been intensively implemented through former mass mobilization campaigns. These projects occurred between 1999 and 2013 and their areas ranged from 1 ha to just

over 200 ha. All interventions included terracing, with varying levels of biological additions ("guassa" grass or tree lucerne). In a separate session, participants mapped the places in their landscape seen as priorities for future conservation initiatives.

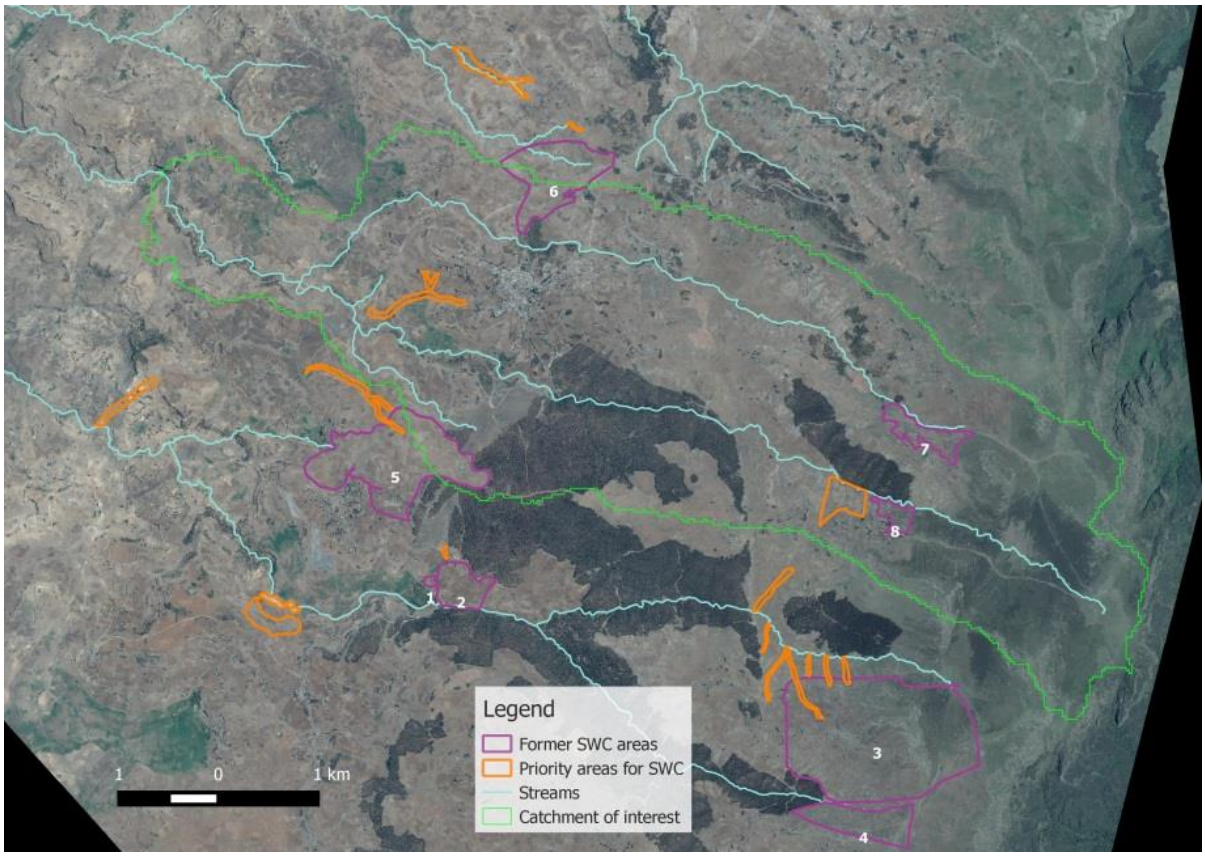

Figure 9: Locations of former conservation undertakings through annual mass mobilization campaigns (numbers correspond to Table 10) and locations seen as most critical for future conservation initiatives

Table 10: Types of SWC projects completed in recent years (IDs correspond to locations in Figure 9)

ID	Area (ha)	Year(s)	Intervention type
1	1	1999	terrace with grass
2	19	2010	terrace no grass
3	207	2010-13	terrace no grass
4	31	2011-13	terrace with grass
5	102	2010-13	terrace with grass + lucerne
6	54	2011-13	terrace with grass + lucerne
7	18	2010-11	terrace with grass ("guassa")
8	8	2011	terrace no grass

3.3 Land use/land cover classification

Based on SPOT imagery from May 2014 (pre-cropping season), a 10-class LULC map was generated (Figure 10). Descriptions of each class are described in Table 11.

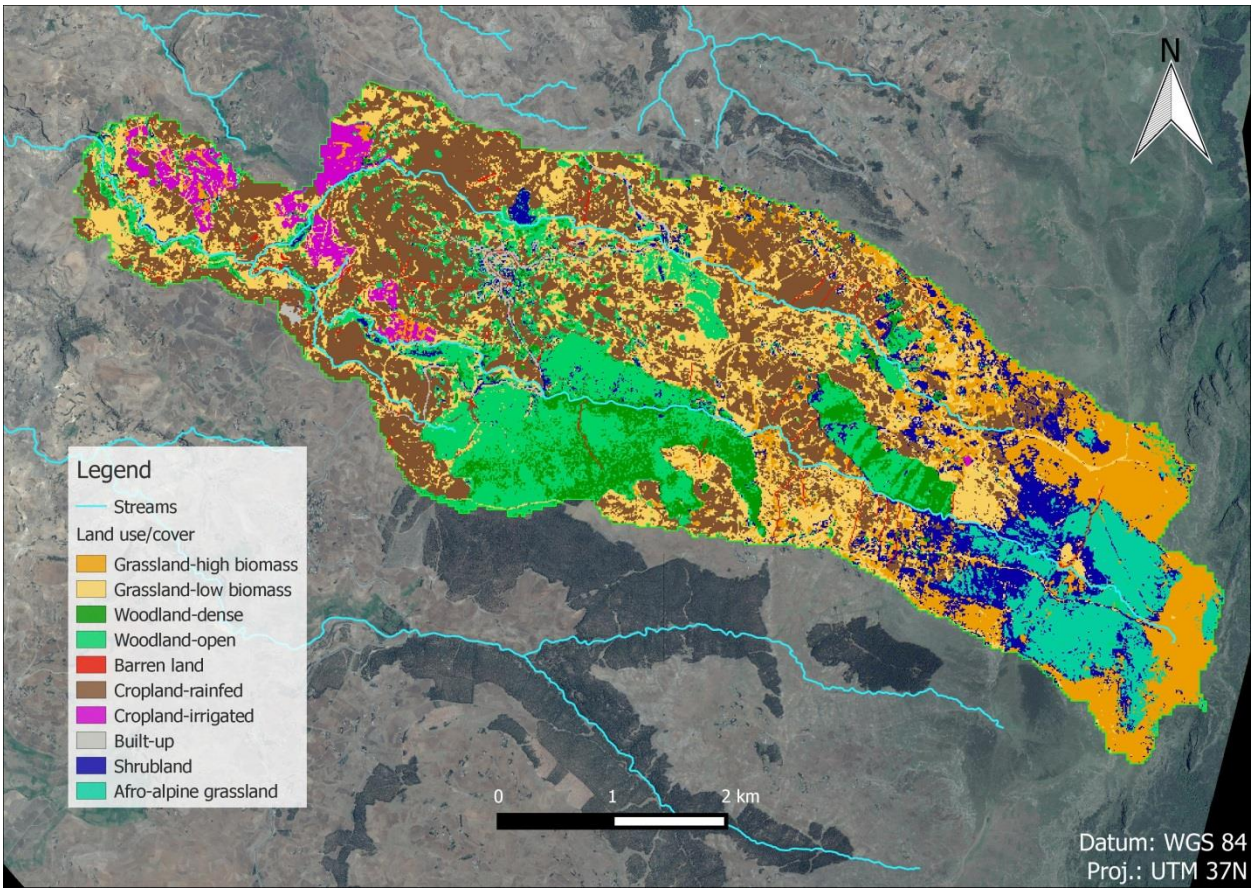

Figure 10: Results of the land cover and land use classification

Table 11: Descriptions and frequency of each LULC class

LU/LC class	No. of hectares	% of study area	Description
Grassland-high biomass	325	12.6	Pasture areas with high grass biomass, often found near springs or in places less accessible to livestock, seen as green areas.
Grassland-low biomass	534	21.0	Pasture areas with low grass biomass, often compacted and intensively grazed, seen as yellow or light brown areas
Dense woodland	137	5.4	Mature *Eucalyptus sp.* and *Cupressus sp.*, almost exclusively representing denser sections of state-owned plantations
Open woodland	358	14.2	Newly transplanted, immature, or regenerating *Eucalyptus sp.* and *Cupressus lusitanica*, mainly in state-owned plantations, but also in small privately-owned stands
Barren land	10	0.4	Unvegetated or sparsely-vegetated areas often derived from soil degradation such as rill erosion common along cattle paths and other severely eroded parts of pasture or cropland. This includes areas so severely eroded that whitish-gray decomposed rock is exposed at the soil surface (Figure 8) as well as gully sites known from the hotspot mapping.

Cropland-rainfed	735	28.9	Seen as bare soil of various shades (due to stone mulches and soil types) or lightly greened (recently sowed) areas in the pre-cropping season imagery
Cropland-irrigated	62	2.4	Seen as dark valley soils or dark green areas confined to specific scheme areas
Built-up area	26	1.0	Rooftops (iron sheets) and paved asphalt roads
Shrubland	206	8.1	Native dense and sparse shrubland, mainly occurring in the higher Afro-alpine eastern parts
Afro-alpine grassland	150	5.9	Native grassland found only on the higher Afro-alpine hilltops in the east, characterized by the dominance of a single tussock species known as "guassa"

A slope analysis of the rendered LULC class data showed that mid- (5-20%) and high- (>20%) slope classes dominated the landscape (Figure 11).

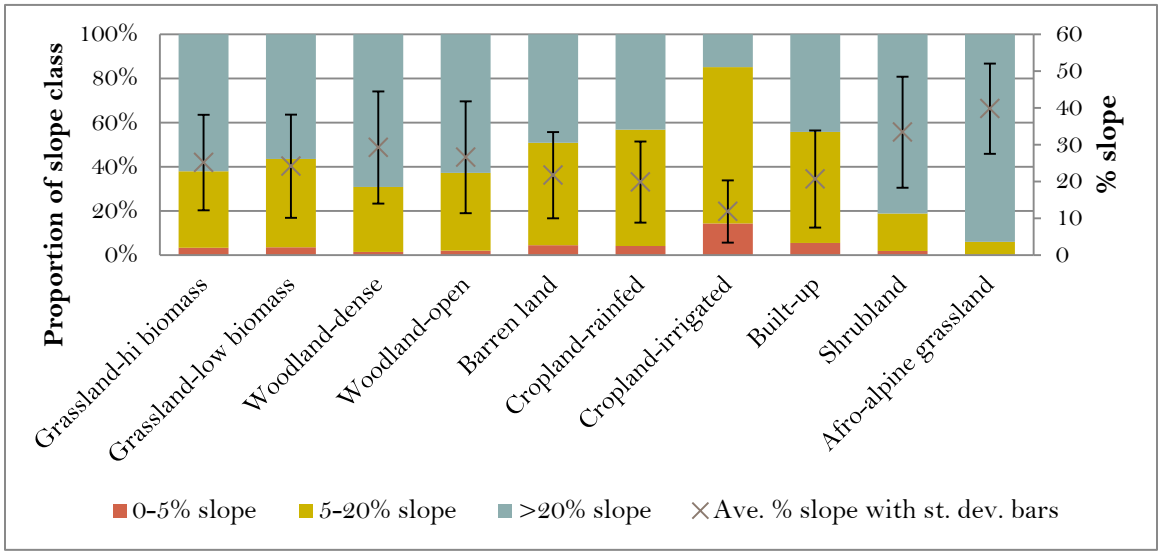

Figure 11: Slope statistics for the LULC classes

A kappa accuracy assessment revealed an overall accuracy of 82.7%, a kappa of 0.749, and a kappa variance of 0.0028. According to Landis & Koch (1977), this kappa is "substantial," (the second highest of five classes) while according to Fleiss (1981), this kappa is "fair to good," (the second highest of three classes). This accuracy was seen as sufficient for the modelling exercise. The main failure of the classification was the false identification of rainfed cropland as pasture. This can be blamed on overlap between the training signatures for the two classes. This could not be avoided for the given imagery since the time of year (May) meant that low-biomass pastures were dead (having minimal chlorophyll) and thus appeared in some cases similar to rainfed cropland dominated by bare soil.

Table 12: Accuracy assessment of the LULC map

↓ LU map	Reference LU points								Total	Error committed
	Pasture	Wood	Degraded	Cropland-rainfed	Roof	Road	Grassland	Cropland-irrigated		
Pasture[1]	17	0	0	15	0	0	0	2	34	50.0
Shrubland[2]	1	0	0	0	0	0	0	0	1	NA
Wood[1]	0	14	0	0	0	0	0	0	14	0
Degraded	0	0	4	0	0	0	0	0	4	0
Cropland-rainfed	0	0	0	47	0	0	0	0	47	0
Roof	0	0	1	0	2	0	0	0	3	33.3
Road	0	0	0	0	0	2	0	0	2	0
Grassland	0	0	0	0	0	0	1	0	1	0
Cropland-irrigated	0	0	0	0	0	0	0	4	4	0
Total	18	14	5	62	2	2	1	6	110	
Error by Omission	5.6	0.0	20.0	24.2	0.0	0.0	0.0	33.3		0.173

[1] A lack of data meant that some classes had to be combined (hi/low biomass pasture and dense/sparse wood).
[2] A lack of data meant that shrubland accuracy could not be assessed.

3.4 Local costs and annual labor

Budgeting for the correct amount of labor available for the study area utilized the following information acquired from Gudo Beret leaders. In Gudo Beret, men and women over the age of 18 must participate in an annual mass mobilization of residents for watershed management projects that occur within in a three-month period (Jan.-March), but normally takes about a total of 30 days. Work is assigned through daily quotas, which are often in terms of the length of a physical structure a participant must construct in a day. Gudo Beret informants confirmed that 4 m and 2 m lengths of stone bunds are required per man or woman, resp., per day. Since 4 m was the person-day equivalent for stone bund construction according to the Ministry's recommendations, no adjustment was made to ensure local labor conditions can be used in conjunction with Ministry-cited labor costs (as calculated in Table 13).

However, the labor budget needed to account for the less work performed by women. The labor force available for the previous two years was comprised of 409 men and 89 women. Thus, the total expected labor budget in person-days available per year was calculated as:

$$L_T = (409 \text{ men} \cdot 30 \text{ PD/man}) + (89 \text{ women} \cdot 15 \text{ PD/woman}) = 13{,}605 \text{ PD/yr} \qquad \text{Equation 16}$$

3.5 RUSLE and RIOS input data

In the next three subsections RUSLE and RIOS are presented together since there is much overlap. Raster data is presented first, followed by the selected SWC activities and restrictions regarded where they could be allocated in RIOS; thirdly, biophysical parameter coefficients are presented.

3.5.1 Geospatial input data

The final raster input data maps at 10 m resolution are shown in Figure 12.

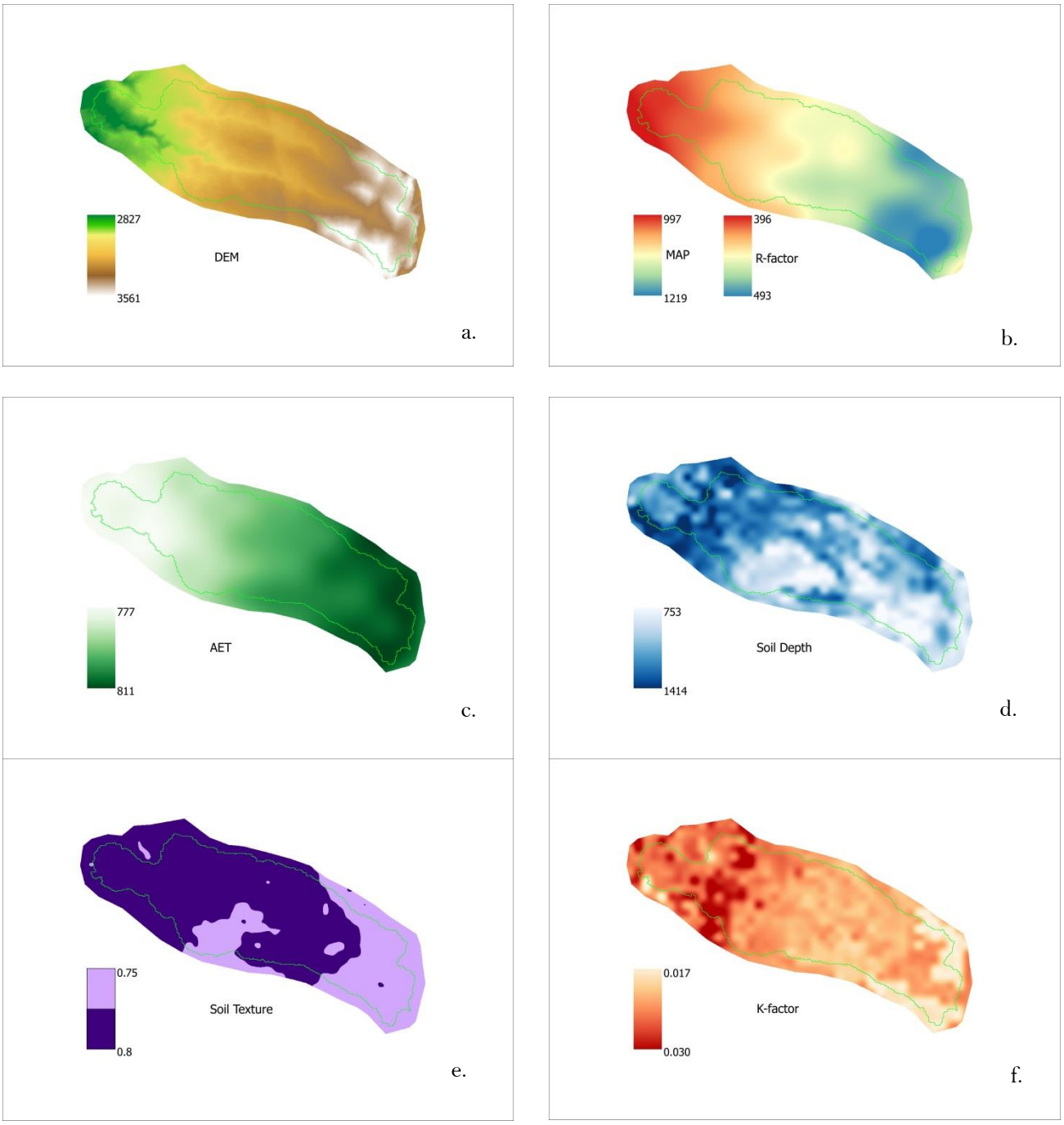

Figure 12: Raster input data: a.) SRTM DEM in meters above-sea-level; b.) Mean annual precipitation in mm and Rainfall erosivity in (MJ mm)/(ha h yr); c.) Annual actual evapotranspiration in mm; d.) Soil depth in mm; e.) Indexed soil texture for two classes (0.75 for clay loam and 0.8 for clay); f.) Soil erodibility in (t h)/(MJ mm) (Note: The catchment is delineated in green.)

The DEM reveals the dramatic elevation gradient of this headwater catchment; the elevation rises by 700 meters from the stream outlet point in the west to the hilltops in the east. Delineation of a sub-catchment with an outlet just downstream of the vast irrigation area rendered a 2576 ha area which became the study area.

The interpolated rainfall data exhibits a similar gradient to the DEM, pointing to the effect of topography on rainfall amounts which is likely in this highland setting. Precipitation is highest at the highest elevations, the peaks on the western side of the East African Rift (on the far right of the map). The range of precipitation values compared favorably with the 2015 precipitation measured at the Gudo Beret weather station, which summed to 1191 mm for the year. Because of the linear relationship used to derive rainfall erosivity, the gradient of these two maps are identical.

Again, a similar gradient is seen in the AET map. This map captures the higher density of native vegetation in the form of shrubland and afro-alpine grassland on the less inhabited hills in the eastern part of the catchment. Raster division of the AET map by the MAP map reveals that AET can be between 66% and 78% of the MAP. As discussed in the Methods section, the inability of the AET data to distinguish between LULC classes rendered it a poor indicator factor for the on-pixel runoff source calculation for the BF objective, and was thus eliminated from the calculation. It was, however, required for the RIOS pre-processor.

The soil depth data additionally revealed a west-east gradient, although less pronounced. This is expected because there is a higher density of steep slopes as one moves to the top (east) of the headwater catchment. As seen from gully banks and rill erosion in these steeper area in the east, soils here were very shallower. Despite some confidence in the relative differences in soil depth between valleys and slopes, the data under-predicts the depth of soil in the valley bottoms. Gully banks and eroded riverbanks seen during transect walks through these low areas exhibited very deep soils, much in excess of the 1.4 m maximum seen in the map.

The soil texture classification derived from clay, silt, and sand data revealed just two texture classes in the study area, clay and clay loam. Clay fractions ranged from 35 to 47% within the study area. Expanding clay Vertisols are indeed found in the valleys in the west. Unfortunately, meaningful validation of this data was not possible.

Soil erodibility values can range from 0.001 to 0.060 (t h)/(MJ mm). Calculated for all of Ethiopia, K-factor values ranged from 0.004 to 0.057 (t h)/(MJ mm). K-factor values for Gudo Beret (0.017 to 0.030) were thus low to moderate. Soils high in clay are resistant to erosion because of their tendency to aggregate. The west-east gradient seen in Fig. 10 (a) is probably due to the higher levels of SOM predicted by the soil data in the higher parts (eastern) of the catchment. The presence of SOM reduces erodibility due to the higher potential for aggregation as well as infiltration. The highest values in the catchment (found on the west side) are due to the high packing density there predicted by the soil data. This indicates a poor (massive) soil structure which would limit infiltration and thus increase the potential for detachment. Highly erodible soils – those with high silt contents which are easily detached and limit infiltration – are not found in the study area.

Three characteristics of the K-factor which have not been well-captured by the data are the widespread depletion of SOM levels, the high frequency of significant stone mulch (rock fragments) on the soil surface of cultivated lands, and the compacted nature of most pastureland. These circumstances have an

effect on soil erodibility but were not taken into account. SOM is not being replenished by decaying biomass on cropland (from which most residues are removed) or woodland plantations (from which leaf litter is collected and sold as a biofuel), meaning that the effect of SOM on aggregation is greatly reduced. Stone mulches have a surface-protecting effect that counters the soil particle detachment-causing effect of raindrop impact, and can thus lower the K-factor. Finally, high livestock densities have rendered hardpans quite commonplace on pasturelands; these hardpans now block the connectivity of the soil surface to the original deep flow paths (Tebebu et al. 2015), thereby augmenting runoff and thus, soil erodibility.

3.5.2 SWC activities and restrictions

The review of SWC activities recommended by the government and consideration of input gained from the participatory sessions led to the selection of twelve SWC options for the Gudo Beret case (Table 13). All options either partially or wholly involve a renewed establishment of vegetation, based on requests that conservation be dual-purpose and provide local benefits in addition to benefits relevant at a larger spatial scale.

SWC activities are restricted to certain slope classes based on the literature. Slopes across the study area ranged from 1.5 to 68.8%. Due to the general ineffectiveness of SWC at slopes above 58%, cropland above this threshold is recommended for conversion to woodland (see "Reforested exclosure" in Table 13). The threshold is less (35% slope) for degraded land which is assumed to be in a precarious state and in need of physical reshaping prior to revegetation efforts (see "Hillside terraces with trenches and agroforestry" in Table 13).

Each SWC activity requires one or several procedures, each of which come with a cost: reshaping of land; construction of physical structures; planting of grass, shrubs, or trees; guarding (or protection by a nearby resident who is paid); and compensation for land when the activity is done on a LU that is normally private and in which the LU will change as a consequence. The costs of SWC activities ranged from 27 to 8614 PDs.

Table 13: SWC activities, restrictions regarding their allocation, and costs

Activity	Description	LU's where allowed	Restricted to…[3]	Costs include…[4]	Cost (person-days/ha)[1,2]
Reforested exclosure	Area is closed off following assisted revegetation with tree species; occurs on cropland that is too steep for safe cultivation	Crop-rainfed	Slopes >58	Compensation for land[2], planting, guarding	276
Passive exclosure	Vegetative fencing to close off land; no assisted revegetation within fence; only allowed on LUs where vegetation exists to facilitate unassisted revegetation	Alp. grassland Shrubland Woodland-open	-	Compensation for land[2], vegetative fencing, guarding	42
		Barren land	Slopes <3		
Hillside terraces with trenches and agroforestry	Reserved for severely eroded areas at high slopes where unassisted revegetation may be hampered by land instability	Barren land	Slopes >35	Structures, planting, guarding	451
Silvopastoral hedgerows	Rows of fruit or fodder species planted on contours, calculated at 10 m inter-row distance on level land	Grassland-low biomass Grassland-hi biomass	-	Planting, guarding	40
Bench terraces with agroforestry	Terraces stabilized with fertilizer/fruit/fodder shrub or tree species	Crop-rainfed	Slopes 35 - 58	Structures, planting	756
Stone bunds with agroforestry	Ditches alongside stone bunds or stone-faced soil bunds stabilized with fertilizer/fruit/fodder shrub or tree species	Crop-rainfed Barren land	Slopes 15 - 35	Structures, planting	290
Soil bunds or fanya juu with agroforestry	Ditches alongside bunds or fanya juu stabilized with fertilizer/fruit/fodder species; 1.5 m vertical interval	Crop-rainfed	Slopes 8 - 15	Structures, planting	140
		Barren land	Slopes 3 - 15		
Grass strips or alley hedgerows	Strips of grass (0.8-1 m wide) or lines of shrubs on parallel contours at a 1 m vertical interval	Crop-rainfed	Slopes 3 - 8	Planting	27
Vegetative fencing	Assisted vegetation of field borders, calculated for an average field size of 0.2 ha	Crop-irrigated	-	Planting	36
		Crop-rainfed	Slopes <3		
Gully reclamation	Reshaping (cut and fill) of sides, assisted revegetation of area up to 8.55 m from gully center, wire-mesh gabion check dams are stone-filled.	All	An 8.55 m buffer of the gully channels	Reshaping, check dams, planting, guarding	7059[5,6]
Riparian buffer establishment	Vegetative fencing of 9 m buffer (from stream center) to exclose streambanks and facilitate unassisted revegetation that will slow streambank erosion	All	A 9 m buffer of stream channels	Planting, guarding	46
Homestead greening	Assisted revegetation of immediate vicinity of homesteads (demarcated from rooftops)	All	Within 4 m of homesteads	Planting	143

[1] Where an activity is restricted to a given slope class, costs are calculated for an average slope within the slope class.
[2] Compensation costs followed Balana et al.'s (2012) approximation of the worth of "less-productive land" at 69 Ethiopian birr (ETB) per ha (in 2007 ETB when 1 ETB = 9.16 USD) and their approximation of wages the state pays for labor, 0.87 USD/PD.
[3] All slopes refer to percent slope.
[4] Guarding not included when LU is likely to be privately-owned.
[5] Calculations utilized average slope (19.2%), depth (3.5 m), and width (9.1 m) of measured gullies; revegetation is established at 1 m from the top of the original (un-cut) gully bank, which means a gully rehabilitation occurs within an 8.55 m buffer of the gully center; a minimum reshape angle of 1:1 was used; Gabion spacing is calculated by: (height x 1.2)/(slope), yielding a 21.9 m spacing for average gullies; Gabion width was 1.5 m (a minimum value), height was 1.25 m (an average value), and foundation width was 0.5 m.
[6] Gully rehabilitation costs were summed from: reshaping at 5555 PD/ha, revegetation at 225 PD/ha, checkdams at 1278 PD/ha, and guarding at 2 PD/ha.
[7] Riparian buffer width was calculated by extending an approximated riverbed width (10 m) an additional 4 m outward; The buffer of 9 m is calculated as half the riverbed width plus the 4 m.

The "activity – LULC" combinations shown in Table 13 are restricted to certain slope classes, landscape features (rivers and gullies) or LULCs (homesteads). However, five additional restrictions were necessary to ensure the model incorporated as much of the background information as possible, as explained in Table 14.

Table 14: Additional restrictions for "activity – LULC" combinations

Activity(-ies)	Restriction description	Justification
Activities other than gully rehabilitation or riparian buffer establishment	Prevent these activities on gully and riparian areas, where only gully rehabilitation and riparian buffer establishment can be done	Prevents cheaper activities from being allocated to gully areas; promotes continuity of a riparian buffer
	Prevent these activities from being allocated on state plantation areas.	Removes areas of less benefit to community from being considered. Except for riparian or gully management, conservation of state-owned plantations would render few benefits to locals.
	Prevent these activities from being allocated to areas where SWC has been performed in recent years.	Avoids duplication of efforts based on participatory delineation of former SWC project areas (see Figure 9).
All activities	Ensure that community-selected priority areas are targeted prior to other areas.	Ensures prioritization of community requests (see Figure 9).
Silvopastoral hedgerows	Prevent these on the high-biomass pastures found on the largely uninhabited alpine hilltops in the far east of the catchment.	This activity would render few benefits in this sparsely populated area.

3.5.3 Biophysical parameter coefficients

Next, biophysical parameter coefficients were sought in the literature for the various LULC classes (Table 15).

Table 15: Selected biophysical parameter coefficients for original LULC classes

	C-factor		Roughness rank		Sediment retention efficiency[3]	Cover rank[3]	P-factor
LU class	Range in literature	Selected value	Range in literature	Selected value			
Grassland-hi biomass	0.003-0.14	0.010[2,5,6]	0.2-0.5	0.390[6]	0.84	1.00	1
Grassland-low biomass	0.003-0.14	0.050[2,5]	0.02-0.24	0.130[6]	0.84	1.00	1
Woodland-dense	0.003-0.07	0.050[5]	0.11-0.15	0.120[4,9]	0.68	0.71	1
Woodland-open	0.003-0.1	0.100[6]	0.10-0.75	0.100[4,9,10]	0.51	0.57	1
Barren land	0.4-1.0	0.600[1]	0.01-0.07	0.030[6]	0.26	0	1
Built-up	0.01-0.5	0.010[2]	0.001-0.02	0.012[6,10]	0.13	0	1
Crop-rainfed	0.01-0.45	0.400[5]	0.006-0.170	0.090[6,8]	0.55	0.81	0.9[13]
Crop-irrigated	0.1-0.4	0.150[1,2,5,8]	0.046-0.300	0.163[3,6]	0.55	0.81	0.9[13]
Alpine grassland	0.001-0.1	0.010[1,5,6,7]	0.06-0.60	0.21[6]	0.67	0.36	1
Shrubland	0.001-0.5	0.001[5,6]	0.069-0.600	0.130[6,10]	0.51	0.36	1

[1] BCEOM 1998; [2] Hurni 1985; [3] RIOS default coefficients (Vogl et al. 2013); [4] Candela et al. 2005; [5]Kaltenrieder 2007; [6] Morgan 2005; [7] Eweg & van Lammeren 1996; [8] SWAT values from Neitsch et al. 2005; [9]Arcement & Schneider 1989; [10] Engman 1986; [11] Cook et al. 2005; [12] SWAT values from Arnold et al. 2012; [13]"contour plowing" value from Haregeweyn et al. 2013

Similarly, biophysical parameter coefficients were established for each possible combination of a LULC class and an activity. Table 16 shows the predicted post-conservation LULC transitions. These transitions represent shifts to a more conserved state. Some combinations transitioned to a new LULC class with new biophysical coefficients while other combinations transitioned to an existing LULC class (shrubland). Newly created LULC classes were needed where an activity causes a shift to a previously non-existing LULC. Activities that affected the vegetation management of agricultural or pastoral areas did not shift toward a native vegetation type, but led to an improved condition of an existing LULC type. For example, cropland usually remained cropland after an activity was implemented, but biophysical coefficients were nevertheless altered depending on the type of activity. Shifts towards shrubland, dense shrubland, or improved alpine grassland – the only classes representing native vegetation types - were used when an area was either converted to or remained under native vegetation. 100% transitions were assumed in all cases except for homestead greening, which produces only an 80% shift to shrubland because these areas near homesteads are not excluded and are being utilized.

Table 16: Predicted post-conservation LULC classes and their chosen biophysical parameter coefficients

Old LULC class	Activity	New LULC class	C-factor	Rough rank	Sed. retention eff.	Cover rank	P-factor
Crop-rainfed	AF fanya juu	AF crop with fanya juu	*0.37*[3]	NC	0.738[3]	0.9[7]	0.375[6]
Grassland-hi biomass Grassland-low biomass	Silvopastoral hedgerows	Pasture with hedgerows	NC	0.48[6]	NC	NC	0.75[6]
Crop-rainfed	Grass strips	Crop with grass strips	*0.36*[3]	*0.105*[5]	*0.580*[3]	0.9[7]	0.25[6]
Crop-rainfed Crop-irrigated	Veg. fencing	Crop with veg. fence	NC	NC	0.738[3]	0.9[7]	0.8[4]
Barren land	AF fanya juu, AF stone bund, AF hillside terracing Gully rehabilitation	Reclaimed barren land	0.03[4]	0.6[5]	0.51[3]	0.357[3]	0.375[6]
Crop-rainfed	Gully rehabilitation						
Shrub	Passive exclosure	Dense shrubland	0.003[5]	0.32[6]	0.668[3] (ave. of old original shrub & grassland values)	0.679[3] (ave. of shrub & grass-land)	NC
Shrub Grassland-low biomass Grassland-	Gully rehabilitation						

high biomass Alp. Grassland Woodland-open Woodland-dense							
Alp. grassland	Passive exclosure	Improved alpine grassland	0.003[5]	0.32[6]	0.83[3]	1.0[3]	NC
Woodland-open Barren land Shrubland Crop-rainfed Grassland-hi biomass	Homestead greening	Shrubland	0.001[8]	0.130[8]	0.51[8]	0.36[8]	1.0[8]
Woodland-open Crop-rainfed Shrubland Crop-irrig. Barren land Grassland-low biomass Alp. grassland Grassland-hi biomass	Riparian buffer mngt						
Barren land Woodland-open	Passive exclosure						
Crop-rainfed	Reforested exclosure						

[1] italicized values indicate weighted averages of the original LU class value and a new value from the literature; [2] NC indicates no change from the original value; [3] Vogl & Wolny 2015; [4] Haregeweyn et al. 2013; [5] SWAT values from Neitsch et al. 2005; [6] Morgan et al. 2005; [7] Calculated by accounting for a 9% increase in vegetative cover; [8] Same as original shrubland values

3.6 Current soil losses in the study area

The RUSLE calculation for current conditions showed significant potential soil loss levels throughout the catchment (Figure 13). The average per-hectare for the catchment was 20.6 ton ha^{-1} (σ = 52.7). Of the five soil loss classes presented in the figure, the first two classes have conveniently been capped at 2.5 and 11 t ha^{-1}, corresponding, respectively, to Lal's (1981) soil loss tolerance rate for shallow tropical highlands and the critical maximum value (among all climate and soil types) used by the NRCS (1999) and many studies utilizing the RUSLE (although the value is sometimes seen as 11.2 t ha^{-1}). Not surprisingly, barren land produced the highest erosion rates among the LU/LC classes (Figure 12).

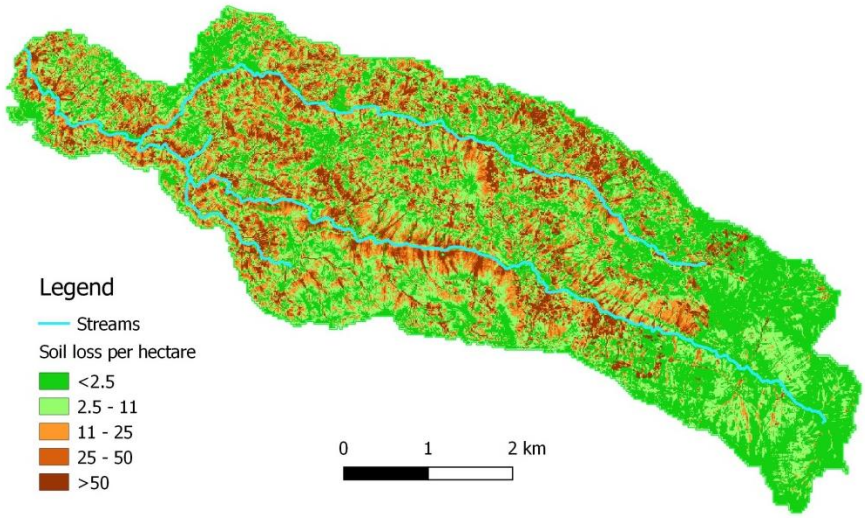

Figure 13: Potential annual soil loss rates for the current condition.

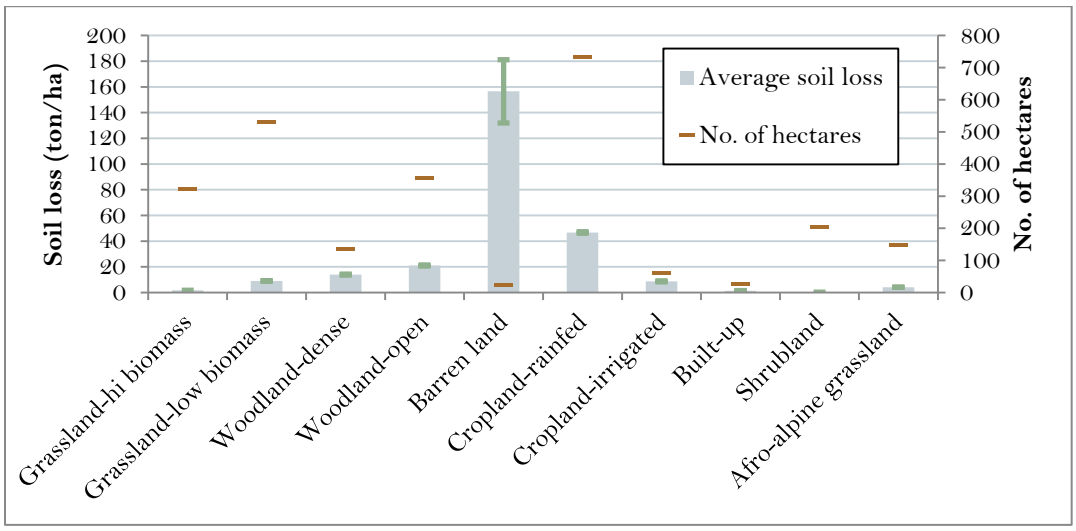

Figure 14: Average soil loss rates and total hectares per LU/LC class; error bars indicate the 95% confidence interval

Despite its high sediment yield, however, barren land constitutes just 0.9% of the total catchment area. The "barren land" LU/LC is largely comprised of known hotspots, all of which are gully and severe rill erosion sites. To check the model's performance at these sites, statistics were derived for soil loss at hotspots (Table 17); the "current" soil loss raster was sampled at 10-m intervals along gully lines, which cumulatively amounted to 13.36 km of gullies. Although the RUSLE is not intended for the estimation of soil losses due to permanent gullies – and therefore greatly under-predicts at these sites – average soil loss and exported sediment values greatly exceeded those of the "barren land" LULC. Known hotspots were shown to yield an average of 215 ton/ha per year, or 37.5% more than the "barren land" class. However, hotspot soil loss was widely spread, having a standard deviation of 861 ton/ha. Soil losses were similarly checked for areas designated as priority areas during focus group discussions (Table 17). These areas – amounting to 107 hectares - exhibited soil loss rates on par with those of rainfed cropland.

Table 17: Current soil loss at hotspots and focus group-selected priority areas

	All barren land		**Hotspots**		**Community priority areas**	
	Soil loss (t/ha)	Exported sediment (t/ha)	Soil loss (t/ha)	Exported sediment (t/ha)	Soil loss (t/ha)	Exported sediment (t/ha)
Average	156.6	19.4	215.3	32.1	43.8	3.8
St. deviation	584.4	1.9	861.2	292.7	119.1	19.1
Maximum	16746.3	62.6	16746.3	6260.3	3506.9	9.9

Far more concerning are the potential annual losses from rainfed cropland (Figure 13), an LU/LC that occupies 28.8% of the catchment. Rainfed cropland lost by far the most soil (63.7% of the total loss of the catchment) and exported a similar proportion (63.2%) to stream channels. The annual total soil loss for the catchment is 52,998 tons, 7.8% of which reaches stream channels. The average soil loss per hectare is 20.8 tons with a standard deviation of 52.7 tons.

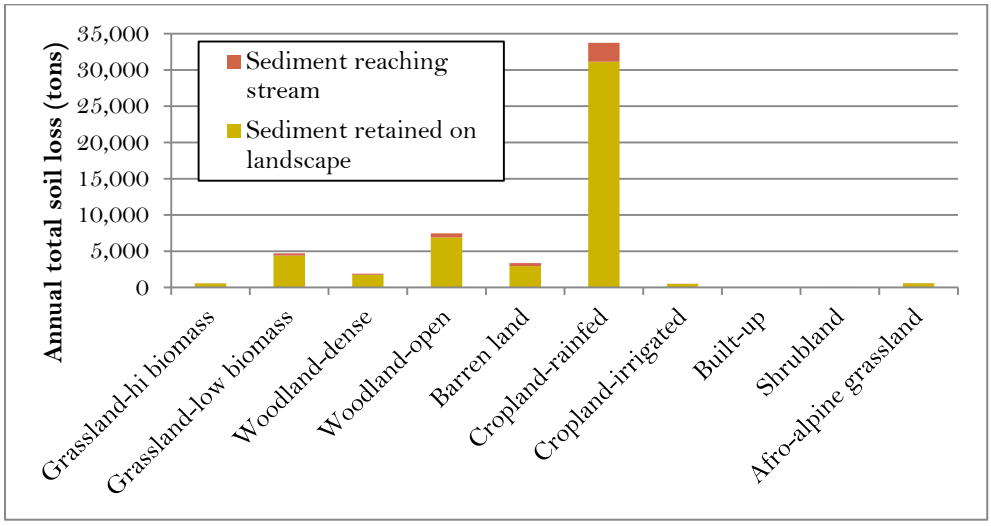

Figure 13: Total annual soil losses per LU/LC class

3.7 Modelling of SWC activities using RIOS

The activity maps produced by RIOS (Figure 15) indicate the sites predicted to be most "responsive" to SWC activities. Allocations were performed in three ways, resulting in three different scenarios. In the first scenario, erosion control was considered only ("EC1 BF0"); in the second, erosion control was weighted as twice that of baseflow enhancement ("EC2 BF1"); in the third, erosion control and baseflow enhancement were weighted equally ("EC1 BF1").

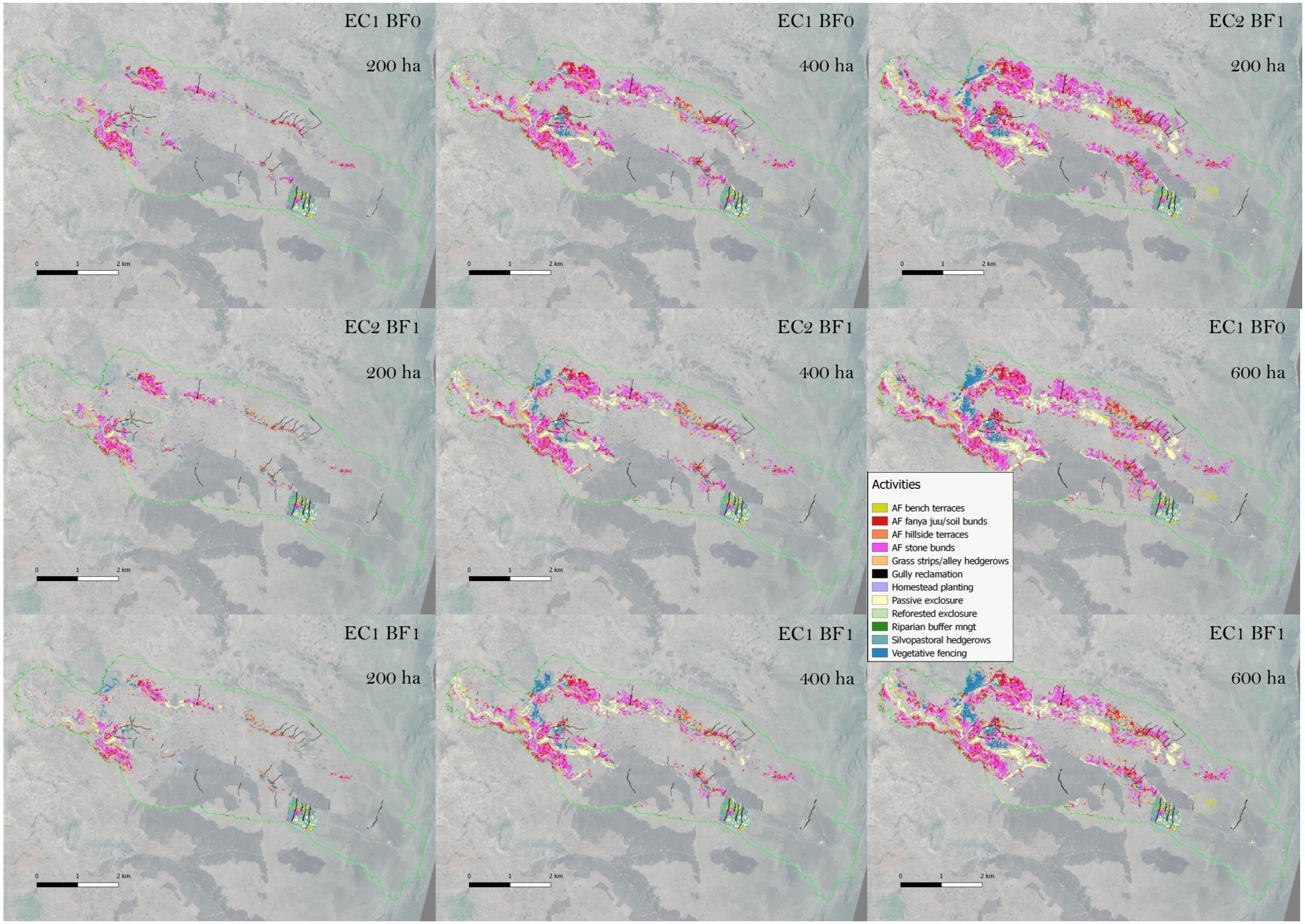

Figure 15: SWC activity maps for three ES objective weighting scenarios (EC1 BF0 / EC2 BF1 / EC1 BF1) following the allocation of 200, 400, and 600 hectares of activities

The pixel allocation procedure by RIOS yielded similar results among the three different objective weighting scenarios (Figure 14). The EC1BF0, EC2BF1 and EC1BF1 scenarios required 17.3, 17.0, and 16.9 years, respectively, to complete activities on 600 hectares. Figure 16 and Figure 17 also show great similarity between the types of activities called for under each scenario. Most importantly, all scenarios show an emphasis on the need to ameliorate cropland. Between the scenarios, some differences could be seen in the amount of pastureland and cropland converted. When the baseflow component is not considered, more activities occur on cropland and fewer activities occur on pastureland. The opposite is true when baseflow is given more weight: cropland has slightly less importance and activities shift to other LULC classes. Degraded lands – considered as gullies and barren land in this case – were treated equally; approximately 48% of the total "barren land" LULC class was converted in every scenario.

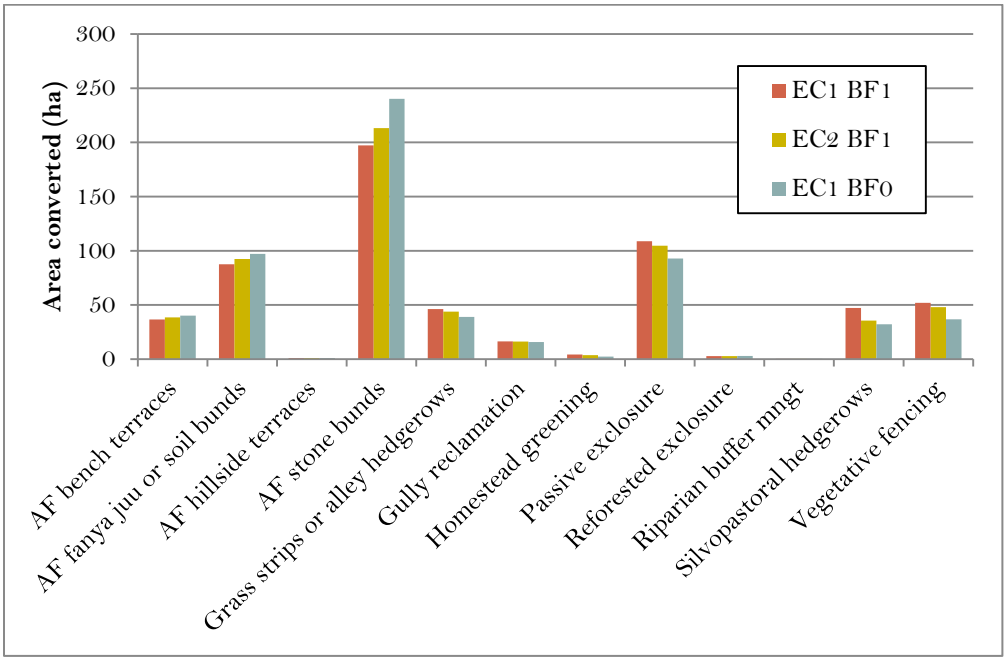

Figure 16: Area designated for each SWC activity for the three scenarios

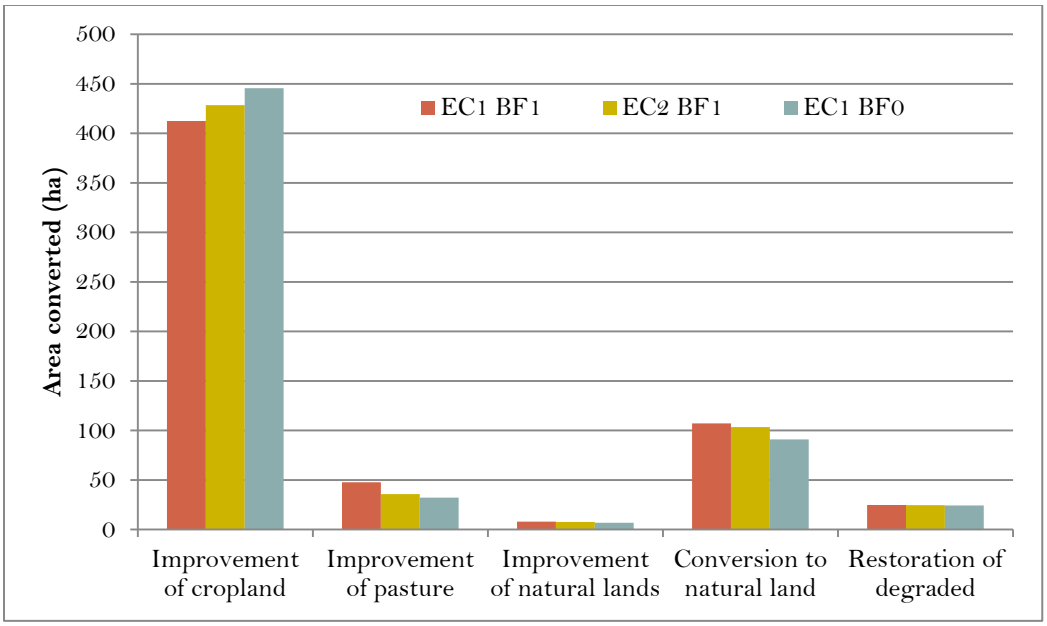

Figure 17: Hectares converted under SWC activities for various LULC transition categories for the three scenarios

3.8 Predicted soil losses after implementation of SWC activities

RUSLE calculations were performed for the post-activity "transitioned" data at the 200, 400, and 600 converted hectare benchmarks for each scenario. Table 18 and Table 19 give the soil loss statistics for the catchment as a whole. Table 18 shows that the scenarios require about the same amount of time to reach each benchmark (200/400/600 hectares converted). These numbers were derived by dividing the total amount of labor used (in PDs) by the annual labor budget.

Table 18: Soil loss statistics for the entire catchment

Hectares converted	Average soil loss (t/ha)			Fraction exported (%)			Time to complete (yrs)		
	EC1 BF1	EC2 BF1	EC1 BF0	EC1 BF1	EC2 BF1	EC1 BF0	EC1 BF1	EC2 BF1	EC1 BF0
none	20.6			7.8	7.8	7.8	-		
200	17.8	17.7	17.3	6.9	7.0	7.1	9.4	9.6	10.1
400	15.5	15.3	14.8	6.4	6.6	6.6	3.7	3.8	4.0
600	13.4	13.1	12.6	6.2	6.4	6.6	3.8	3.6	3.2
						Totals:	16.9	17.0	17.3

Table 19: Incremental soil loss statistics for each set of 200 ha converted

Hectares converted	Soil loss avoided (t)			Soil loss avoided per unit time (t/yr)			Soil loss avoided per area converted (t/ha)		
	EC1 BF1	EC2 BF1	EC1 BF0	EC1 BF1	EC2 BF1	EC1 BF0	EC1 BF1	EC2 BF1	EC1 BF0
200	7045	7482	8513	750	776	842	35.2	37.4	42.6
400	6140	6182	6239	1653	1643	1562	30.7	30.9	31.2
600	5356	5664	5696	1422	1574	1761	26.8	28.3	28.5
Totals:	18541	19329	20448						

The data shows that when baseflow is not considered, more soil loss is avoided. However, the difference is marginal. Plus, this option takes slightly more time and does not reduce the fraction of sediment lost exported as much as other options. In terms of soil loss avoided per unit area, EC1 BF0 performs better at the outset (the first 10 years), but afterwards is similar to the other options.

The soil loss map for the first allocation of 200 hectares was subtracted from the "current" situation soil loss map to give a "soil loss avoided" map. The map was sampled at intervals of 100 m in order to test for significance between the three objective weighting scenarios. A single-factor analysis of variance revealed that the means of each dataset could not be considered statistically dissimilar. The same procedure was also performed for the 600-hectare benchmark. Again, the means of soil loss avoided in the catchment were found to be statistically equivalent.

Average (or total) soil loss fell by 10% in only three LULC classes: open woodland, barren land, and rainfed cropland (Figure 18). These classes were responsible for 14.1%, 6.4%, and 63.7%, resp., of the total soil loss from the catchment for the current situation. For this reason, rainfed cropland becomes the focal point of this study. Figure 18 shows the progress made by each objective weighting scenarios after the 200, 400, and 600 hectare benchmarks. When baseflow is given less weight, the average soil loss from rainfed cropland is less. All scenarios require about 17 years to reach the 600-ha benchmark (Table 18), at which point soil losses have been reduced by nearly half in the best scenario (Figure 18). Further conservation is needed to reach "safe" levels of soil loss (see 4.1.1).

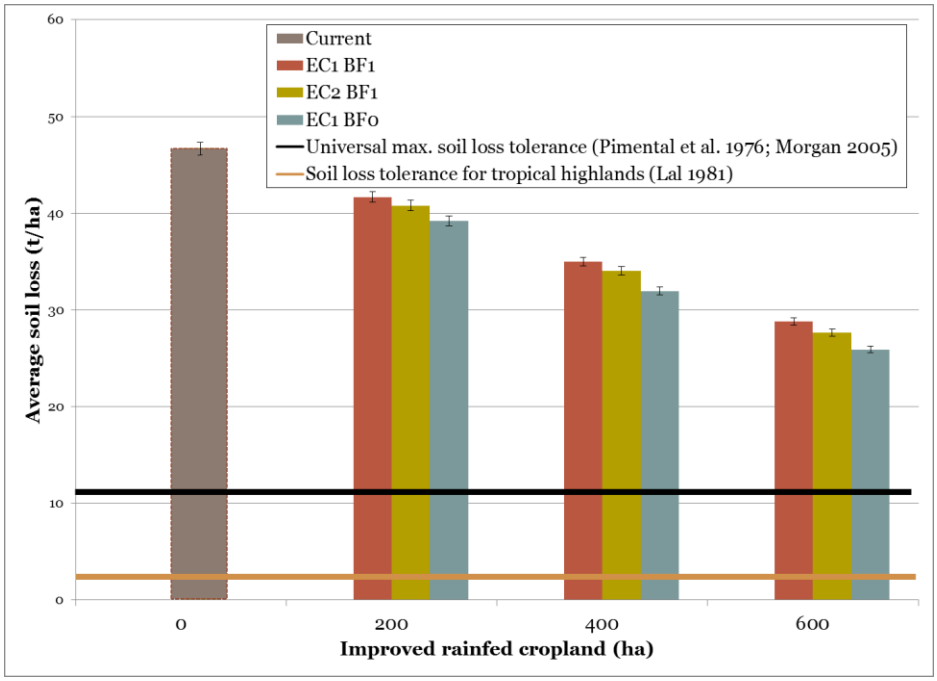

Figure 18: Post-activity average soil loss on rainfed cropland (bars show 95% confidence interval)

In terms of labor efficiency, grass strips out-performed the other cropland activities while vegetative fencing performed very poorly (Table 20). These results are based on the post-SWC biophysical coefficients chosen for each activity.

Table 20: Labor efficiency in soil loss avoidance for SWC activities on rainfed cropland (for the EC1BF0/600 ha benchmark)

Activity	Ave. reduction in soil loss (t/ha)	Labor req't (PD/ha)	Labor per soil loss avoided (PD/t)
Bench terrace	107.8	756	7.0
Stone bund	37.7	290	7.7
Fanya juu/soil bund	14.3	140	9.8
Grass strips	8.1	27	3.3
Vegetative fencing	0.3	36	137.2

3.9 Water balance predictions

A water balance was calculated using the 2015 daily meteorological data. The current situation (before activities) was compared to that of the EC1BF1 and EC1BF0 scenarios since these two scenarios represent the greatest difference in the importance of the baseflow component. The calculations are for an average three-dimension soil column of rainfed cropland in the study area. Post-activity scenarios were calculated at the 600-ha benchmark. Evapotranspiration, calculated at daily time steps, used the simulated Kc values shown in Figure 19. The influence of the shrub (representing agroforestry) on 9% of the land surface is seen to raise the overall K_c during the dry season. Differences in K_c for the two post-SWC scenarios were negligible.

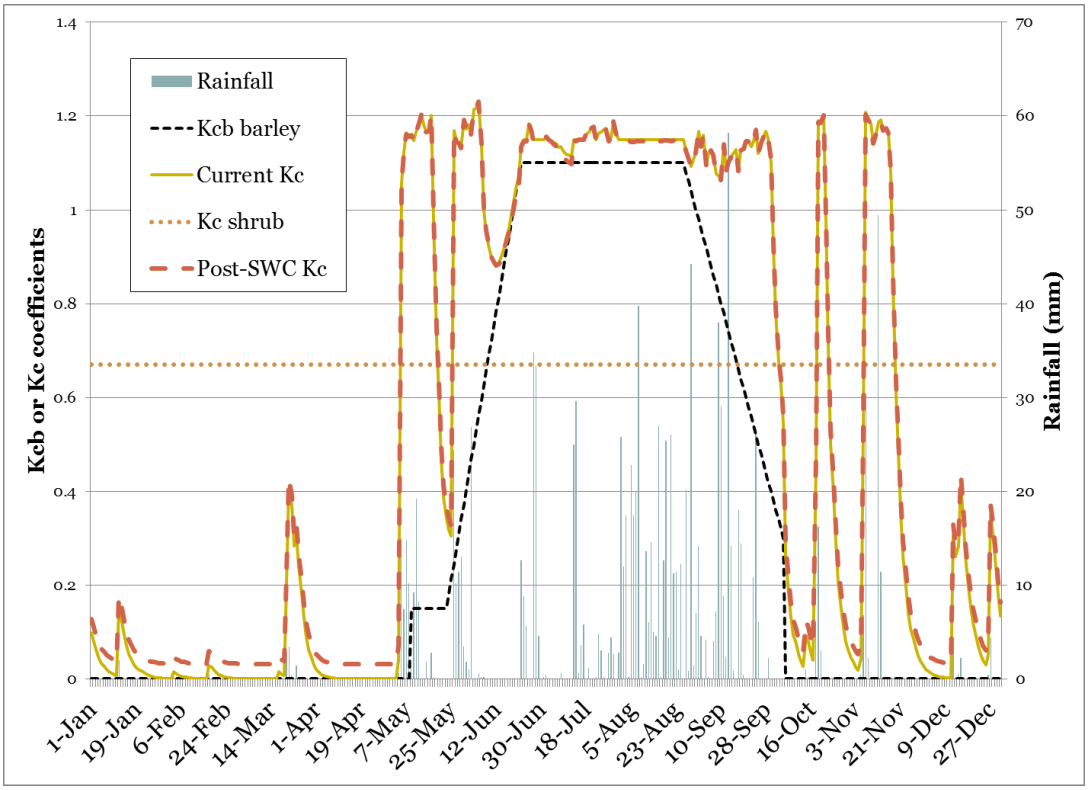

Figure 19: Simulated crop coefficients (K_c) and their transpiration components (K_{cb}) for 2015 climate conditions. (A "general" post-SWC K_c value is given here since the difference between the two scenarios was negligible.)

The runoff component of the water balance is reduced for the average plot of rainfed cropland after conservation activities, but differences between the scenarios were marginal (Figure 20). Annual runoff depths from rainfed cropland for the current, EC1BF1, and EC1BF0 scenarios were 467, 402, and 394 mm. These compare favorably to depths measured at the Andit Tid research site (also located in the central highlands and experiencing similar climatic conditions) where runoff averaged 354 mm annually (Herweg & Ludi 1999).

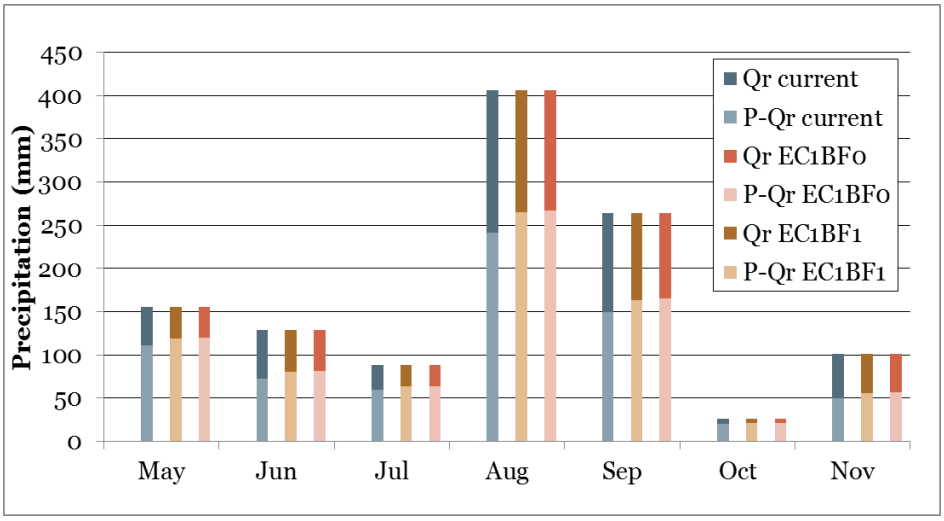

Figure 20: Monthly precipitation divided into the infiltration ($P-Q_r$) and runoff (Q_r) components for the scenarios (for wet months only)

Figure 21 shows the flux of water to and from the ΔS + D (soil water storage plus drainage) term described in 2.9. This term describes the cumulative change in water that infiltrates the soil (is not lost to runoff) and is not lost to either soil evaporation or plant transpiration. It should be noted that within the ΔS + D term, ΔS can be positive or negative but D is always positive since the soil column touches the water table and thus accounts for positive changes in groundwater. Therefore, positive changes in ΔS + D have positive implications for stream baseflow.

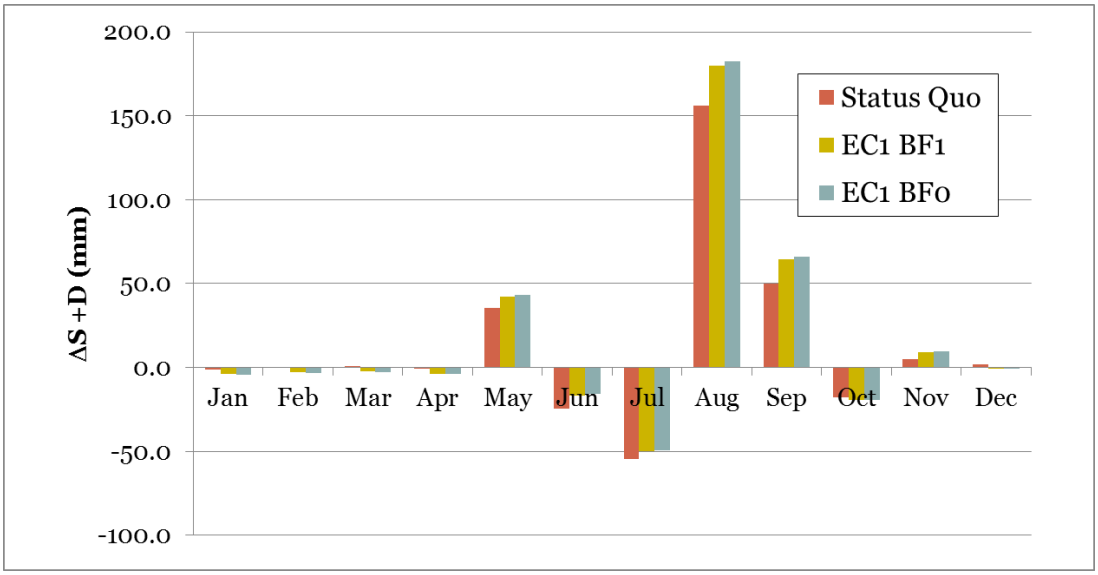

Figure 21: Monthly change in the sum of soil water storage plus drainage for 2015 climatic conditions

The current, EC1BF1, and EC1BF0 conditions yielded positive values for ΔS + D when summed for the year; they were 151, 196, and 305 mm, respectively, for the 2015 weather conditions. Surprisingly, the objective weighting scenario that did not account for baseflow seems to be most likely to enhance baseflow according to these results. A paired two-sample T-test was used to compared monthly values for the two scenarios. The test indicated that the null hypothesis (the supposition that the means are statistically equal) cannot be rejected. However, it should be remembered that these results represent only the average water flux on a unit of rainfed cropland. A catchment-wide analysis could yield contrasting results.

4 Discussion

4.1 Current soil losses

4.1.1 Seeking a tolerable soil loss rate for the Ethiopian highlands

In order to appreciate the severity of the current soil loss status at Gudo Beret – disregarding, momentarily, the validity of the rates predicted in this study – it is necessary to consider the soil loss rate that can be considered tolerable since complete avoidance of erosion is not achievable. An acceptable soil loss rate is generally held to be equivalent to the rate of soil formation for a given area. Unfortunately, the measurement of soil formation rates is a time-intensive process, so literature estimates must be relied upon. An estimated maximum tolerable soil erosion rate of 11 t ha^{-1} (or 11.2 as is sometimes reported) is often seen in the literature (Morgan 2005). This value was first suggested by Pimental et al. (1976) and later became an upper limit used by the NRCS in the US (Nill et al. 1996).

Soil formation in (sub-) humid areas is, however, catalyzed by more intense weathering processes than are typical in the US; at the same time, monsoonal climatic regimes mean that erosive forces are more intense. Furthermore, shallow soils on sloped land like those of Gudo Beret are even more susceptible to erosive forces. Hence, more conservative values of soil loss tolerance have been given by various sources: 2.2 t ha^{-1} for shallow soils over hard rock (NRCS 1993); 2 t ha^{-1} for Ethiopia (Hurni 1981); 2-5 t ha^{-1} for shallow erodible tropical soils (Hudson 1986); and 2.5 t ha^{-1} for shallow tropical highland soils (Lal 1981).

Nevertheless, to regard the soil formation rate as an acceptable threshold for soil loss is to value top soil the same as soil from the bottom of the profile. When nutrients and SOM are factored into the mass balance of soil formation and erosion, it becomes clear that the tolerable soil loss rate must be set at some margin below that of soil formation to guarantee sustainable land use in the long-term (Rensch & Harbor 2002). New approaches for establishing a tolerable rate (Lal 1998 or Botschek 1997) suggest the consideration of more parameters but no consensus has been reached.

If Lal's (1981) threshold (2.5 t ha^{-1}) is taken, then all LULC classes in Gudo Beret other than high-biomass grassland, built-up areas, and shrubland exceed the allowable limit. Rainfed cropland, the dominant LULC class in the catchment, exceeds this limit 19-fold on average. Even after accounting for some error in either direction, it can be ascertained with reasonable confidence that rainfed cropland in Gudo Beret is not being managed in a way that will ensure long-term utility for agriculture.

4.1.2 Comparisons with relevant studies

Soil erosion rates given in the literature normally distinguish between sheet/rill and gully erosion. Rill and sheet (also known as interrill) erosion can be measured from runoff plots; other times, estimates have been based on rill dimensions measured within a study area and then adjusted for the added losses due to interrill erosion. Moreover, there are multiple models of varying complexity (RUSLE, SWAT, WEPP) that are used to approximate rill and interrill erosion. On the other hand, models predicting gully erosion – excluding ephemeral gully erosion - are uncommon; most studies reporting gully

erosion rates have utilized aerial photography or field measurements of gully dimensions (see Haregeweyn et al 2015).

Many erosion studies have been performed in Ethiopia's highlands (Haregeweyn et al. 2015 provides an overview of these) and a wide range of results have been achieved. One must be cautious when making comparisons between studies due to large differences between agro-climatic zones as well as scaling effects. The Soil Conservation Research Program (SCRP) that established 7 stations in Ethiopia for the purpose of monitoring SWC practices distinguished between three regions for the guiding of SWC measures: semi-arid areas, subhumid areas with insecure rainfall, and subhumid areas with secure high rainfall (Herweg & Ludi 1999). The combination of high secure rainfall and fine textured soils that saturate during substantial rainfall events at Gudo Beret renders the location unique in the dynamics of its soil and water processes, and non-comparable to drier or sandier places. Furthermore, extrapolations from runoff plot measurements to catchment or larger scales normally lead to overestimates since small plot experiments cannot capture the effect of downslope soil retention. For this reason, a number of early basin-scale and national-scale erosion estimates that extrapolated from plot-scale data from the SCRP stations in Ethiopia have since been realized as greatly overestimated (Rahmato 2001).

Of the SCRP stations, the one most comparable to Gudo Beret is Andit Tid, also located in the North Shewa Zone of the Amhara region. The two sites share the same climatic regime (sub-humid with high rainfall), have similar altitudinal ranges (about 3100 m average), mean annual rainfalls (over 1200 mm), and mean annual erosivities (averages of 450 and 500 MJ mm ha^{-1} h^{-1} yr^{-1} at Gudo Beret and Andit Tid); the Andit Tid plots had 24% gradients while the average cropland gradient at Gudo Beret was 19% (Herweg & Ludi 1999). Plot experiments on rainfed cropland using traditional cultivation techniques between 1983 and 1992 at Andit Tid yielded average soil losses of 48 t ha^{-1} yr-1 (±50) (Herweg & Ludi 1999). Clearly this compares favorably to our estimates at Gudo Beret (47 ± 82 t ha^{-1} yr^{-1}). However, as discussed previously, the Andit Tid experiment is likely an overestimation. A second site for comparison is Debrew Mewi, which is not an SCRP site, but has similar rainfall and altitudinal characteristics as Gudo Beret; here, Zegeye et al (2010) measured rill dimensions on crop fields and later adjusted for a 30% contribution of interrill erosion; their result was an average of 36 t ha^{-1} yr-1. Among the SCRP sites, the highest highland rates (110 ± 29 t ha^{-1} yr^{-1}) were measured at Anjeni where the altitude is similar, but slopes (28%), rainfall (1690 mm), and erosivity (633 MJ mm ha^{-1} h^{-1} yr^{-1}) are all higher (Herweg & Ludi 1999).

Erosion predictions at the watershed level are either generated from time-series sediment yield measurements at the watershed outlet or reservoir or through various modelling approaches like the one used in this exercise. Gessesse et al. (2014) used SWAT to approximate the sediment yield of the Modjo watershed, which is found geographically close to Gudo Beret in the neighboring Awash Basin in the central highlands, and having similar altitudinal and climatic characteristics as Gudo Beret, although receiving about 300 mm less rainfall; their result was an average sediment yield of 24.2 t ha^{-1} yr^{-1} (with a Nash-Sutcliffe efficiency >0.79) for the meso-scale watershed. Again, this compares favorably with our catchment results at Gudo Beret (20.6 ± 52.7 t ha^{-1} yr^{-1}). Furthermore, the study found significant correlations between soil erosion and soil types, LULC types, and slope positions.

Gully erosion predictions in Ethiopia have utilized farmer knowledge, field measurements and (often low-resolution) aerial imagery. Nevertheless, Tebebu et al's (2010) gully headcut retreat measurements and imagery analysis at Debre Mewi (the same as above) led to a worrying estimation of 530 t ha^{-1} yr^{-1}

soil loss from gullies, a value 20 times larger than the rill and interrill erosion occurring on surrounding lands – and therefore accounting for 97% of the total soil loss in the study area.

Other gully erosion measurement studies from the sub-humid high rainfall central highlands could not be found. Most studies on gullies have occurred in the northern part of the country (especially in the Tigrai region) where the climate is semi-arid and where widespread implementation of SWC from the late 1970s onwards has had a notable influence on gully control (Haregeweyn et al. 2015). Nyssen et al. (2007) found the contribution of gully erosion to total soil losses in the semi-arid Tigrai highlands to be about 28%. It is logical that gullying in wetter agro-climatic zones is more severe since high water tables are associated with instable (and thus active) gully sections (Tebebu et al. 2010). Tebebu et al. (2010) and Nyssen et al. (2007) agree that the conditions that foster gully initiation are human-caused; their studies find that the pronounced removal of vegetation – which significantly lowers the evapotranspiration component of the water balance (and can significantly raise the water table in wetter regions) – allows for the initial incisions on saturated soils that become gullies. In Gudo Beret, the collapse of saturated gully banks (composed of heavy soils) is a frequent sight and apparently a key mechanism for their expansion. Tebebu et al. (2010) suggest the planting of water table-lowering Eucalyptus at gully sites to increase the shear strength of gully walls (and thus their stability). Ironically, non-targeted conversion of Vertisol bottomlands to Eucalyptus can lead to water table lowering that *promotes* cracking, piping, and gully development (Nyssen et al. 2007).

Although more studies in sub-humid highland regions will be needed to draw firmer conclusions as to the dominance of gully erosion, Poesen et al. (2003) points out that the presence of gullies has a compounding effect on overall soil loss because they increase the sediment connectivity of a landscape, thereby rendering the products of rill and interrill erosion lost to the system (non-recoverable) far sooner than in a gully-free landscape. The presence of gullies reduces flow lengths, meaning that detached sediments have less opportunity to be retained on the downslope path. Gullies of varying degrees of stability are a frequent sight in Gudo Beret. While some have been recolonized by native vegetation and can be considered stable, others showed signs of slumping (wall collapse) and uphill migration. While gully erosion contributions are not known for Gudo Beret, their frequency across the Gudo Beret landscape seems to point to a significant contribution to total soil losses. It is therefore likely that soil loss predictions for the Gudo Beret catchment have been significantly under-predicted.

4.1.3 A critique of the RUSLE

Developed in 1958 by the SCS (now the NRCS), the USLE was based on empirical data from experiments in the US. Although it was developed for use by conservation planners and not for research this "universal" model was soon being used (and misused) globally in the absence of other easy-to-use erosion assessment tools. Though today the model has much more competition with more sophisticated conceptual and process-based models, it remains widely used due to its low data requirement and overall simplicity. Wischmeier & Smith's (1958, 1978) original model was updated in 1991 in the form of the Revised USLE (RUSLE) which changed the LS factor calculation (as discussed in 2.7.1) and extended its usability to more land types and conditions (Renard et al. 1991).

Nonetheless, it is necessary to be cognizant of the shortcomings of the RUSLE, especially those of greatest relevance to this study. Perhaps the two greatest limitations of the model regarding the needs of this study are its inability to predict gully erosion losses and its failure to capture seasonality of some factors. As a rill/interrill prediction model, the RUSLE does not account for ephemeral or permanent

gullies or streambank erosion. Therefore, adjustments to the sediment yield predictions have to be made using measured or estimated values if possible. In this study, known permanent gully sites were given higher C-factor values to emphasize their vulnerability to detachment; this resulted in an average soil loss at hotspots of 215 (±861) t ha^{-1} yr^{-1}, approximately half the yield found at the Debre Mewi watershed (see 4.1.2). Field observations showed that gullies were primarily found to originate from or transect four LULCs: rainfed cropland, low-biomass grassland pasture, sparse woodland, and barren land. However, for the purpose of altering their C-factor value, all known gully sites were reclassified as barren land. This means that soil losses on rainfed cropland, low-biomass grassland pastures, and sparse woodlands are technically under-predicted. It should also be emphasized that soil compaction due to overgrazing, which was practically synonymous with pastureland in Gudo Beret, is ignored by the RUSLE due to its simplification of hydrological concepts. Although they are one of the main hosts of gullies, soil loss from pasturelands were artificially low in this study.

Although adaptations of the (R)USLE have facilitated event-based predictions (Kinnell 2010), the model was developed to predict *annual* average soil losses. The factors that suffer from a lack of temporal variability in the RUSLE are the C-factor and the R-factor; additionally, sediment retention values used by InVEST to predict sediment retention and export should fluctuate with the seasons since soil surface characteristics change, especially on cropland. Like most studies utilizing the RUSLE, input data for these factors are clumped to represent the annual timeframe. A cumulative annual R-factor based on annual precipitation was used in this study. Despite the significant temporal variability in cover on rainfed cropland, C-factor and sediment retention values representing mid-season cover were used because these are most representative of the cover status when rainfall is hitting the soil surface.

Furthermore, the RUSLE ignores heterogeneity within single spatial units. Rather, each unit – a 10 by 10 meter pixel in this case - is treated as a homogenous unit whose cover and management is solely represented in its C-factor, P-factor, and sediment retention efficiency. This causes issues when trying to evaluate the effects of intra-unit (within the pixel) land cover or management changes. Practices like intercropping, alley cropping, border cropping as well as physical SWC measures must therefore be represented by changing C-, P- and sediment retention values for the entire pixel, which does not accurately reflect the processes of sediment export and retention that can occur within a pixel. Vegetative (and soil) heterogeneity can highly influence runoff and thus detachment from shear flow although the RUSLE assumes uniform flow of runoff (Kinnell 2010). Nevertheless, these limitations are overcome in this study through the assumption that vegetative SWC measures result in an increase of a certain percentage of these factor values in order to capture enhanced cover, retention, and management. Generally, however, C- and P- values for the pre- and post-SWC scenarios were a large source of uncertainty in this study. This was dealt with by consulting a large number of Ethiopian and highland-specific studies. In studies where more precise modelling is needed, an iterative process of calibration followed by validation with local measurements is pursued. A physically-based model would be preferred to the RUSLE if more detail is needed; this class of models uses a larger number of parameters to describe processes, which translates to a greater data requirement (Aksoy 2005).

Finally, although the RUSLE's R- and K-factors incorporate a number of parameters that correlate with runoff generation (rainfall intensity, soil texture, porosity/bulk density, SOM, and drainage class), the model makes no distinction between runoff generation mechanisms, which can cause different types and magnitudes of soil particle detachment. Raindrop splash, flow shear, or a combination of these two - the possible mechanisms for downslope transport – are rather lumped together since the empirical model is based on linear regressions derived from experiments that simply measured sediment yield at the lower

border of plots (Kinnell 2010). This shortcoming is apparently particularly seen when an adapted form of the RUSLE is used to predict event-based erosion; indeed, for these short-term predictions, the failure to consider runoff explicitly means that temporal variations (e.g. the degree to which the soil surface is saturated) or spatial variations (e.g. differences in antecedent moisture conditions of the soil) are not well accounted for (Kinnell 2010).

4.2 Spatial allocation of activities with RIOS

4.2.1 RIOS used elsewhere

According to the documentation for RIOS, the simulation tool "introduces a science-based approach to prioritizing watershed investments by identifying where protection or restoration activities are likely to yield the greatest benefits for both people and nature at the lowest cost" (Vogl et al. 2013). The tool has only been available since 2013 and literature on its use is scarce. Internet searches reveal that the utility of RIOS has at least been explored for water funds in Costa Rica, Colombia, Kenya, and Ecuador, of which only the last of these was the subject of a peer-reviewed article (see Mulligan et al. 2015).

However, the most relevant employment of the tool to this study in terms of geographic proximity and objectives is the Upper Tana-Nairobi Water Fund project in which RIOS was used to determine intervention locations for different investment budgets in order to make a business case for the conservation of upland areas responsible for the sediment and water yields in the Tana River – Nairobi's main source of hydroelectric power. Although not yet published, the use and evaluation of RIOS's performance is well-documented in technical reports (see TNC 2015; Kizito et al. 2014; Vogl & Wolny 2015; Hunink & Droogers 2015).The study focused on the same two ES objectives as this study, erosion control and baseflow enhancement, since high siltation and ever-decreasing dry season flows have been recognized as stifling to the generation of hydroelectric power.

The premise of the water fund is that by protecting the watershed through long-term investments using targeted interventions at strategically-chosen sites, the environment could be protected, water supply could be enhanced, and more power could be generated. In the study, RIOS is first used to choose the sites that would be most "responsive" to interventions. Unlike this study, their study incorporated SWC activity costs in RIOS so that cost-effectiveness played a role in site selection, and scenarios were created based on different budget levels.

Next, benefits were calculated for both the farmers that would implement SWC activities and for the hydroelectric company, which would be able to produce more power with a greater water yield and would save money on removing silt from the dam. The impacts of the various portfolios were quantified in terms of soil loss, river flows, and turbidity using SWAT (Hunink & Droogers 2015).

At the farmer site (source of erosion), SWAT was used to investigate the change in soil losses as well as the soil water balance. Then, a productivity index equation was used to index the relative change in soil productivity; this index is a function of soil pH, amount of clay, rooting density, SOM content, and water holding capacity, and is calculated for each soil layer within the rooting depth and then summed (Pierce et al. 1983; Mulengera & Patyton 1999; Duan et al. 2011). Of these factors, only SOM and water holding capacity were assumed to have changed significantly as a result of SWC. Since an increase in

soil productivity leads to an increase in biomass production (coupled with a decrease in soil evaporation and an increase in crop transpiration), productivity index – calculated for the pre- and post-SWC conditions – was used to predict the "new" crop transpiration rate; a positive linear relationship between productivity index and crop transpiration was assumed (Rockström, 2003; Adgo et al., 2013). As a final step, the new crop transpiration rates were translated to economic benefits using locally-derived economic water productivity coefficients ($/volume transpired) for each crop. By doing this for the pre- and post-SWC conditions, a net economic benefit for the farmers could be predicted.

In this way, the avoidance of soil erosion was shown to yield monetary benefits due to relative increases in soil productivity as a result of enhanced soil moisture (water-holding capacity) and fertility (SOM) (Hunink & Droogers 2015). While assuming that soil productivity would reach the new predicted equilibrium about ten years following the introduction of a SWC activity, the authors forecasted that from that time onwards, the long-term change in annual revenues for farmers in the three targeted watersheds (spanning 3329 km^2) would be around 3 million USD annually in the case that 10 million USD was invested into the water fund.

In addition to the increases in agricultural productivity estimated for the farmers upstream, the same 10 million USD investment mentioned above was predicted to result in up to a 15% water yield increase during the dry season; coupled with an estimated 18% decrease in reservoir sedimentation meant that the hydroelectric company would increase revenues by 600,000 USD annually (TNC 2015). The return on investment for various stakeholders was presented as a business case for the strategic investment in SWC by the water fund.

4.2.2 Understanding the RIOS results

A preliminary run of the RIOS model that differentiated between activity costs showed that pixel selection by RIOS was dominated by activity cost-effectiveness. This meant that activity selection was skewed to the cheaper activities and highly degraded areas remained unconverted because they required activities that were too expensive. It was decided that cost-effectiveness was not as relevant to the Gudo Beret case where labor campaigns provide a fixed labor source annually.

Rather, this study turned to the question of how ES objectives influence RIOS outputs. Costs were no longer utilized in the model and the focus shifted to the basic premise of RIOS – that the most "responsive" sites can be selected by ranking a small set of biophysical factors that control one or more ES's.

The weighting of one ES objective relative to another could, in practice, represent the value that stakeholders express for one ES over the other. Since, focus group discussions revealed that soil loss and seasonal water scarcity were highly prioritized challenges in the study area, erosion control and baseflow enhancement became the focal ES objectives for the RIOS modelling. RIOS leaves the weighting of objectives as well as the factors controlling each objective up to the user. It was decided to weight factors controlling each objective by the data quality associated with that factor. However, it was decided to maintain RIOS's suggestion that each factor category is equal (on-pixel source, on-pixel retention, downslope retention, and upslope source). This left the question as to how the weighting of ES objectives would affect the results.

The results (summarized in Figure 22) demonstrated that differences between the ES objective weighting scenarios were minimal and insignificant for the analysis techniques used. The technique used

to check for differences in "soil loss avoided" was a regular sampling (100-m spacing) of the raster containing values for the soil loss avoided. Sampling at activity sites only was not possible because the three scenarios are not doing activities at the same locations. The technique used was therefore "fair" but unable to capture differences at the catchment scale; hence the insignificant difference between means. Despite this, a difference of about 2,000 tons existed between the scenarios weighting baseflow as the highest and lowest (as seen in the third column of Figure 22).

Figure 22: Results summary for the three scenarios at the 600-hectare benchmark

Scenario	Ave. soil loss avoided at sampled points (± st. dev)[1]	Cumulative soil loss avoided for whole catchment (tons)	Change in annual ΔS+D on rainfed cropland (mm)
EC1 BF1	6.74 ± 31.6	18,541	+46
EC2 BF1	7.01 ± 31.9	19,329	-
EC1 BF0	7.75 ± 32.7	20,448	+51

[1] At regularly-spaced (100-m) sample points throughout catchment

Impact on baseflow was predicted through a simplified water balance, calculated for a typical soil column of rainfed cropland. Only the precipitation, evapotranspiration, runoff, and soil storage/drainage (ΔS + D) terms were considered. The most differently weighted scenarios (EC1BF1 and EC1BF0) were checked for differences between their monthly ΔS+D values, and again significance could not be proven. This was also quite apparent from the annual ΔS+D values, which varied by just a few millimeters between scenarios.

Despite the apparent insignificant differences between the weighting of ES objectives in RIOS, it is necessary to take a look at why a smaller BF weighting produced better (even if only marginally better) soil loss and ΔS+D results. When EC was weighted higher, it produced better erosion control results; however, it also produced marginally better DS+D results. The answer could be quite simple. The water balance analysis looked at only rainfed cropland, of which 50 additional hectares were converted under the EC1BF0 scenario relative to the EC1BF1 scenario. This meant that the average soil column for the EC1BF0 scenario lost more to ETc but lost less due to runoff. Interestingly, the associated increase in ETc for EC1BF0 (just 2 mm annually) was dwarfed by the savings due to less runoff (8 mm annually). Although these numbers are small and uncertainty is high because of the simplicity of the analysis, they could tell us something about the effect of SWC measures on the annual water balance. Measures that integrate biological and physical components (e.g. shrubs planted at the terrace edge) render more water lost to ETc but more runoff retained; however, it seems that the bigger change is produced by the greater retention of runoff.

It should be noted that several factors were not accounted for in the simplified water balance analysis. The assumptions of the analysis are given in the Methods section. It is necessary to discuss how some of these assumptions could have had an impact on the results obtained, and particularly how the neglect of some "small" factors could have potentially widened the gap between scenarios had they been considered. Since the analysis regarded a soil column unit as the control volume, upslope or downslope effects such as runoff retention or flow convergence/divergence was not considered. Since upslope source and downslope retention are key factors in RIOS's spatial selection (accounting for half of the total factor weights), these important aspects of RIOS are not captured in the analysis. Secondly, the effect of mulch (like leaf litter produced by the shrub) and shading by the shrub is not considered, although it could have had implications on soil evaporation. Thirdly, the ability of shrub roots to

reestablish the original flow paths from the soil surface to deeper layers is not considered even though the use of deep-rooting species has been identified as a mechanism for re-establishing these runoff-reducing pathways (Tebebu et al. 2015). Fourth, since spatial variation was neglected in the analysis, the influence of soil physical properties on runoff generation played no role. Finally, the ability of SWC measures to increase productivity due to the saving of fertile top soil – and the associated increases in SOM and water-holding capacity – would influence the ETc and runoff terms of the water balance; this is, however, only captured in the runoff calculation from the post-SWC curve numbers.

Despite some differences between scenarios and the possibility that the choice of analysis techniques simply did not capture these differences, we must conclude that ES objective weighting in RIOS produced insignificant differences. To discover why this was the case, we must turn to the various factors used in the relative rankings for the EC and BF objectives (Table 7 and Table 8). Among these two sets of factors were two pairs of factors that matched identically after normalization: the upslope source index rasters were identical due to the weighted flow accumulation algorithm used (see 2.8.1.4), and the R-factor and mean annual rainfall rasters were identical since they are linearly related. These two matches accounted for just over 28% similarity. Furthermore, sediment retention efficiency in the EC ranking and Manning's surface roughness in the BF ranking are more-or-less linearly related, leading to an additional partial similarity of 15%.

The remaining 57% of the total weights of the factors were technically different. It is these factors that had the potential of creating dissimilarities between the EC and BF rankings. These factors were K-factor for EC and soil texture, slope, and soil depth for BF. Of these, K-factor (for EC) and soil depth (for BF) – both sourced from 250-m resolution AfSIS predictions – exhibited east-to-west gradients that would have produced a similar rankings for either objective (and had similar weights). This left soil texture and slope index as the two datasets that could potentially produce different rankings for the BF objective. Unfortunately, soil texture's weight was reduced due to low data quality (see 0), and slope, representing about 9% of the total BF ranking, thus became the main differentiator.

Clearly the problem was partially one of data quality. Future runs of RIOS that wish to investigate the weighting of ES objectives should realize that producing distinctive rankings for different objectives depends on the extent to which input data varies spatially, showing local peaks and minima or differences between LULC types. Moreover, the problem just described was exacerbated by the relative small size of the catchment (~25 km² versus one of the ~1000 km² catchments from TNC 2015). Spatial variations often become more pronounced when you "zoom out," even when using lower quality data.

Nevertheless, this experience raises the question as to whether the appropriate factors and factor weights are being used by RIOS. The literature review for this study has made it apparent that between the two ES's, far more is known about the factors that control soil stability (erosion) than those that control baseflow. In her review of watershed characteristics' effects on baseflow, Price (2011) highlights some of the known key drivers (topography, soils, land cover, and climate) of baseflow, but concludes that still relatively little is known about baseflow response to mitigation strategies and the relative influences of various factors; this is partially because studies have not explored multiple addressed multiple aspects of the watershed in explaining baseflow and because of the range of methodologies used that make comparisons difficult. RIOS simplifies the matter by assuming that locations that have the most potential to infiltrate water will be the most likely to enhance baseflow. Regardless of whether or not this is an oversimplification, future research will be necessary to improve these current assumptions.

4.2.3 A critique of RIOS

A number of models that can be used to investigate SWC at the catchment scale are available today; widely used models include conceptual models such as SWAT, AGNPS, or AGWA as well as physical models such as ANSWERS and WEPP (Fakhri et al. 2014). All of these models allow the user to predict runoff, erosion, and watershed sediment yield for a given set of conditions. Some tools that have even been designed for the valuation of ES's are available; InVEST (which contains 15 different terrestrial, freshwater, and marine modules) and ARIES represent "a new breed" of ES models allowing for the spatial visualization of ES's across a landscape (Vigerstol 2011).

RIOS, however, fulfills a different niche. Its utility is unique in two ways. Firstly, it attempts to guide the spatial distribution of interventions based on the "responsiveness" of a land unit relative to other land units. Secondly, it attempts to find "responsive" places based upon set of factors that control the ES or ES's of interest. Since the above models (or any other models known to the author) do not attempt to inform the user of most "responsive" locations, the RIOS approach could be said to fill a unique gap in the realm of conservation planning.

Its premise would seem attractive given the trend for increased regard for ES and targeting them. However, little literature is thus far available on the use of RIOS, and no studies have yet compared the RIOS approach to targeting ES objectives to other means of performing the same task. In fact, studies investigating the impacts of SWC utilize a variety of approaches for selecting areas for conservation. Oftentimes, areas are selected based upon a baseline soil loss prediction which is used to distinguish erosion risk classes across a landscape, and intervention is suggested to start with the most severe erosion risk class. Such approaches mean that only a single ES is targeted. Ideally, RIOS could help a practitioner decide which areas to conserve while targeting multiple ES objectives, and perhaps even weight them differently according to stakeholder preferences.

Other strengths of RIOS include the flexibility to adapt the simulation to the available data quality (as in this study) or to use new knowledge regarding the contribution of biophysical factors to an ES objective in order to improve the model. Additionally, the tool is open-source and can be used in conjunction with other open-source tools like QGIS, GRASS, and InVEST.

Despite its unique niche and advantages, this study recognizes a number of shortcomings of RIOS. Some of these have already been mentioned. Biophysical inputs do not take into account relative differences in compaction between LULC classes. The upslope source index raster is the same for both ES and BF after normalization due to the weighted flow accumulation algorithm used. Though originally thought to be a disadvantage, the annual time step in RIOS (as opposed to shorter time steps) seems to be appropriate since this is a planning tool that must consider "average" conditions (long-term rainfall, etc).

The greatest shortcomings of RIOS were identified as the following:

1. The high uncertainty of the user regarding the weighting of the key factors for each ES objective (discussed in 4.2.2).

2. The failure to integrate post-SWC benefits into the selection of activities. This could be achieved either by a.) a cost/monetary basis or b.) a biophysical parameter basis.

a. Cost/monetary basis: Pixel and activity selection is currently cost-dominated if the activity prices differ greatly (if costs are included). If the tool allowed the user to distinguish between the immediate costs and future benefits, the "return-on-investment" maps used to select pixels would also incorporate those benefits, thereby lessening the dominance of costs on the output. This is more realistic since often the most degraded areas require the most investment to rehabilitate but also offer great benefit in doing so. Ayele et al. (2015) found a marginal rate of return of 10 for gully rehabilitation in the Ethiopian highlands. Accounting for the benefits within the cost calculation is currently not practical because RIOS uses these costs to decide when the budget has been spent.

b. Biophysical parameter basis: During its ranking procedure, RIOS does not take into account the extent to which an activity will alter the C-factor, P-factor and sediment retention of a piece of land. In this study, this led to RIOS choosing to implement about the same amount of vegetative fencing as grass strips (Figure 16), although the former is highly labor inefficient (Table 20) in terms of the labor input per ton of soil loss avoided. Accounting for the relative change in biophysical coefficients that an activity can achieve could improve the "return-on-investment" calculation by incorporating soil loss avoidance as a benefit with a user-given value.

3. The non-availability of a companion tool capable of predicting the post-SWC impact on catchment baseflow. This study attempted to quantify the impact of following RIOS recommendations by analyzing soil loss with the InVEST tool and baseflow with a simple water balance. InVEST makes the post-analysis easy by requiring nearly identical data inputs to RIOS. A parallel tool for quantifying baseflow at the catchment scale is necessary. Hunink & Droogers (2015) paired RIOS with SWAT for the analysis, but data adaptation was necessary and time-consuming. Within InVEST is also an annual water yield model, but this is not useful for quantifying impact on dry season baseflow. Fortunately, the Natural Capital Project (the creators of RIOS and InVEST) has said that a "seasonal water yield model" is in development.

4.3 Soil and water conservation: a broader perspective

This study focused on erosion and spatial modelling of SWC activities and not the characteristic differences between activities. Activities were pre-determined for LULC - slope class combinations based on government recommendations. Differences between the effects of the activities were only captured in the selection of the post-SWC biophysical coefficients (C-factor, sediment retention, and P-factor). While focusing on maximizing EC and BF ecosystem service objectives, in reality, a multitude of factors determine the appropriateness of a measure to a certain area, the attractiveness of a measure to the farmer, and the short- and long-term costs and benefits associated it.

Through a multi-criteria analysis of farmer preferences among SWC activities, Adimassu et al. (2013) found that farmers from a central highlands watershed weighted economic criteria over technical or stability criteria. Table 21 attempts to illustrate the financial aspect of three commonly-seen activities suited to cropland. The adoption or (forced adoption) of SWC has two predominant financial implications for the farmer: a loss in total cropped area due to the space taken up by the structure or new vegetation, and a long-term relative yield increase due to the enhancement of on-site ES's (see 1.2) (Herweg & Ludi 1999). There is clearly a large variability between activities in terms of their financial

attractiveness (Table 21). When an activity is not implemented as part of a mass movement labor campaign, significantly more resources (labor) have to be invested by the farmer.

Table 21: Cost-benefit breakdown for the farmer for three common SWC activities

SWC activity	Labor cost (PD/ha)[1]	Fraction of cropping area lost [2]	Relative long-term impact on yield	For 10 years[8]		Benefits minus costs for 10 years	
				Costs to farmer (birr/ha)[6]	Benefits to farmer (birr/ha)[7]	...if labor is free (birr/ha)	... if self-implemented (birr/ha)[9]
Fanya juu or soil bunds	140	5.8% (2-5%)	10%[3]	3499	3619	121	-2492
Grass strips	27	9%	25%[4]	5429	9048	3619	3115
Stone bunds	290	10% (5-25%)	8%[5]	6032	2895	-3137	-8548

[1] as discussed in 2.8.4; [2] calculated based on slope class where activity is recommended; in parenthesis are values from Teshome et al. for NW Ethiopia; [3] Teshome et al. (2013) for semi-arid NW Ethiopia; [4] Tenge et al. (2005) for humid Tanzanian highlands; [5] Nyssen et al. (2007) for semi-arid N Ethiopia; [6] in terms of crop yield forfeited due to loss of cropping area; [7] in term of positive impacts on yield seen starting in the 5th year based on Herweg & Ludi's (1999) estimation; [8] based on an 2010-16 average wheat (as proxy for barley) price of 7.13 ETB (Ethiopian birr) per kg at Debre Markos (Amhara Region) (FAO 2016) and an average barley yield of 846 kg/ha for Vertisol cultivation in central highlands (Gebre 1988); [9] based on Balana et al.'s (2012) approximation of wages the state pays for labor, 0.87 USD/PD and the current exchange rate as of March 2016 of 21.45 ETB/USD

The analysis in Table 21 disregards the substantial value gained from increased fodder resources as a result of incorporating agroforestry with SWC structures. While Herweg & Ludi (1999) state that this can hardly replace food production from the farmer's perspective, Adimassu et al. (2013) found that when given a choice between SWC structures with or without multi-purpose vegetation planted atop (a leguminous shrub and two grasses were the options), vegetative options were ranked higher.

What is clear from this study and many other studies is that conservation of soil and water is a key issue for Ethiopia. This particular study shows that it takes many years to make a dent in human-induced soil erosion that has had centuries to grow in severity. Waiting for labor campaigns to rehabilitate or preserve parts of the highland landscape means that many areas will become severely degraded before there is time to attend to them. SWC planning approaches like the one attempted in this study are, of course, important to public sector land resource planners. Approaches that integrate field observations, participatory input, and spatial analysis tools like GIS add dimension and perspective to land use planning. More effective means of SWC planning should continually be explored.

There is also a niche to be filled in making SWC more attractive to individual land users so as to promote individual adoption. One way could be to further explore the possibility of making SWC multi-purpose, as with agroforestry. Another option to increase widespread adoption is through payments for ecosystem services. One concept currently being explored in Kenya is the payment by offsite beneficiaries (bottling companies, hydropower companies, and other downstream water users) for SWC of the upland contributing areas (see Hunink et al. 2012 or Kauffman et al. 2014).

Indeed, a potential key to the future of SWC is to take into account its offsite benefits in addition to onsite benefits. In Gudo Beret, SWC implemented on 52% of the total cropland resulted in a 30% increase in annual soil water storage and drainage. This could have meaningful implications in an area where farmers report the lowering of the water table, the disappearance of natural springs, and dry season stream discharge at all-time lows. These forms of degradation have impacts on livestock (traveling times to watering holes), the usability of water access infrastructure, and irrigation capacity. Nevertheless, in rural areas like Gudo Beret, it is problematic to encourage SWC in uplands based on the offsite benefit premise since these outcomes primarily benefit downslope or downstream users.

5 Conclusions

This thesis focused on the use of SWC planning tools to address two ES's, erosion control and dry season baseflow enhancement. The study site was the Gudo Beret catchment located in the central highlands of Ethiopia. The aims of the thesis were to 1) model the current soil loss risk for the catchment, 2) to simulate a spatial allocation of recommended SWC activities throughout the catchment while giving different weights to the ES objectives, and 3) to estimate potential changes in soil loss and in the water balance as a result of those simulated activity scenarios. In the study, a number of tools and procedures were used. Field observations and measurements were taken in order to map erosion hotspots. Community focus groups were consulted in order to prioritize land management-related issues and to locate areas of the landscape seen as priorities for SWC implementation. A LULC map was generated with the help of remote sensing tools and field observations. The spatial modelling procedures were performed using GIS-based tools. A water balance was calculated with the help of daily meteorological data recorded at Gudo Beret. Literature reviews helped to fill data gaps.

The current soil loss risk was predicted for the Gudo Beret catchment using the RUSLE model. Regardless of the metric being used as a tolerable soil loss rate, erosion at Gudo Beret was found to far exceed safe limits. Soil loss on rainfed cropland exceeded one of the suitable metrics by 19-fold. Estimates of soil loss compared favorably with measurements and estimates from other sub-humid highland catchments in Ethiopia. Both the estimates for rainfed cropland and the catchment-wide estimates seem well within reason for a typical central highland area. However, these estimates have not fully accounted for the contribution of gullies to total soil loss. Due to the prevalence of gullies across the Gudo Beret landscape and the results of other studies that show that gullies contribute significantly to total losses – it is presumed that soil loss estimates have been under-predicted for some LULC classes and for the catchment at-large. Among a number of discussed limitations of the RUSLE model, two were discussed as expressly confining; that is, the inability of the model to predict gully erosion and the inability of the model to capture seasonality (which is especially pronounced in the study region). It is, however, recognized that work-arounds are possible.

The next part of the study was a simulation of SWC activities across the Gudo Beret catchment using the RIOS tool. RIOS is a relatively new tool based on a unique approach. It's based upon the assumption that a small set of spatially-mapped biophysical factors can be used to locate those places in the landscape most likely to be "responsive" to SWC. Literature describing its application at other sites is scarce and studies comparing it to other techniques are not yet available. One recent application of the tool in Kenya has used RIOS to generate different scenarios featuring different spatial allocations of activities and then SWAT to assess the impact of implementing those scenarios. In this way, the study was able to quantify the benefits of SWC in monetary terms for the onsite and offsite beneficiaries, the farmer and downstream water users, respectively.

Since the RIOS tool allows for the relative weighting of different ES objectives, it was perceived that this function could potentially be used as a means for producing alternative outcomes to meet different onsite and offsite conservation goals. Under this premise, three scenarios were investigated to see how ES objective weighting in RIOS affects the outcome. These scenarios focused on two ES's: erosion control (EC) and dry season baseflow (BF) enhancement – two conservation goals of the Gudo Beret community. In the scenarios, EC and BF were weighted according to three ratios: 1:1, 2:1, and 1:0.

The RIOS-generated activity maps showed some differences in the locations chosen for activities as well as the degree to which certain activities were chosen. Soil loss was then estimated for the entire catchment for the hypothetical scenarios. A simplified water balance was performed to represent the typical changes in runoff, evapotranspiration, and soil water storage/drainage for all the rainfed cropland in the catchment. The analysis that followed found that soil loss and water balance calculations performed for the post-SWC scenarios resulted in insignificant differences.

The lack of significance between outcomes of the scenarios was attributed to low data quality for some inputs and the relatively small catchment size – both of which suppressed spatial variability which is needed to produce different relative rankings for the ES objectives in RIOS. It is also recognized that controls on baseflow are not fully understood by the scientific community; the set of factors used in RIOS could therefore improve in the future. Three main criticisms of RIOS were given. There is a high uncertainty in the weighting of the key factors for each of the ES objectives. The tool does not account for post-SWC benefits during the activity selection and allocation process. There is not yet an easy-to-use companion tool to aid in estimating the impact of a RIOS scenario on baseflow.

Modelling approaches for SWC planning are of relevance to scientists as well as land use planners. Participatory tools, field observations, and spatial analysis tools (GIS) tools can be especially useful when used in combination, as in this study. They can be used to develop SWC options that are compelling to stakeholders, both on- and off-site. It was also recognized that the success of SWC has to involve farmers, for which short- and long-term costs and benefits are of particular relevance. As Ethiopia continues to experience declines in land productivity estimated at 2.2% per annum (Tamene & Vlek 2008), the need for effective SWC measures on a larger scale has never been so poignant. Enhancing the onsite benefits derived from SWC adoption will be key as well as paying more attention to offsite benefits. The future of SWC efforts in Ethiopia will need to be creative and innovative in designing pathways for uptake that see beyond business-as-usual.

6 References

Adgo, E., A. Teshome, and B. Mati (2013), Impacts of long-term soil and water conservation on agricultural productivity: The case of Anjeni watershed, Ethiopia, Agric. Water Manag., 117, 55–61, doi:10.1016/j.agwat.2012.10.026.

Adimassu, Z., Gorfu, B., Nigussie, D., Mowo, J., & Hilemichael, K. (2013). Farmers' preference for soil and water conservation practices in central highlands of Ethiopia. African Crop Science Journal, 21(1), 781-790.

Adimassu, Z., Mekonnen, K., Yirga, C., & Kessler, A. (2014). Effect of soil bunds on runoff, soil and nutrient losses, and crop yield in the central highlands of Ethiopia. *Land Degradation & Development*, *25*(6), 554-564.Aksoy, H., & Kavvas, M. L. (2005). A review of hillslope and watershed scale erosion and sediment transport models. *Catena*, *64*(2), 247-271.

Allen, R. G., Pereira, L. S., Raes, D., & Smith, M. (1998). Crop evapotranspiration-Guidelines for computing crop water requirements-FAO Irrigation and drainage paper 56 (M-56, ISBN 92-5-104219-). *Food and Agriculture Organization of the United Nations, Rome (http://www. fao. org/docrep/X0490E/x0490e00. htm# Contents).*

Arcement Jr, G. J., & Schneider, V. R. (1989). Guide for Selecting Manning's Roughness Coefficients for Natural Channels and Flood Plains United States Geological Survey Water-supply Paper 2339. *pubs. usgs. gov/wsp/2339/report. pdf.*

Arnold, J. G., J. R. Kiniry, R. Srinivasan, J. R. Williams, E. B. Haney and S. L. Neitsch (2012). Appendix A: Model databases. In: Soil and Water Assessment Tool (SWAT) input/output documentation. Temple, Texas, Texas Water Resources Institute, US Department of Agriculture - Agricultural Research Service. pp 563-617.

Auerswald, K., Fiener, P., Martin, W., & Elhaus, D. (2014). Use and misuse of the K factor equation in soil erosion modeling: An alternative equation for determining USLE nomograph soil erodibility values. *Catena*, *118*, 220-225.

Auerswald, K., Fiener, P., Martin, W., & Elhaus, D. (2015). Corrigendum to "Use and misuse of the K factor equation in soil erosion modeling"[Catena 118 (2014) 220–225]. *Catena.*

Ayele, G. K., Gessess, A. A., Addisie, M. B., Tilahun, S. A., Tebebu, T. Y., Tenessa, D. B., ... & Steenhuis, T. S. (2015). A Biophysical and Economic Assessment of a Community-based Rehabilitated Gully in the Ethiopian Highlands. Land Degradation & Development.

Badege, B. (2001). Deforestation and land degradation in the Ethiopian highlands: a strategy for physical recovery. Northeast African Studies 8 (1), 7–25.

Balana, B. B., Muys, B., Haregeweyn, N., Descheemaeker, K., Deckers, J., Poesen, J., ... & Mathijs, E. (2012). Cost-benefit analysis of soil and water conservation measure: The case of exclosures in northern Ethiopia. *Forest Policy and Economics*, *15*, 27-36.

BCEOM. (1998). Abbay River Basin Integrated Development Master Plan, Main Report. Ministry of Water Resources: Addis Ababa.

Bewket, W., & Sterk, G. (2005). Dynamics in land cover and its effect on stream flow in the Chemoga watershed, Blue Nile basin, Ethiopia. Hydrological Processes, 19(2), 445-458.

Bewket, W., Sterk, G. (2002). Farmers' participation in soil and water conservation activities in the Chemoga watershed, Blue Nile basin, Ethiopia. Land Degradation and Development, 13, 189–200.

Botschek, J., Sauerborn, P., Skowronek, A., Wolff, R. (1997). Tolerierbarer Bodenabtrag und Bodenbildung—Konzepte und Perspektiven. Mitt. Dtsch. Bodenkdl. Ges. 83, 87–90.

Candela, A.N.G.E.L.A., Noto, L. V., & Aronica, G. (2005). Influence of surface roughness in hydrological response of semiarid catchments. *Journal of Hydrology*, *313*(3), 119-131.

Cook, B.G., Pengelly, B.C., Brown, S.D., Donnelly, J.L., Eagles, D.A., Franco, M.A., Hanson, J., Mullen, B.F., Partridge, I.J., Peters, M. and Schultze-Kraft, R. (2005). Tropical Forages: an interactive selection tool., [CD-ROM], CSIRO, DPI&F(Qld), CIAT and ILRI, Brisbane, Australia.

Dagnew, D. C., Guzman, C. D., Zegeye, A. D., Tibebu, T. Y., Getaneh, M., Abate, S., ... & Steenhuis, T. S. (2015). Impact of conservation practices on runoff and soil loss in the sub-humid Ethiopian Highlands: The Debre Mawi watershed. Journal of Hydrology and Hydromechanics, 63(3), 214-223.

Datta, P. S., & Schack-Kirchner, H. (2010). Erosion relevant topographical parameters derived from different DEMs—A comparative study from the Indian Lesser Himalayas. *Remote Sensing*,*2* (8), 1941-1961.

Descheemaeker, K., Poesen, J., Borselli, L., Nyssen, J., Raes, D., Haile, M., ... & Deckers, J. (2008). Runoff curve numbers for steep hillslopes with natural vegetation in semi-arid tropical highlands, northern Ethiopia. Hydrological Processes, 22(20), 4097-4105.

Desmet, P.J.J., Govers, G. (1996). A GIS procedure for automatically calculating the USLE LS factor on topographically complex landscape units. J. Soi 51, 427–433.

Desta, L., Carucci, V., Wendem-Ageňehu, A., and Abebe, Y. (eds). (2005). Community Based Participatory Watershed Development: A Guideline. Ministry of Agriculture and Rural Development, Addis Ababa, Ethiopia.

Duan, X., Y. Xie, T. Ou, and H. Lu (2011). Effects of soil erosion on long-term soil productivity in the black soil region of northeastern China, CATENA, 87(2), 268–275, doi:10.1016/j.catena.2011.06.012.

EFAP (Ethiopian Forestry Action Program) (1994). The Challenge for Development. Volume II. Addis Ababa, Ethiopia.

Ellis-Jones, J. Mekonnen, K., Gebreselassie, S. and Schulz, S. (2013). Challenges and opportunities to the intensification of farming systems in the Highlands of Ethiopia: Results of a participatory community analysis. Addis Ababa: International Potato Center.

Engman, E. T. (1986). Roughness coefficients for routing surface runoff. *Journal of Irrigation and Drainage Engineering*, *112*(1), 39-53.

EPA (Environmental Protection Authority) (1997). Environmental Policy of Ethiopia, Addis Ababa.

Eweg HPA, van Lammeren R. (1996). The application of geographic information system at the rehabilitation of degraded and degrading areas of Tigray, Ethiopia. Research Report, Wageningen Agricultural University, Wageningen.

Fakhri, M., Dokohaki, H., Eslamian, S., Farsani, I. F., & Farzaneh, R. (2014). Flow and Sediment Transport Modeling in Rivers (Chapter 13). In: Eslamian, S. (Ed.). (2014). Handbook of engineering hydrology: Fundamentals and applications. CRC Press.

FAO (2016). Food Price Monitoring and Analysis (FPMA) Tool. FAO Global Information and Early Warning System. Online database http://www.fao.org/statistics/databases/en/ (accessed 25 March 2016).

FAO, I. (1990). Guidelines for soil profile description. *FAO, Rome, Italy.*

Fleiss, J. (1981). Statistical Methods for Rates and Proportions. 2nd edn John Wiley: New York.

Gebre, H. (1988). Crop agronomy research on Vertisols in the central highlands of Ethiopia: Iar's experience. In *The Fifth Regional Wheat Workshop: For Eastern, Central, and Southern Africa and the Indian Ocean: Antsirabe, Madagascar, October 5-10, 1987* (p. 152). CIMMYT.

Gessesse, B., Bewket, W., & Bräuning, A. (2015). Model-based characterization and monitoring of runoff and soil erosion in response to land use/land cover changes in the Modjo watershed, Ethiopia. *Land Degradation & Development*, *26*(7), 711-724.

GRASS Development Team (2015). Geographic Resources Analysis Support System (GRASS) Software, Version 7.0. Open Source Geospatial Foundation. http://grass.osgeo.org

Haregeweyn, N., Poesen, J., Verstraeten, G., Govers, G., Vente, J., Nyssen, J., ... & Moeyersons, J. (2013). Assessing the performance of a spatially distributed soil erosion and sediment delivery model (WATEM/SEDEM) in Northern Ethiopia. *Land Degradation & Development*, *24*(2), 188-204.

Haregeweyn, N., Tsunekawa, A., Nyssen, J., Poesen, J., Tsubo, M., Meshesha, D. T., ... & Tegegne, F. (2015). Soil erosion and conservation in Ethiopia A review. *Progress in Physical Geography.*

Hargreaves, G. H., & Samani, Z. A. (1985). Reference crop evapotranspiration from temperature. Applied engineering in agriculture,1(2), 96-99.

Hawkins, R. H., Ward, T. J., Woodward, D. E., & Van Mullem, J. A. (2009). Curve number hydrology. ASCE publication.

Healy, R. W. (2010). Estimating groundwater recharge. Cambridge University Press.

Hengl T, de Jesus JM, MacMillan RA, Batjes NH, Heuvelink GBM, et al. (2014). SoilGrids1km — Global Soil Information Based on Automated Mapping. PLoS ONE 9(8): e105992. doi:10.1371/journal.pone.0105992

Hengl T, Heuvelink GBM, Kempen B, Leenaars JGB, Walsh MG, Shepherd KD, et al. (2015) Mapping Soil Properties of Africa at 250 m Resolution: Random Forests Significantly Improve Current Predictions. PLoS ONE 10(6): e0125814.doi:10.1371/journal.pone.0125814

Herweg, K., & Ludi, E. (1999). The performance of selected soil and water conservation measures—case studies from Ethiopia and Eritrea. *Catena*,*36*(1), 99-114.

Hijmans, R. J., Cameron, S. E., Parra, J. L., Jones, P. G., & Jarvis, A. (2005). Very high resolution interpolated climate surfaces for global land areas. *International journal of climatology*, *25*(15), 1965-1978.

Hudson, N.W. (1986): Soil conservation. Batsford Ltd, London, UK: 324 pp

Hunink, J. E., & Droogers, P. (2015). Impact assessment of investment portfolios for business case development of the Nairobi Water Fund in the Upper Tana River, Kenya. *Wageningen, The Netherlands.*

Hunink, J. E., Droogers, P., Kauffman, S., Mwaniki, B. M., & Bouma, J. (2012). Quantitative simulation tools to analyze up-and downstream interactions of soil and water conservation measures: Supporting policy making in the Green Water Credits program of Kenya. *Journal of environmental management*,*111*, 187-194.

Hurni, H. (1981). Nomograph for the design of labour-intensive soil conservation measures in rain-fed cultivations. In *Soil conservation problems and prospects:[proceedings of Conservation 80, the International Conference on Soil Conservation, held at the National College of Agricultural Engineering, Silsoe, Beford, UK, 21st-25th July, 1980]/edited by RPC Morgan.* Chichester [England], Wiley, c1981.

Hurni, H. (1985). Soil conservation manual for Ethiopia: a field manual for conservation implementation. *Soil Conservation Research Project, Addis Ababa.*

Hurni, H. (1998). Agroecological Belts of Ethiopia: Explanatory notes on three maps at a scale of 1: 1,000,000. *Soil conservation research program of Ethiopia, Addis Ababa, Ethiopia*, 31.

Kauffman, S., Droogers, P., Hunink, J., Mwaniki, B., Muchena, F., Gicheru, P., ... & Bouma, J. (2014). Green Water Credits–exploring its potential to enhance ecosystem services by reducing soil erosion in the Upper Tana basin, Kenya. *International Journal of Biodiversity Science, Ecosystem Services & Management*, *10*(2), 133-143.

Kelemu, K., Gebrekirstos, A., and Hadgu, K. (2014). Innovation platforms for improving productivity in mixed farming systems in Ethiopia: Institutions and Modalities. Nairobi: ICRAF.

Kinnell, P. I. A. (2010). Event soil loss, runoff and the Universal Soil Loss Equation family of models: A review. *Journal of Hydrology*, *385*(1), 384-397.

Kizito, F., Cordingley, J., Nganga, K., Bossio, D., & Kihara, F. (2014). WLE Innovation Fund, 2013/2014 CIAT Technical Report Submitted to the Water Land and Ecosystems Program. *Using an ecosystems approach for securing water and land resources in the Upper Tana Basin.*

Kuria, A., Lamond, G., Pagella, T., Gebrekirstos, A., Hadgu, K., and Sinclair, F. (2014). *Local Knowledge of Farmers on Opportunities and Constraints to Sustainable Intensification of Crop-Livestock-Trees Mixed Systems in Basona Woreda, Amhara Region, Ethiopian Highlands.* Addis Ababa: ILRI.

Lal, R. (1981). Soil conservation: Preventive and control measures. In *Soil conservation problems and prospects:[proceedings of Conservation 80, the International Conference on Soil Conservation, held at the National College of Agricultural Engineering, Silsoe, Beford, UK, 21st-25th July, 1980]/edited by RPC Morgan.* Chichester [England], Wiley, c1981.

Lal, R. (1998). Agronomic consequences of soil erosion. In: DeVries, P., Agus, F., Kerr, J. (Eds.), Soil Erosion at Multiple Scales: Principals and Methods for Assessing Causes and Impacts. International Board for Soil Research and Management (IBSRAM), CABI Publishers, Wallingford, UK, pp. 149–160.

Landis, J. R., & Koch, G. G. (1977). The measurement of observer agreement for categorical data. *Biometrics*, 159-174.

Millennium Ecosystem Assessment (2005). Ecosystem and human well-being: biodiversity synthesis. World Resources Institute, Washington, DC.WBISPP. (2004). A National Strategic Plan for the Biomass Energy Sector, Addis Ababa, Ethiopia.

Morgan, D. L. (1996). Focus groups as qualitative research (Vol. 16). Sage publications.

Morgan, R. P. C. (2005). Soil erosion and conservation. National Soil Resources Institute. Cranfield University.

Mulengera, M. K., and R. W. Payton (1999), Modification of the productivity index model, Soil Tillage Res., *52*(1-2), 11–19, doi:10.1016/S0167-1987(99)00022-7.

Mulligan, M., Benıtez-Ponce, S., Lozano-V, J. S., & Sarmiento, J. L. (2015). 12 Policy support systems for the development of benefit-sharing mechanisms for water-related ecosystem services. *Water Ecosystem Services: A Global Perspective*, 99.

Natural Resources Conservation Service (NRCS), 1999. National Soil Survey Handbook—Title 430-VI, http://www.statlab.iastate. edu/soils/nssh/.

Neitsch, S. L., Arnold, J. G., Kiniry, J. R., Williams, J. R., & King, K. W. (2005). SWAT theoretical documentation version 2005. *Soil and Water Research Laboratory, ARS, Temple Texas, USA.*

Neteler, M. & Mitasova, H. (2008). Open Source GIS - A GRASS GIS Approach. 3d Ed. Springer Science+Buisness Media. New York.

Nigussie, T. A., Fanta, A., Melesse, A. M., & Quraishi, S. (2014). Modeling rainfall erosivity from daily rainfall events, upper Blue Nile basin, Ethiopia. In *Nile River Basin* (pp. 307-335). Springer International Publishing.

Nill, D., Schwertmann, U., Sabel-Koschella, U., Berhard, M. B. J., & Breuer, J. (1996). Soil erosion by water in Africa. Principles, prediction and protection. GTZ, Germany, 292.

NRCS (2004). National Engineering Handbook: Part 630—Hydrology. USDA Soil Conservation Service: Washington, DC, USA.

NRCS, U. Soil Survey Division Staff (1993) Soil Survey Manual. Soil Conservation Service. *US Department of Agriculture Handbook*, *18*, 315.

Nyssen, J., Poesen, J., Gebremichael, D., Vancampenhout, K., D'aes, M., Yihdego, G., ... & Haregeweyn, N. (2007). Interdisciplinary on-site evaluation of stone bunds to control soil erosion on cropland in Northern Ethiopia. *Soil and Tillage Research*, *94*(1), 151-163.

Nyssen, J., Poesen, J., Moeyersons, J., Haile, M., & Deckers, J. (2008). Dynamics of soil erosion rates and controlling factors in the Northern Ethiopian Highlands–towards a sediment budget. *Earth surface processes and landforms*, *33*(5), 695-711.

Osman, M. (2001). Rainfall and its erosivity in Ethiopia with special consideration of the central highlands.

Panagos, P., Meusburger, K., Ballabio, C., Borrelli, P., & Alewell, C. (2014). Soil erodibility in Europe: A high-resolution dataset based on LUCAS. *Science of the total environment*, *479*, 189-200.

Pierce, F. J., W. E. Larson, R. H. Dowdy, and W. A. P. Graham (1983), Productivity of soils: Assessing long-term changes due to erosion, J. Soil Water Conserv., 38(1), 39–44.

Pimentel, D., Terhune, E. C., Dyson-Hudson, R., Rochereau, S., Samis, R., Smith, E. A., ... & Shepard, M. (1976). Land degradation: effects on food and energy resources. Science, 194(4261), 149-155.

Poesen, J., Nachtergaele, J., Verstraeten, G., & Valentin, C. (2003). Gully erosion and environmental change: importance and research needs. *Catena*, *50*(2), 91-133.

Price, K. (2011). Effects of watershed topography, soils, land use, and climate on baseflow hydrology in humid regions: A review. *Progress in physical geography*, *35*(4), 465-492.

Rahmato, D. (2001). Environmental change and state policy in Ethiopia: lessons from past experience. Forum for Social Studies.

Renard, K. G., Foster, G. A., Weesies, G. A. & McCool, D. K. (1997). Predicting soil erosion by water: a guide to conservation planning with RUSLE. USDA. Agriculture Handbook No. 703, Washington, DC, USA.

Renard, K. G., Foster, G. R., Weesies, G. A., & Porter, J. P. (1991). RUSLE: Revised universal soil loss equation. *Journal of soil and Water Conservation*, *46*(1), 30-33.K value.

Renschler, C. S., & Harbor, J. (2002). Soil erosion assessment tools from point to regional scales—the role of geomorphologists in land management research and implementation. *Geomorphology,47*(2), 189-209.

Reusing, Matthias (1998). Monitoring of forest resources in Ethiopia, Ministry of Agriculture in cooperation with German Agency for Technical Cooperation (GTZ), April, Addis Ababa.

Rockström, J. (2003), Water for food and nature in drought-prone tropics: vapour shift in rainfed agriculture., Philos. Trans. R. Soc. Lond. B. Biol. Sci., *358*(1440), 1997–2009, doi:10.1098/rstb.2003.1400.

Roose, E. (1996). *Land husbandry: components and strategy* (Vol. 70). Rome: FAO.

Sharp, R., Tallis, H.T., Ricketts, T., Guerry, A.D., Wood, S.A., Chaplin-Kramer, R., Nelson, E., Ennaanay, D., Wolny, S., Olwero, N., Vigerstol, K., Pennington, D., Mendoza, G., Aukema, J., Foster, J., Forrest, J., Cameron, D., Arkema, K., Lonsdorf, E., Kennedy, C., Verutes, G., Kim, C.K., Guannel, G., Papenfus, M., Toft, J., Marsik, M., Bernhardt, J., Griffin, R., Glowinski, K., Chaumont, N., Perelman, A., Lacayo, M. Mandle, L., Hamel, P., Vogl, A.L., Rogers, L., and Bierbower, W. (2015). InVEST +VERSION+ User's Guide. The Natural Capital Project, Stanford University, University of Minnesota, The Nature Conservancy, and World Wildlife Fund.

Shiferaw, B., & Holden, S. (1999). Soil erosion and smallholders' conservation decisions in the highlands of Ethiopia. *World development*, *27*(4), 739-752.

Tamene, L., & Le, Q. B. (2015). Estimating soil erosion in sub-Saharan Africa based on landscape similarity mapping and using the revised universal soil loss equation (RUSLE). *Nutrient Cycling in Agroecosystems*, *102*(1), 17-31.

Tamene, L., & Vlek, P. L. (2008). Soil erosion studies in northern Ethiopia. In Land use and soil resources (pp. 73-100). Springer Netherlands.

Tarboton, D. G. (2011). TauDEM 5.0 Watershed Delineation Using Taudem: A tutorial for using TauDEM to delineate a single watershed. Utah State University. (http://hydrology.usu.edu/taudem/taudem5/TauDEM5DelineatingASingleWatershed.pdf)

Tebebu, T. Y., Abiy, A. Z., Zegeye, A. D., Dahlke, H. E., Easton, Z. M., Tilahun, S. A., ... & Steenhuis, T. S. (2010). Surface and subsurface flow effect on permanent gully formation and upland erosion near Lake Tana in the northern highlands of Ethiopia. *Hydrology and Earth System Sciences,14*(11), 2207-2217.

Tebebu, T. Y., Steenhuis, T. S., Dagnew, D. C., Guzman, C. D., Bayabil, H. K., Zegeye, A. D., ... & Yitaferu, B. (2015). Improving efficacy of landscape interventions in the (sub) humid Ethiopian highlands by improved understanding of runoff processes. *Frontiers in Earth Science*, *3*, 49.

Tekle, K. (1999). Land degradation problems and their implications for food shortage in south Wello, Ethiopia Environmental Management 23:419 - 427.

Tenge, A. J., J. De Graaff, and J. P. Hella (2005), Financial efficiency of major soil and water conservation measures in West Usambara highlands, Tanzania, Appl. Geogr., 25(4), 348–366, doi:10.1016/j.apgeog.2005.08.003.

Teshome, A., D. Rolker, and J. de Graaff (2013), Financial viability of soil and water conservation technologies in northwestern Ethiopian highlands, Appl. Geogr., 37, 139–149, doi:10.1016/j.apgeog.2012.11.007.

TNC (2015). Upper Tana-Nairobi Water Fund Business Case. Version 2. The Nature Conservancy: Nairobi, Kenya.

Trabucco, A., and Zomer, R.J. (2010). *Global Soil Water Balance Geospatial Database. CGIAR Consortium for Spatial Information.* Published online, available from the CGIAR-CSI GeoPortal at: http://www.cgiar-csi.org

Tumcha Belguda (2004). The vision of Ministry of Agriculture on Natural Resources of Ethiopia by 2025, pp. 1-11, In: Seyoum and Negussu (eds.)

Van Mullem JA, Woodward DE, Hawkins RH, Hjelmfelt AT Jr. (2002). Runoff curve number method: beyond the handbook. In Hydrologic Modeling for the 21st Century. Second Federal Interagency Hydrologic Modeling Conference, 28 July to 1 August, Las Vegas, Nevada, USA.

Vigerstol, K. L., & Aukema, J. E. (2011). A comparison of tools for modeling freshwater ecosystem services. Journal of environmental management, 92(10), 2403-2409.

Vogl, A., & Wolny, S. (2015). Developing cost-effective investment portfolios for the Upper Tana-Nairobi Water Fund, Kenya. The Natural Capital Project. Unpublished. (http://www.nature.org/ourinitiatives/regions/africa/rios-technical-appendix.pdf)

Vogl, A., Tallis, H., Douglass, J., Sharp, R., Wolny, S., Veiga, F., ... & Guimarães, J. (2013). Resource Investment Optimization System: Introduction & Theoretical Documentation.

Williams JR. (1995). The EPIC model. In Singh VP. (Ed). Computer models of watershed hydrology. Water resources Publications, Highlands Ranch, CO. Chapter 25, pp. 909-1000.

Wischmeier, W.H., Johnson, C.B., Cross, B.V. (1971). A soil erodibility nomograph for farmland and construction sites. J. Soil Water Conserv. 26, 189–193.

Wischmeier, W.H., Smith, D.D. (1978). Predicting Rainfall Erosion Losses: A Guide to Conservation Planning. Agric. Handb., 537. U.S. Dep. Agric., Washington, D.C.

Wolancho, K. W. (2015). Evaluating watershed management activities of campaign work in Southern nations, nationalities and peoples' regional state of Ethiopia. *Environmental Systems Research*, *4*(1), 1-13.

Woodward, D. E., Hawkins, R. H., Jiang, R., Hjelmfelt, A. T., Van Mullem, J. A., & Quan, Q. D. (2003). Runoff curve number method: Examination of the initial abstraction ratio. In World Water & Environmental Resources Congress 2003(pp. 1-10). ASCE.

Zegeye, A. D., Steenhuis, T. S., Blake, R. W., Kidnau, S., Collick, A. S., & Dadgari, F. (2010). Assessment of soil erosion processes and farmer perception of land conservation in Debre Mewi watershed near Lake Tana, Ethiopia. *Ecohydrology & Hydrobiology*, *10*(2), 297-306.

ANNEX: Results of running 9-year RIOS simulation using SWC costs and yearly budgets

The following simulation results were not a part of this study. However, they are given here to show how use of activity costs dramatically changes the results. In this case, cost-effectiveness drives the pixel selection, and pixels are allocated activities more based on activities costs than on "responsiveness." This was because differences between activities varied greatly. The dominance of "cheap activities" allows half of the catchment (about 1200 ha) to be converted in just 9 years. In the thesis, simulation was based only on "responsiveness." For the 600-ha benchmark, about 17 years were estimated to be needed.

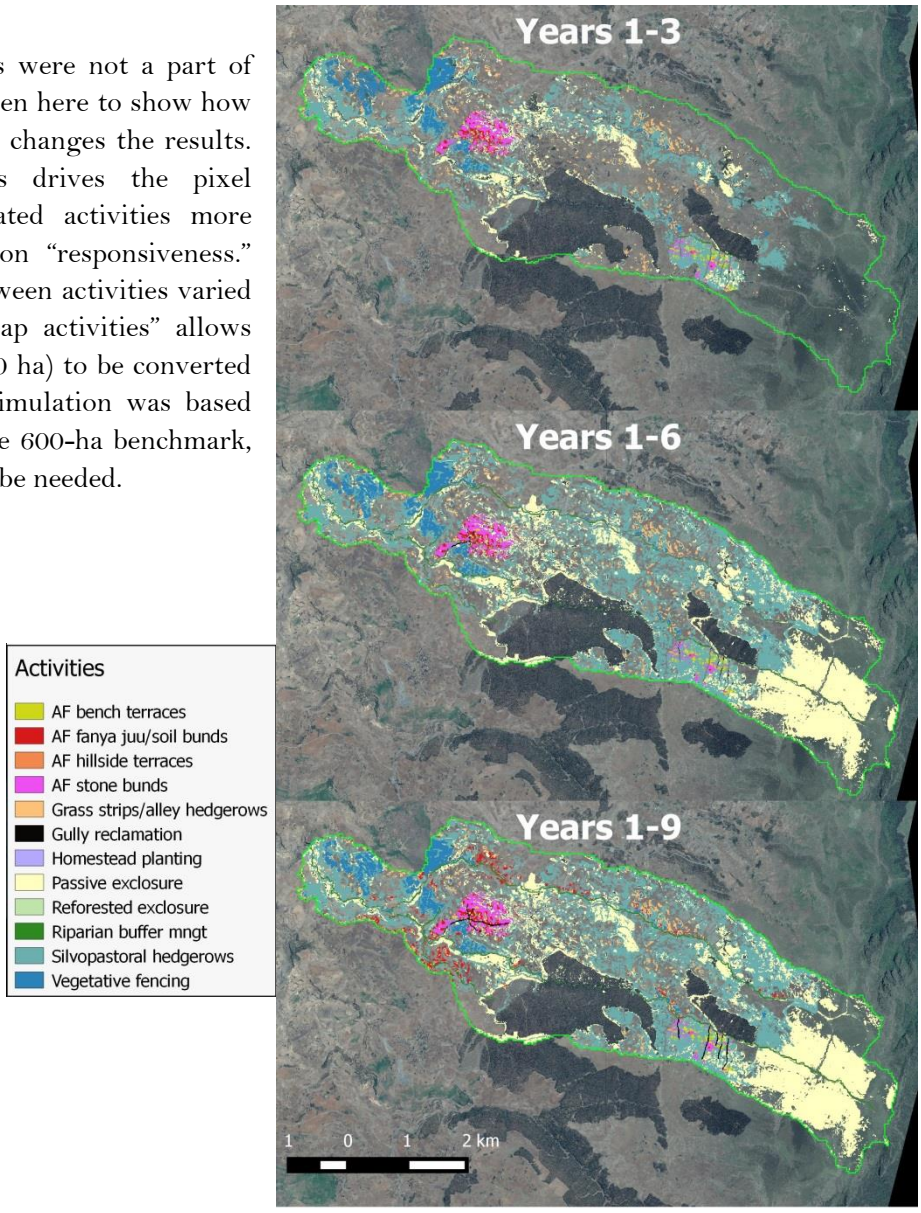

Figure 23: RIOS simulation when based on costs and annual budgets

Table 22: No. of hectares converted by each activity when RIOS simulation is based on costs and annual budgets

Activity	Years 1-3	Years 4-6	Years 7-9	All years
AF bench terraces	9.0			9.0
AF fanya juu/soil bunds	10.5		30.9	41.4
AF hillside terraces				0.0
AF stone bunds	30.7			30.7
Grass strips/alley hedgerows	61.6			61.6
Gully reclamation		1.9	5.0	6.9
Homestead greening	0.6		0.6	1.2
Passive exclosure	153.6	351.3	12.6	517.5
Reforested exclosure	0.7			0.7
Riparian buffer mngt	1.4	22.0	12.5	35.8
Silvopastoral hedgerows	310.5	289.0		599.5
Vegetative fencing	77.9	0.2		78.1
Total	**656.4**	**664.4**	**61.6**	**1382.3**

Statement

Herewith I assure that I have composed by myself the present paper, without any help from any other person and only with the sources and auxiliary means explicitly indicated in the paper.

Also parts verbally or analogously adopted from other papers are indicated.

I have taken due account of the "Guidelines of Good Scientific Practice" released by the University of Göttingen.

Date: Signature: